

Electronic supplemental information for:

Direct mechanocatalysis by Resonant Acoustic Mixing (RAM)

Cameron B. Lennox^{a,b} Tristan H. Borchers,^{a,b} Lori Gonnet,^{a,b} Christopher Barrett,^b Stefan Koenig,^{*c}
Karthik Nagapudi,^{*c} and Tomislav Friščić^{*a,b}

a. School of Chemistry, University of Birmingham, Edgbaston, Birmingham, B152TT, UK

b. Department of Chemistry, McGill University, 801 Sherbrooke St. W., Montreal, Quebec, H3H 0B8, Canada,

c. Small Molecule Pharmaceutical Sciences, Genentech Inc., One DNA Way, South San Francisco, CA, 94080, USA

Table of contents

	Page	
S1	Experimental section	2
S1.1	Materials and Methods	2
S1.2	Solution nuclear magnetic resonance (NMR) spectroscopy	2
S1.3	High resolution mass spectrometry (HR-MS)	2
S1.4	Fourier-transform infrared attenuated total reflectance (FTIR-ATR) spectroscopy	2
S1.5	Inductively coupled plasma mass spectrometry (ICP-MS)	2
S1.6	Scanning electron microscopy (SEM)	2
S1.7	X-ray photoelectron spectroscopy (XPS)	2
S1.8	Single-crystal X-ray diffraction	2
S1.9	Real-time Raman spectroscopy	2
S1.10	Resonant acoustic mixing	3
S1.11	General procedure for RAM direct mechanocatalysis	3
S1.12	Rufinamide synthesis by RAM direct mechanocatalysis	3
S1.13	Procedure for stoichiometrically selective reactions	3
S2	Reaction outcomes under static conditions	4
S3	Summary of reaction outcomes for reaction screening conditions	4
S4	Summary of reaction outcomes for stoichiometrically selective experiments	6
S5	Summary of copper loss compared to reaction conversion	8
S6	Summary of reaction outcomes following different copper treatment procedures	9
S7	Summary of ¹H-, ¹³C-NMR, HR-MS data, and isolated yields	9
S8	Scanning electron microscopy (SEM) micrographs	12
S9	X-ray photoelectron spectroscopy (XPS) spectra	13
S10	¹H-, ¹³C-NMR spectra	16
S11	Fourier-transform infrared attenuated total reflectance (FTIR-ATR) spectra	59
S12	<i>In situ</i> Raman measurements	71
S13	Summary of single crystal X-ray diffraction data	72
S14	References	72

S1. Experimental section

S1.1 Materials and Methods

Unless otherwise specified, all reagents and solvents were obtained from commercial sources and were used without further purification. Copper wire used was FisherBrand, #20-gauge (0.9 mm diameter) copper wire was manually wrapped around a standard NMR tube to create a 1 cm x 4.5 cm coil.

S1.2 Solution nuclear magnetic resonance (NMR) spectroscopy

^1H and ^{13}C NMR spectra were recorded on a Varian Inova 500 MHz NMR spectrometer. Chemical shifts are reported relative to CDCl_3 (δ 7.26 ppm), or DMSO (δ 2.50 ppm) and data is presented as chemical shifts, and integration.

S1.3 High resolution mass spectrometry (HR-MS)

The molecular weights of the purified products were obtained using high resolution mass spectrometry with an Exactive Plus Orbitrap-API.

S1.4 Fourier-transform infrared attenuated total reflectance (FTIR-ATR) spectroscopy

Infrared spectra were obtained using a Bruker Platinum ATR spectrometer, and are reported in wavenumber (cm^{-1}) units.

S1.5 Inductively coupled plasma mass spectrometry (ICP-MS)

Analysis was performed on a FINNIGAN iCapQ SOLUTION ICP-MS, with samples pre-digested with 50 % H_2O_2 and TMG HNO_3 , before serial dilution to appropriate concentration for analysis. For analysis of copper content, a calibration curve was prepared following standard operating procedures and copper content was extrapolated.

S1.6 Scanning electron microscopy (SEM)

SEM images were recorded on a QUANTA FED 450 electron microscopy. Samples were loaded on carbon tape without prior purification, and were coated with 4 nm Pt prior to measurement.

S1.7 X-ray photoelectron spectroscopy (XPS)

Analysis was performed on a Fisher Scientific $\text{K}\alpha$ spectrometer using a spot size of 200 μm , running 3 survey scans at 200 mV for 50 ms residence times and 10 scans for specific elements (similarly at residence times of 50 ms). Deconvolution and peak position were determined using Avantage software.

S1.8 Single-crystal X-ray diffraction

Single crystal X-ray diffraction (scXRD) data was measured on a Bruker D8 Venture diffractometer equipped with a Photon 200 area detector, and 1 μs microfocus X-ray source (Bruker AXS, $\text{CuK}\alpha$ source). Measurements were carried out at 298(2) K. Crystals were coated with a thin layer of paratone oil before mounting on a diffractometer, and structure solution was carried out using the SHELXTL package. The parameters were refined for all data by full-matrix-least-squares refinement of F^2 using SHELXL. All of the non-hydrogen atoms were refined with anisotropic thermal parameters, and the coordinates of all hydrogen atoms were constrained to reside on their carrier atom.

Crystallographic data in CIF format for all herein determined crystal structures can be accessed using the joint CCDC/FIZ Karlsruhe online deposition service (www.ccdc.cam.ac.uk/structures/2223762), under the deposition number 2223762.

S1.9 Real-time Raman spectroscopy

Real-time reaction monitoring was done using a RamanRxn1™ analyzer by Kaiser Optical Systems Inc., equipped with a power tunable 1-400 mW 785 nm Raman probe. Spectra were recorded with an integration time of 5-10 seconds and 3-5 accumulations to optimize the signal-to-noise ratio. All spectra were dark and intensity corrected using the Holograms® software package before being processed with MATLAB.

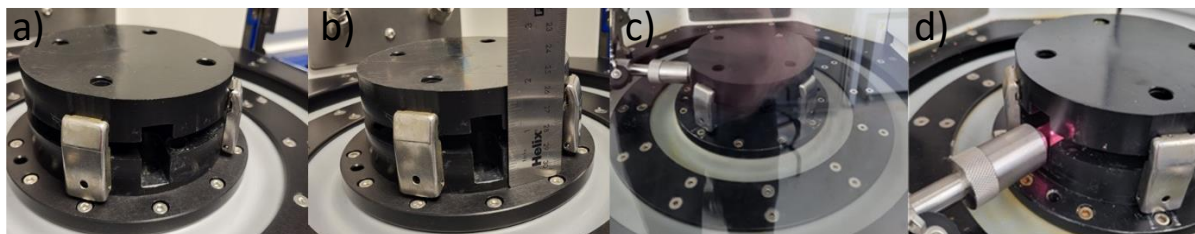


Figure S1.1 a) Image of custom-made RAM holder including an entrance slit, b) highlight of size of the entrance slit (ca. 33 mm) ensuring that the probe does not enter into contact with holder during RAM operation, c) image of Raman monitoring experiment taken from outside of the LabRam II, and d) image of Raman probe and the relative distance from the sample vial and entrance slit.

In a typical Raman monitoring experiment, a 1 dram glass vial was placed in the custom-made sample holder containing an entrance slit (Figure S1.1a, b). The 785 nm Raman probe was then placed approximately 10 mm from the vial, with the probe's focal length focused on the center of the vial. The probe was mounted to an optical breadboard, placed on a separate table to the LabRam II, and then placed inside the instrument through the open side-door and held in place with various posts and clamps, ensuring no contact with the instrument. This allowed for continuous monitoring without damaging the Raman probe through vibrations. The probe was shielded from invasive background light by covering the exterior windows and open door of the LabRam II with tinfoil.

S1.10 Resonant acoustic mixing

All synthesis was carried out using a Resodyn LabRAM II instrument with 1 dram (3.5 mL) volume glass vials (Figure S1a) and a copper coil (Figure S1b).

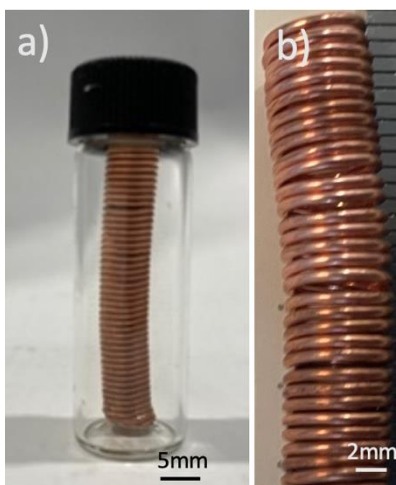


Figure S1.2 a) Pristine coil in vial, b) close-up of copper coil following priming, showing a change in material luster.

S1.11 General procedure for RAM direct mechanocatalysis

In a typical reaction benzyl bromide **1a** (2 mmol, 238 μL), ethynylbenzene **2a** (2 mmol, 256 μL), NaN_3 (3 mmol, 195 mg), and DMSO (436 μL , $\eta = 0.50 \mu\text{L}/\text{mg}$) were added to a 3.5 mL reaction vial containing a copper coil that had previously been "primed" by RAM for 60 minutes at 90 g with 300 mg of SiO_2 , **2a** and DMSO ($\eta = 0.50 \mu\text{L}/\text{mg}$) (see S6). After RAM for 60 minutes, **4a** was purified by extraction into EtOAc and subsequent RAM with a 1:2 by volume mixture of water and MeOH. Product **4a** was obtained as a white solid, and was characterised by ^1H -, ^{13}C -NMR, FTIR and HR-MS.

S1.12 Rufinamide synthesis by RAM direct mechanocatalysis

2,6-Difluorobenzyl bromide (4 mmol, 517.5 mg), propiolamide (4 mmol, 172.5 mg), NaN_3 (5 mmol, 325 mg), and DMSO (507 μL , $\eta = 0.50 \mu\text{L}/\text{mg}$) were added to a 3.5 mL reaction vial containing a copper coil that had previously been activated by RAM for 60 minutes at 90 g with 300 mg of SiO_2 , **2a** and DMSO ($\eta = 0.50 \mu\text{L}/\text{mg}$) (see S6). After 60 minutes at 90 g the crude reaction product was analysed by dissolution of the entire reaction mixture in d_6 -DMSO and analysis by ^1H -NMR. Purification consisted of dissolution in EtOAc, washing with aqueous NH_4Cl , aqueous NaHCO_3 , brine, after which the organic solvent was evaporated *in vacuo* to yield white powder, characterised by ^1H -, ^{13}C -NMR, FTIR and HR-MS.

S1.13 Procedure for stoichiometrically selective reactions

In a typical reaction benzyl bromide **1a** (2 mmol, 238 μL), *p*-diethynylbenzene **2d** (1 mmol, 126 mg), NaN_3 (3 mmol, 195 mg), and DMSO (507 μL , $\eta = 0.50 \mu\text{L}/\text{mg}$) were added to a 3.5 mL reaction vial containing a copper coil that had previously been activated by RAM for 60 minutes at 90 g with 300 mg of SiO_2 , **2a** and DMSO ($\eta = 0.50 \mu\text{L}/\text{mg}$) (see S6). After 60 minutes RAM leads to the preferred formation of **4s**, while after 120 minutes at $\eta = 1.00 \mu\text{L}/\text{mg}$ the product is **4t**. Reaction products were purified by dissolution in EtOAc, filtration and solvent evaporation under reduced pressure to yield a white powder in each case, characterised by ^1H -, ^{13}C -NMR, FTIR and HR-MS.

S2. Summary of reaction outcomes for static reactions

Table S2.1 Reaction conversion to **4a** from **1a** and **2a** without any mixing

Entry	liquid additive	copper catalyst	time (hours)	conversion (%) ^[a]
1	none	Copper coil	0.5	0
2			24	0
3		CuCl ^[c]	0.5	0
4			24	0
5	DMSO ^[d]	Copper coil ^[b]	0.5	0
6			24	trace
7		CuCl ^[c]	0.5	0
8			24	trace

^[a] The vial was allowed to stand at room temperature for 30 minutes or 24 hours, before full sample dissolution in CDCl₃ and analysis by ¹H-NMR. ^[b] 1 cm x 4.5 cm coil from #20 gauge copper wire. ^[c] 3 mol% relative to **2a**.

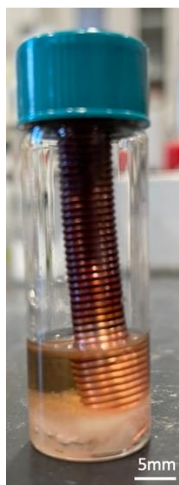


Figure S2.1 Example image of a reaction vial following 24 h static reaction, conducted without any mixing (entry 6 in table S2.1).

S3. Summary of reaction outcomes for screening conditions

Table S3.1 Conversions to **3a** or **4a** with different liquid additives after 60 minutes of RAM at 90 g.

entry	liquid additive ($\eta = 0.50 \mu\text{L}/\text{mg}$)	conversion to 3a (%) ^[a]	conversion to 4a (%) ^[a]
1	no additive	0	0
2	water	13 \pm 3	32 \pm 1
3	DMSO	28 \pm 4	>95
4	<i>N</i> -methylpyrrolidine	>95	45 \pm 1
5	acetonitrile	5 \pm 3	45 \pm 1
6	methanol	29 \pm 1	82 \pm 1

^[a] Accessed by ¹H-NMR of the entire reaction mixture after dissolution in CDCl₃.

Table S3.2 Conversions to **4a** with DMSO as a liquid additive after 60 minutes of RAM at 90 g.

Entry	η ($\mu\text{L}/\text{mg}$)	conversion (%) ^[a]
1	0	0
2	0.25	91 \pm 1
3	0.50	>95
4	0.75	>95
5	1.00	>95
6	1.25	>95

^[a] Accessed by ¹H-NMR of the entire reaction mixture after dissolution in CDCl₃.

Table S3.3 Conversions to **4a** with MeOH as a liquid additive after 60 minutes of RAM at 90 g.

Entry	η ($\mu\text{L}/\text{mg}$)	conversion (%) ^[a]
1	0	0
2	0.25	23 \pm 1
3	0.50	82 \pm 1
4	0.75	49 \pm 2
5	1.00	47 \pm 1
6	1.25	44 \pm 3

^[a] Accessed by ¹H-NMR of the entire reaction mixture after dissolution in CDCl₃.

Table S3.4 Conversions to **4a** with H₂O as a liquid additive after 60 minutes of RAM at 90 g.

Entry	η ($\mu\text{L}/\text{mg}$)	conversion (%) ^[a]
1	0	0
2	0.25	17 \pm 4
3	0.50	32 \pm 3
4	0.75	5 \pm 4
5	1.00	9 \pm 2
6	1.25	7 \pm 2

^[a] Accessed by ¹H-NMR of the entire reaction mixture after dissolution in CDCl₃.

Table S3.5 Conversions to **4a** with a 1:1 (v/v) mixture of DMSO and H₂O as a liquid additive after 60 minutes of RAM at 90 g.

Entry	η ($\mu\text{L}/\text{mg}$)	conversion (%) ^[a]
1	0	0
2	0.25	5 \pm 1
3	0.50	5 \pm 4
4	0.75	6 \pm 3
5	1.00	9 \pm 4
6	1.25	9 \pm 6

^[a] Accessed by ¹H-NMR of the entire reaction mixture after dissolution in CDCl₃.

Table S3.6 Conversions to **4a** with 1:1 (v/v) mixture of DMSO and MeOH as a liquid additive after 60 minutes of RAM at 90 g.

Entry	η ($\mu\text{L}/\text{mg}$)	conversion (%) ^[a]
1	0	0
2	0.25	23 \pm 1
3	0.50	82 \pm 1
4	0.75	49 \pm 2
5	1.00	47 \pm 1
6	1.25	44 \pm 3

^[a] Accessed by ¹H-NMR of the entire reaction mixture after dissolution in CDCl₃.

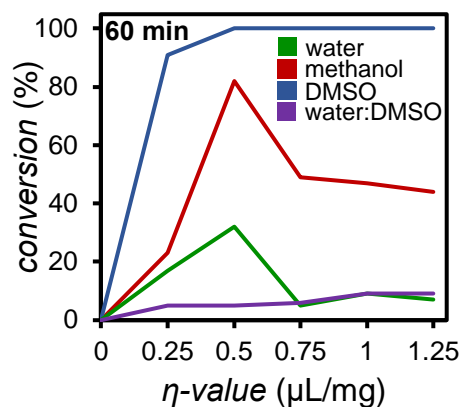
**Figure S3.1** Effect of liquid additive choice and η -value on the direct mechanosynthesis of **4a** in the presence of different liquid additives: MeOH, DMSO, water, and 1:1 by volume mixture of DMSO and water.

Table S3.7 Conversions to **4a** with DMSO ($\eta = 0.50 \mu\text{L}/\text{mg}$) as liquid additive after 60 minutes of RAM at 90 g.

Entry	Cu source	Conversion (%) ^[a]
1	-	0
2	CuCl ^[b]	31 ± 4
3	CuO ^[b]	0
4	Cu ₂ O ^[b]	23 ± 3
5	Cu(OAc) ₂ • H ₂ O ^[b]	26 ± 6
6	Cu wire ^[c]	24 ± 4
7	Cu coil ^[d]	>95

^[a] Accessed by full dissolution of product for ¹H-NMR analysis in CDCl₃. ^[b] 3 mol% relative to **2a**; ^[c] 45 mm x 0.9 mm; ^[d] 0.9 mm copper wire formed into a 45 mm x 10 mm coil.

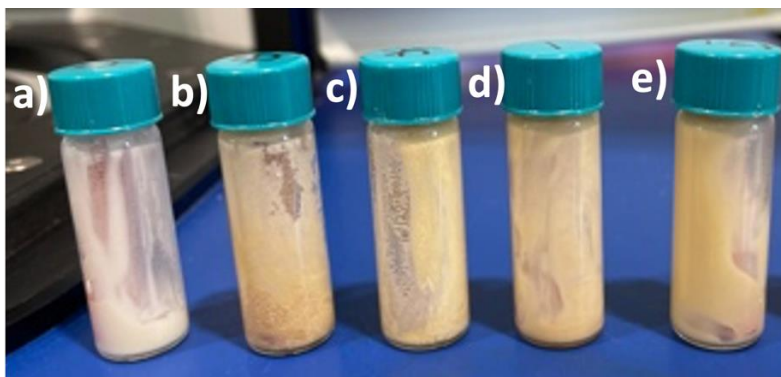


Figure S3.2 Result of RAM direct mechanocatalysis reactions to form **4a**, following 60 minutes of mixing at 90 g with a) $\eta = 0.25 \mu\text{L}/\text{mg}$, b) $\eta = 0.50 \mu\text{L}/\text{mg}$, c) $\eta = 0.75 \mu\text{L}/\text{mg}$, d) $\eta = 1 \mu\text{L}/\text{mg}$, or e) $\eta = 1.25 \mu\text{L}/\text{mg}$ of DMSO.

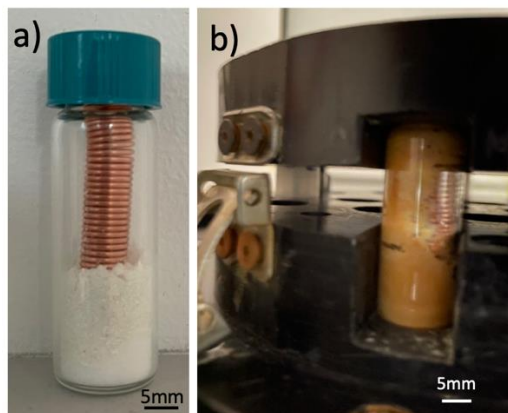


Figure S3.3 a) Reaction mixture **1e** and NaN₃ (before addition of **2a** and DMSO), and b) reaction mixture immediately following reaction, with quantitative conversion to **4e**.

S4. Summary of reaction outcomes for stoichiometrically selective reactions

All conversions are based on ¹H-NMR analysis following full sample dissolution in CDCl₃. All reactions were conducted by RAM at 90 g with 2 mmol of **1a**, 1 mmol of **2d**, 5 mmol of NaN₃ and a 45 mm x 10 mm copper coil in the presence of DMSO as a liquid additive.

Table S4.1 Conversion to **4s** or **4t** following RAM at 90 g with $\eta = 0.25 \mu\text{L}/\text{mg}$.

Entry	time (min)	conversion to 4s (%)	conversion to 4t (%)
1	0	0	0
2	40	43 ± 5	2 ± 2
3	60	78 ± 2	9 ± 3
4	80	78 ± 3	16 ± 4
5	120	82 ± 4	13 ± 3

Table S4.2 Conversion to **4s** or **4t** following RAM at 90 g with $\eta = 0.50 \mu\text{L}/\text{mg}$.

Entry	time (min)	conversion to 4s (%)	conversion to 4t (%)
	0	0	0
1	40	93 \pm 4	7 \pm 3
2	60	87 \pm 3	10 \pm 4
3	80	84 \pm 1	13 \pm 2
4	120	79 \pm 3	21 \pm 3

Table S4.3 Conversion to **4s** or **4t** following RAM at 90 g with $\eta = 0.75 \mu\text{L}/\text{mg}$.

Entry	time (min)	conversion to 4s (%)	conversion to 4t (%)
1	40	88 \pm 6	12 \pm 2
2	60	84 \pm 1	16 \pm 3
3	80	46 \pm 2	54 \pm 4
4	120	18 \pm 1	82 \pm 2

Table S4.4 Conversion to **4s** or **4t** following RAM at 90 g with $\eta = 1.0 \mu\text{L}/\text{mg}$.

Entry	time (min)	conversion to 4s (%)	conversion to 4t (%)
1	40	91 \pm 1	9 \pm 3
2	60	79 \pm 4	21 \pm 3
3	80	21 \pm 3	79 \pm 2
4	120	0	>95

Table S4.5 Conversion to **4s** or **4t** following RAM of **1a** and **2d** in a 1:1 molar ratio, 1.5 equivalents of NaN_3 and DMSO at 90 g for 60 minutes.

Entry	η ($\mu\text{L}/\text{mg}$)	conversion to 4s (%)	conversion to 4t (%)
1	0	0	0
2	0.25	70 \pm 1	11 \pm 2
3	0.50	69 \pm 3	13 \pm 3
4	0.75	78 \pm 1	18 \pm 1
5	1.00	74 \pm 2	12 \pm 2

Table S4.6 Conversion to **4u** following RAM of 2 mmol of **1e**, 1 mmol **2d**, 5 mmol NaN_3 and DMSO at 90 g for 60 minutes.

Entry	η ($\mu\text{L}/\text{mg}$)	conversion to non-symmetric product (%)	conversion to 4u (%)
1	0	0	0
2	0.25	64 \pm 1	33 \pm 1
3	0.50	11 \pm 2	89 \pm 1
4	0.75	4 \pm 1	96 \pm 2
5	1.00	0	>95

S5. Summary of copper loss compared to reaction conversion

Table S5.1. Reaction conversion following sequential 20-minute cycles for the RAM reaction of equimolar amounts of **1a** and **2a** with 1.5 equivalents of NaN_3 in the presence of DMSO ($\eta = 0.50 \mu\text{L}/\text{mg}$). Reactions were conducted at 90 g and the coil was washed with EtOAc between cycles.

RAM cycle	total time in reaction (min)	Cu loss (mg)	Cu loss (mol%)	reaction conversion (%)
1	20	0.72 ± 0.3	0.57 ± 0.3	9 ± 3
2	40	1.49 ± 0.5	1.18 ± 0.5	1 ± 4
3	60	0.55 ± 0.2	0.44 ± 0.2	4 ± 5
4	120	1.23 ± 0.2	0.97 ± 0.2	36 ± 2
5	140	1.18 ± 0.7	0.93 ± 0.7	28 ± 4

Table S5.2. Reaction conversion following sequential 60-minute cycles for the RAM reaction of equimolar amounts of **1a** and **2a** with 1.5 equivalents of NaN_3 in the presence of DMSO ($\eta = 0.50 \mu\text{L}/\text{mg}$). Reactions were conducted at 90 g and the coil was washed with EtOAc between cycles. The mean values and standard deviations are based on a set of four independent 10-cycle experiments, each started with a fresh coil.

RAM cycle	total time in reaction (min)	Cu loss (mg) ^[a]	Cu loss (mol%) ^[b]	reaction conversion (%) ^[c]
1	60	0.925 ± 0.2	0.73 ± 0.2	4 ± 3
2	120	1.30 ± 0.4	1.02 ± 0.4	>95
3	180	1.60 ± 0.7	1.26 ± 0.7	>95
4	240	2.11 ± 0.7	1.47 ± 0.7	>95
5	300	1.19 ± 1.0	0.94 ± 1.0	>95
6	360	0.85 ± 0.2	0.67 ± 0.2	>95
7	420	0.96 ± 0.4	0.76 ± 0.4	>95
8	480	1.68 ± 0.5	0.54 ± 0.5	>95
9	540	0.97 ± 0.2	0.76 ± 0.2	>95
10	600	1.08 ± 0.3	0.94 ± 0.3	>95

^[a]Average of four identical reactions, each done with a different coil, with standard deviation from the mean shown. ^[b]Relative to **1a**. ^[c]Average of four identical reactions, based on analysis of the entire reaction mixture by $^1\text{H-NMR}$.

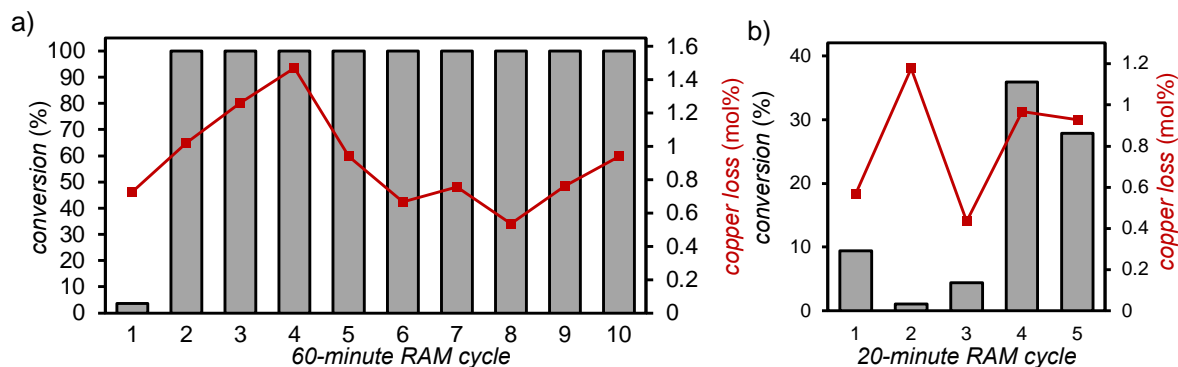


Figure S5. Reaction conversion and average loss of copper for: a) 10 RAM reaction cycles of 60 minutes and b) 5 RAM reaction cycles of 20 minutes. The provided values are an average across four sets of identical experiments.

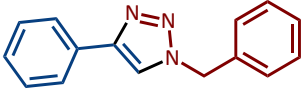
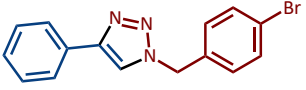
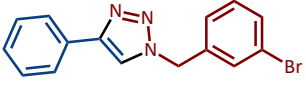
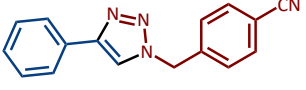
S6. Summary of reaction outcomes following different copper treatment procedures

Table S6.1 Reaction outcomes following different treatments of a copper coil.

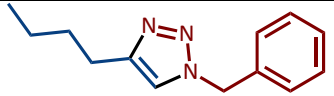
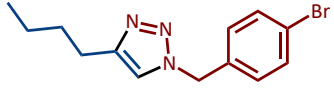
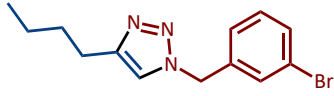
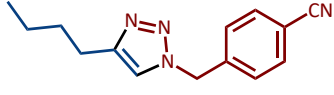
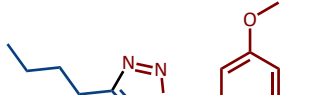
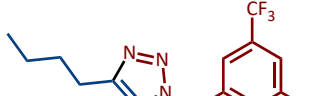
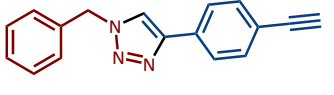
entry	conditions	conversion (%) ^[b]
1	/	5 ± 4
2	1a , 2a , NaN ₃ ^[a]	> 95
7	celite ^[c]	6 ± 2
8	SiO ₂ ^[c]	36 ± 4
9	2a ^[d]	14 ± 4
10	SiO ₂ ^[d] followed by 2a ^[d]	> 95
11	2a and SiO ₂ ^[e]	> 95
12	125°C for 24 hours	34 ± 2
13	CH ₃ COOH, ^[e] followed by 125°C for 24 hours	68 ± 1

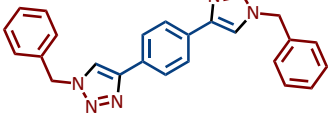
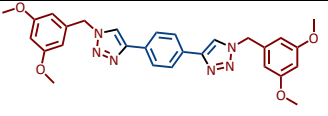
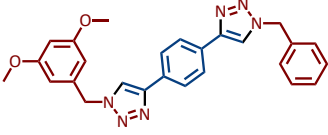
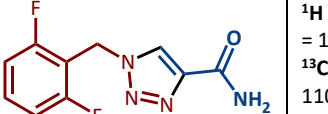
^[a] Reactions conducted by RAM of equimolar amounts of **1a** and **2a** with 1.5 equivalents of NaN₃, in the presence of DMSO liquid additive ($\eta = 0.5 \mu\text{L}/\text{mg}$) at 90 g for 60 minutes. ^[b] Based on triplicate experiments and ¹H NMR analysis following dissolution of the entire reaction mixture in CDCl₃; ^[c] 300mg of solid and DMSO ($\eta = 0.5 \mu\text{L}/\text{mg}$). ^[d] Soaked in 2 mL of **2a** in a sealed vial at room temperature for 24h. ^[e] RAM of 300 mg SiO₂, 256 μL of **2a** and DMSO as the liquid additive ($\eta = 0.5 \mu\text{L}/\text{mg}$) at 90 g for 60 minutes, followed by washing with EtOAc.

S7. Summary of ¹H-, ¹³C-NMR, HR-MS, and isolated yield data

<p>1-benzyl-4-phenyl-1H-1,2,3-triazole (4a)</p> 	<p>¹H NMR (500 MHz, CDCl₃): δ 7.78 (m, 2H), 7.66 (s, 1H), 7.4 (m, 5H), 7.31 (m, 3H), 5.58 (s, 2H). ¹³C NMR (500 MHz, CDCl₃): δ 148.27, 134.70, 130.55, 129.18 (2C), 128.09 (2C), 125.72 (2C), 119.46 (2C), 44.27. HR-MS ESI (+): calculated for C₁₄H₁₄N₃ [M + H]⁺: 236.1182; measured: 236.1177. Isolated yield: >95%</p>
<p>1-(4-bromobenzyl)-4-phenyl-1H-1,2,3-triazole (4b)</p> 	<p>¹H NMR (500 MHz, CDCl₃): δ 7.80 (m, 2H), 7.66 (s, 1H), 7.52 (m, 2H), 7.32 (m, 1H), 7.19 (m, 2H) 5.54 (s, 2H). ¹³C NMR (500 MHz, CDCl₃): δ 148.46, 133.70, 132.37, 130.35 (2C), 129.66 (2C), 128.86, 128.31, 125.73 (2C), 123.00, 119.41, 53.56, 41.00. HR-MS ESI (+): calculated for C₁₄H₁₂BrN₃Na [M + Na]⁺: 336.0107; measured: 336.0119. Isolated yield: >95%</p>
<p>1-(3-bromobenzyl)-4-phenyl-1H-1,2,3-triazole (4c)</p> 	<p>¹H NMR (500 MHz, CDCl₃): δ 7.81 (m, 2H), 7.69 (s, 1H), 7.48 (m, 1), 7.41 (m, 2H), 7.33 (m, 1H), 7.24 (m, 1H), 5.58 (s, 2H). ¹³C NMR (500 MHz, CDCl₃): δ 148.48, 136.90, 131.98, 130.99, 130.74, 130.36, 128.32, 126.56, 125.75, 123.15, 119.51, 53.46. HR-MS ESI (+): calculated for C₁₅H₁₃N₃Br [M + H]⁺: 314.0280; measured: 314.0287. Isolated yield: 94%</p>
<p>4-((4-phenyl-1H-1,2,3-triazol-1-yl)methyl)benzonitrile (4d)</p> 	<p>¹H NMR (500 MHz, CDCl₃): δ 7.81 (m, 2H), 7.72 (s, 1H), 7.68 (m, 2H), 7.41 (m, 4H), 7.34 (m, 1H) 5.66 (s, 2H). ¹³C NMR (500 MHz, CDCl₃): δ 139.90, 132.96, 128.92, 128.65, 128.49, 128.36, 135.77, 53.49. HR-MS ESI (+): calculated for C₁₆H₁₅N₄O [M + H₂O]⁺: 279.1168; measured: 279.1038. Isolated yield: 92%</p>

1-(3,5-dimethoxybenzyl)-4-phenyl-1H-1,2,3-triazole (4e)	
	<p>¹H NMR (500 MHz, CDCl₃): δ 7.81 (m, 2H), 7.68 (s, 1H), 7.40 (m, 2H), 7.32 (m, 1H), 6.44 (m, 3H), 5.59 (s, 2H), 3.77 (s, 6H).</p> <p>¹³C NMR (500 MHz, CDCl₃): δ 161.38, 148.26, 136.79, 130.55, 128.82, 128.18, 125.72, 119.48, 106.11, 100.48, 55.46, 54.33.</p> <p>HR-MS ESI (+): calculated for C₁₇H₁₈N₃O₂ [M + H]⁺: 296.1394; measured: 296.1392.</p> <p>Isolated yield: >95%</p>
1-(3,5-bis(trifluoromethyl)benzyl)-4-phenyl-1H-1,2,3-triazole (4f)	
	<p>¹H NMR (500 MHz, CDCl₃): δ 7.90 (s, 1H), 7.83 (m, 2H), 7.77 (m, 3H), 7.43 (m, 2H), 7.35 (m, 1H), 5.71 (s, 2H).</p> <p>¹³C NMR (500 MHz, CDCl₃): δ 137.27, 128.94, 128.58, 156.82, 119.53, 53.06, 41.02.</p> <p>HR-MS ESI (+): calculated for C₁₇H₁₂F₆N₃ [M + H]⁺: 372.0924; measured: 372.0930.</p> <p>Isolated yield: >95%</p>
1-benzyl-4-(trimethylsilyl)-1H-1,2,3-triazole (4g)	
	<p>¹H NMR (500 MHz, CDCl₃): δ 8.19 (s, 1H), 7.37 (m, 2H), 7.32 (m, 3H), 5.59 (s, 2H), 0.24 (s, 9H).</p> <p>¹³C NMR (500 MHz, CDCl₃): δ 129.13, 129.07, 128.61, 128.61, 128.10, 128.03, 53.49, -1.11.</p> <p>HR-MS ESI (+): calculated for C₁₂H₁₈N₃Si [M + H]⁺: 232.1265; measured: 232.1265.</p> <p>Isolated yield: 88%</p>
1-(4-bromobenzyl)-4-(trimethylsilyl)-1H-1,2,3-triazole (4h)	
	<p>¹H NMR (500 MHz, CDCl₃): δ 7.51 (m, 2H), 7.41 (s, 1H), 7.14 (m, 2H), 5.51 (s, 2H), 0.30 (s, 9H).</p> <p>¹³C NMR (500 MHz, CDCl₃): δ 148.1, 134.6, 130.5, 129.1 (2C), 128.7 (2C), 128.2, 126.4, 125.6 (2C), 122.9, 119.6, 53.3.</p> <p>HR-MS ESI (+): calculated for C₁₂H₁₆BrN₃NaSi [M + Na]⁺: 310.0189; measured: 310.0200.</p> <p>Isolated yield: >95%</p>
1-(3-bromobenzyl)-4-(trimethylsilyl)-1H-1,2,3-triazole (4i)	
	<p>¹H NMR (500 MHz, CDCl₃): δ 8.24 (s, 1H), 7.56 (m, 1H), 7.52 (m, 3H), 5.62 (s, 2H), 0.25 (s, 9H).</p> <p>¹³C NMR (500 MHz, CDCl₃): δ 145.68, 139.33, 143.14, 131.47, 131.44, 131.30, 131.18, 131.05, 127.62, 127.40, 125.65, 122.28.</p> <p>HR-MS ESI (+): calculated for C₁₂H₁₇BrN₃Si [M + H]⁺: 310.0370; measured: 310.0367.</p> <p>Isolated yield: 80%</p>
3-((4-(trimethylsilyl)-1H-1,2,3-triazol-1-yl)methyl)benzonitrile (4j)	
	<p>¹H NMR (500 MHz, DMSO): δ 8.25 (s, 1H), 7.85 (m, 2H), 7.45 (m, 2H), 5.70 (s, 2H), 0.25 (s, 9H).</p> <p>¹³C NMR (500 MHz, DMSO): δ 145.27, 141.68, 132.72, 130.92, 128.72, 110.84, 51.61, 1.02 (3C).</p> <p>HR-MS ESI (+): calculated for C₁₂H₁₇N₄Si [M + H]⁺: 356.1144; measured: 356.0161.</p> <p>Isolated yield: 94%</p>
1-(3,5-dimethoxybenzyl)-4-(trimethylsilyl)-1H-1,2,3-triazole (4k)	
	<p>¹H NMR (500 MHz, CDCl₃): δ 8.19 (s, 1H), 6.46 (m, 3H), 5.50 (s, 2H), 3.72 (s, 6H), 0.25 (s, 9H).</p> <p>¹³C NMR (500 MHz, CDCl₃): δ 161.28, 161.13, 160.92, 137.61, 106.97, 106.15, 106.03, 100.62, 100.30, 100.19, 55.43, 55.40, 54.89, 53.55, 33.63, -1.10 (3C).</p> <p>HR-MS ESI (+): calculated for C₁₄H₂₂O₂N₃Si [M + H]⁺: 292.1476; measured: 292.1475.</p> <p>Isolated yield: 93%</p>
1-(3,5-bis(trifluoromethyl)benzyl)-4-(trimethylsilyl)-1H-1,2,3-triazole (4l)	
	<p>¹H NMR (500 MHz, CDCl₃): δ 8.32 (s, 1H), 8.09 (m, 1H), 8.05 (m, 2H), 5.84 (s, 2H), 0.24 (s, 9H).</p> <p>¹³C NMR (500 MHz, CDCl₃): δ 206.96, 138.22, 137.60, 132.70, 132.43, 132.17, 128.95, 128.08, 127.88, 128.95, 128.08, 127.77, 123.99, 122.77, 122.74, 122.71, 122.17, 121.82, 53.55, 52.32, 30.93, -1.18.</p> <p>HR-MS ESI (+): calculated for C₁₄H₁₆F₆N₃Si [M + H]⁺: 368.1012; measured: 368.1014.</p> <p>Isolated yield: 84%</p>

<p>1-benzyl-4-butyl-1<i>H</i>-1,2,3-triazole (4m)</p> 	<p>¹H NMR (500 MHz, CDCl₃) δ 7.89 (s, 1H), 7.32 (m, 5H), 5.53 (s, 2H), 2.59 (t, <i>J</i> = 15.3 Hz, 2H), 1.55 (quintet, <i>J</i> = 30.4 Hz, 2H), 1.30 (sextet, <i>J</i> = 37 Hz, 2H), 0.88 (t, <i>J</i> = 14.7, 3H). ¹³C NMR (500 MHz, CDCl₃) δ .149.28, 134.08, 132.26, 129.66, 122.72, 120.41, 53.34, 31.69, 24.45, 22.37, 13.88. HR-MS ESI (+): calculated for C₁₃H₁₈N₃ [M + H]⁺: 216.1495; measured: 216.1489. Isolated yield: 93%</p>
<p>1-(4-bromobenzyl)-4-butyl-1<i>H</i>-1,2,3-triazole (4n)</p> 	<p>¹H NMR (500 MHz, CDCl₃) δ 7.49 (m, 2H), 7.17 (s, 1H), 7.11 (m, 2H), 5.44 (s, 2H), 2.69 (t, <i>J</i> = 15.5 Hz, 2H), 1.62 (quintet, <i>J</i> = 30.7 Hz, 2H), 1.35 (sextet, <i>J</i> = 37.1 Hz, 2H), 0.91 (t, <i>J</i> = 14.8 Hz, 3H). ¹³C NMR (500 MHz, CDCl₃) δ 149.3, 134.50, 132.4, 129.7, 122.9, 120.5, 53.3, 31.6, 25.6, 22.4, 13.9. HR-MS ESI (+): calculated for C₁₃H₁₇N₃Br [M + H]⁺: 294.0600; measured: 294.0595. Isolated yield: 87%</p>
<p>1-(3-bromobenzyl)-4-butyl-1<i>H</i>-1,2,3-triazole (4o)</p> 	<p>¹H NMR (500 MHz, CDCl₃) δ 7.53 (m, 1H), 7.45 (s, 1H), 7.29 (m, 1H), 7.23 (m, 1H), 5.51 (s, 2H), 2.76 (t, <i>J</i> = 14.9 Hz, 2H), 1.69 (quintet, <i>J</i> = 29.8 Hz, 2H), 1.42 (sextet, <i>J</i> = 37.3 Hz, 2H), 0.97 (t, <i>J</i> = 16.8 Hz, 3H). ¹³C NMR (500 MHz, CDCl₃) δ 149.2, 137.2, 131.7, 131.4, 131.1, 130.8, 130.6, 130.4, 126.6, 126.4, 123.0, 120.5, 54.0, 53.2, 31.4, 25.4, 22.3, 13.8. HR-MS ESI (+): calculated for C₁₃H₁₆N₃BrNa [M + Na]⁺: 316.0420; measured: 316.0414. Isolated yield: 62%</p>
<p>4-((4-butyl-1<i>H</i>-1,2,3-triazol-1-yl)methyl)benzonitrile (4p)</p> 	<p>¹H NMR (500 MHz, CDCl₃) δ 7.65 (m, 2H), 7.31 (m, 2H), 7.23 (s, 1H), 5.56 (s, 2H), 2.71 (t, <i>J</i> = 15.6 Hz, 2H), 1.64 (quintet, <i>J</i> = 30.6 Hz, 2H), 1.36 (sextet, <i>J</i> = 36.9 Hz, 2H), 0.92 (t, <i>J</i> = 14.8 Hz, 3H). ¹³C NMR (500 MHz, CDCl₃) δ 207.0, 142.8, 140.7, 132.6, 132.6, 129.7, 128.5, 118.4, 112.2, 54.0, 31.4, 30.9, 14.2. HR-MS ESI (+): calculated for C₁₄H₁₇N₄ [M + H]⁺: 241.1375; measured: 241.0682. Isolated yield: 55%</p>
<p>1-(3,5-dimethoxybenzyl)-4-butyl-1<i>H</i>-1,2,3-triazole (4q)</p> 	<p>¹H NMR (500 MHz, CDCl₃) δ 7.19 (s, 1H), 6.41 (s, 1H), 6.38 (m, 2H), 5.40 (s, 2H), 3.75 (s, 6H), 2.69 (t, <i>J</i> = 14.8 Hz, 2H), 1.62 (quintet, <i>J</i> = 30.7 Hz, 2H), 1.35 (sextet, <i>J</i> = 37.8 Hz, 2H), 0.91 (t, <i>J</i> = 15.3 Hz, 3H). ¹³C NMR (500 MHz, CDCl₃) : δ. 161.2, 148.9, 137.1, 120.5, 105.9, 100.3, 55.4, 54.0, 31.5, 25.4, 22.3, 13.8. HR-MS ESI (+): calculated for C₁₅H₂₂O₂N₃ [M + H]⁺: 276.1707; measured: 276.1702. Isolated yield: 91%</p>
<p>1-(3,5-bis(trifluoromethyl)benzyl)-4-butyl-1<i>H</i>-1,2,3-triazole (4r)</p> 	<p>¹H NMR (500 MHz, DMSO): δ 8.11 (s, 1H), 8.02 (s, 1H), 7.98 (s, 2H), 5.78 (s, 2H), 2.62 (t, <i>J</i> = 16.2 Hz, 2H), 1.56 (quintet, <i>J</i> = 30.8 Hz, 2H), 1.29 (sextet, <i>J</i> = 37.8 Hz, 2H), 0.88 (t, <i>J</i> = 14 Hz, 3H). ¹³C NMR (500 MHz, CDCl₃): δ 121.2, 148.9, 137.1, 120.5, 105.9, 100.3, 55.4, 55.0, 31.5, 25.4, 22.3, 13.8. HR-MS ESI (+): calculated for C₁₅H₁₅F₆N [M]⁺: 352.1243; measured: 352.1247. Isolated yield: 92%</p>
<p>1-benzyl-4-(4-ethynylphenyl)-1<i>H</i>-1,2,3-triazole (4s)</p> 	<p>¹H NMR (500 MHz, CDCl₃) δ 7.75 (m, 3H), 7.52 (m, 2H), 7.38 (m, 3H), 7.31 (m, 2H), 5.57 (s, 2H), 3.12 (s, 1H). ¹³C NMR (500 MHz, DMSO): δ 146.3, 136.3, 132.7, 131.5, 129.3, 128.6, 128.3, 125.7, 122.6, 121.4. HR-MS ESI (+): calculated for C₁₇H₁₄N₃ [M + H]⁺: 260.1109; measured: 260.1025. Isolated yield: 94%</p>

1,4-bis(1-benzyl-1 <i>H</i> -1,2,3-triazol-4-yl)benzene (4t)	 <p>¹H NMR (500 MHz, CDCl₃): δ 8.68 (m, 2H), 7.91 (s, 4H), 7.37 (m, 10H), 5.65 (s, 4H). ¹³C NMR (500 MHz, CDCl₃): δ 150.2, 146.8, 136.4, 129.2, 128.6, 128.4, 126.1, 122.1, 53.5. HR-MS ESI (+): calculated for C₂₄H₂₀N₆Na [M + Na]⁺: 415.1642; measured: 415.1645. Isolated yield: > 95%</p>
1,4-bis(1-(3,5-dimethoxybenzyl)-1 <i>H</i> -1,2,3-triazol-4-yl)benzene (4u)	 <p>¹H NMR (500 MHz, CDCl₃): δ 7.84 (s, 2H), 7.70 (s, 2H), 6.44 (m, 4H), 5.49 (s, 4H), 3.77 (s, 12H). ¹³C NMR (500 MHz, CDCl₃): δ 161.2, 137.7, 136.5, 130.1, 125.9, 119.4, 106.0, 105.9, 100.3, 100.0, 55.3, 55.2, 54.2, 40.9. HR-MS ESI (+): calculated for C₂₈H₂₈N₆O₄Na [M + Na]⁺: 535.2064; measured: 535.2071. Isolated yield: 91%</p>
1-benzyl-4-(4-(1-(3,5-dimethoxybenzyl)-1 <i>H</i> -1,2,3-triazol-4-yl)phenyl)-1 <i>H</i> -1,2,3-triazole (4v)	 <p>¹H NMR (500 MHz, DMSO): δ 8.68 (d, <i>J</i> = 7.6 Hz, 2H), 7.92 (m, 6H), 7.37 (m, 5H), 6.53 (m, 2H), 6.47 (m, 1H), 5.65 (s, 2H), 5.56 (s, 2H), 3.74 (s, 6H). ¹³C NMR (500 MHz, DMSO): δ 160.8, 146.5, 138.0, 136.2, 130.1, 128.8, 127.9, 125.6, 121.6, 106.1, 99.6, 55.3, 53.0. HR-MS MALDI: calculated for C₂₆H₂₅N₆O₂ [M + H]⁺: 453.2027; measured: 453.2033. Isolated yield: >95%</p>
1-(2,6-difluorobenzyl)-1 <i>H</i> -1,2,3-triazole-4-carboxamide, <i>Rufinamide</i>	 <p>¹H NMR (500 MHz, DMSO-<i>d</i>₆) δ 8.54 (s, 1H), 7.84 (s, 1H), 7.53 (quintet, <i>J</i> = 31.3Hz, 2H), 7.19 (t, <i>J</i> = 14.4 Hz, 2H), 5.72 (s, 2H). ¹³C NMR (500 MHz, DMSO-<i>d</i>₆) δ 161.11 (3C), 142.66, 131.68, 126.63, 115.00, 111.92, 111.72, 110.89, 41.03. HR-MS ESI (+): calculated for C₁₀H₈N₄F₂Na [M + Na]⁺: 261.056; measured: 261.0555. Isolated yield: 88%</p>

S8. Scanning electron microscopy (SEM) micrographs

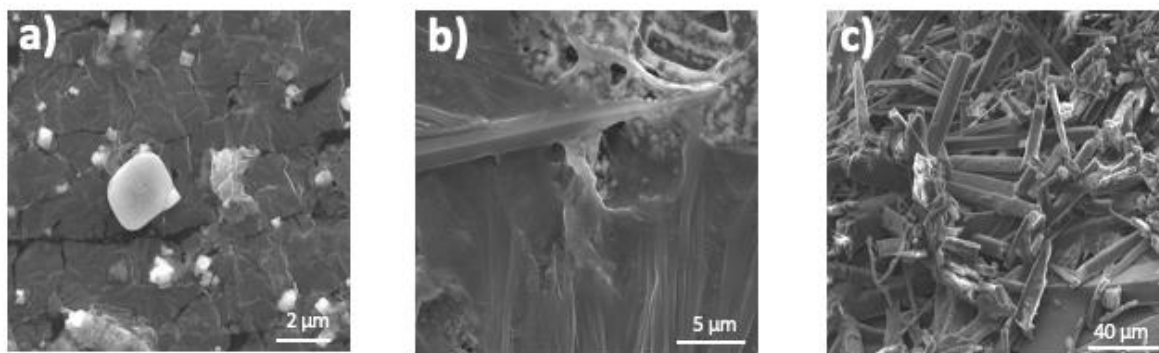


Figure S8.1 Selected micrographs of the crude reaction mixture of **1a** (liquid), **2a** and NaN₃ following RAM at 90 g for: (a) 20 minutes, (b) 40 minutes, and (c) 60 minutes. Scale bar shown in bottom right of each micrograph.

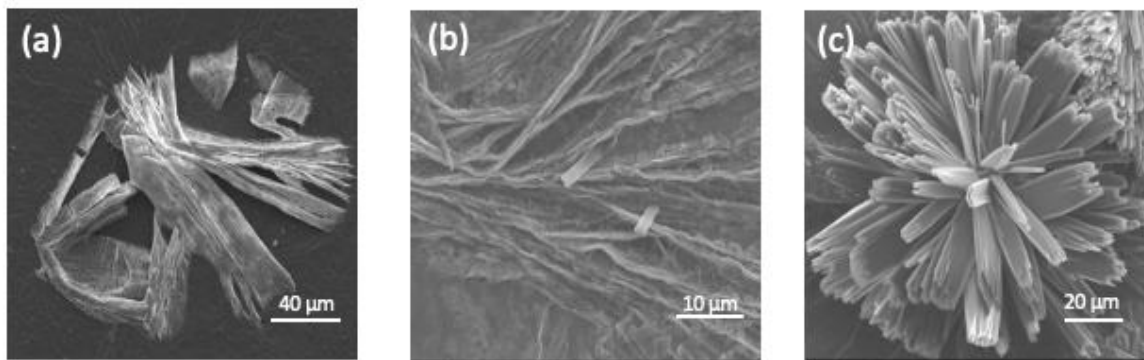


Figure S8.2 Selected micrographs of the crude reaction mixture of **1e** (solid), **2a** and NaN_3 following RAM at 90 g for: (a) 20 minutes, (b) 40 minutes, and (c) 60 minutes. Scale bar shown in bottom right of each micrograph.

S9. X-ray photoelectron spectroscopy (XPS) spectra

Analysis was done based on the positions of the $\text{Cu}2p_{3/2}$ signals, and the satellite features of the $\text{Cu}2p$ signal. For copper metal the $\text{Cu}2p_{3/2}$ signal is expected at 933 eV, for Cu_2O the $\text{Cu}2p_{3/2}$ signal is expected at 933 eV and a weak $\text{Cu}2p$ satellite at ~ 945 eV, and for $\text{Cu}^{\text{II}}\text{O}$ the $\text{Cu}2p_{3/2}$ signal is expected at 933.5 eV with a strong $\text{Cu}2p$ satellite at ~ 943 eV.^[1]

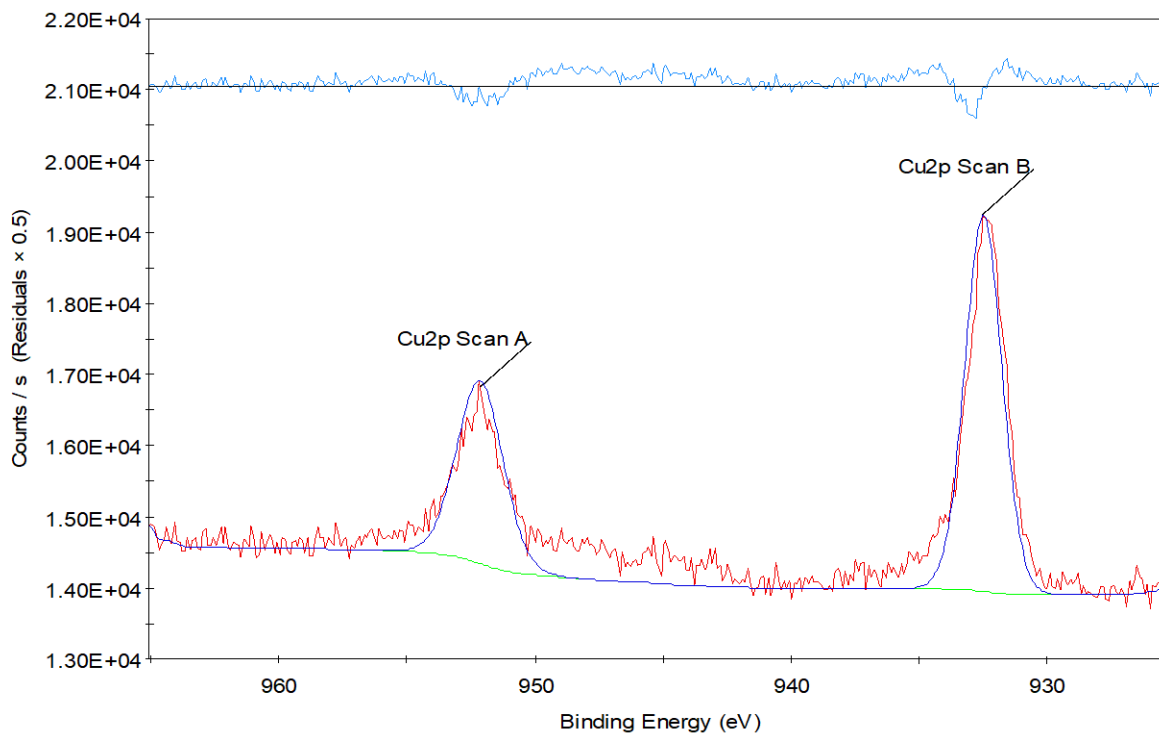


Figure S9.1 The XPS spectrum of fresh, untreated, commercial copper wire, showing characteristic spectrum of copper metal. Spectrum shown in red, fitted curved and residual in blue, and corrected baseline in green.

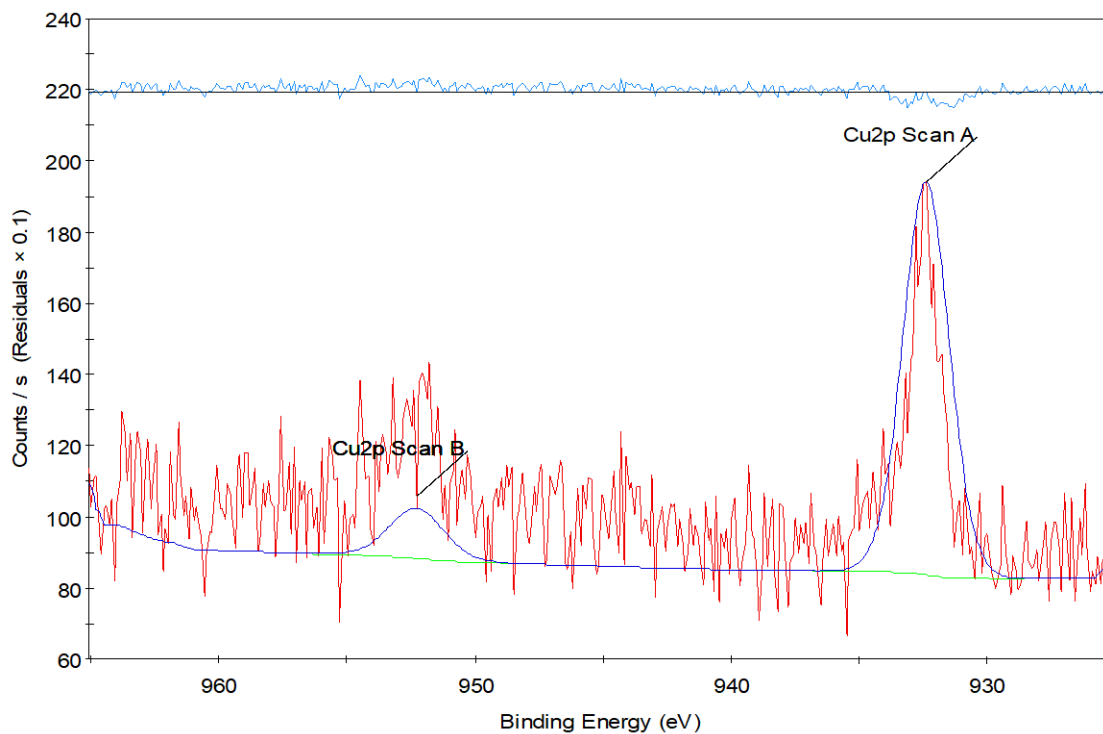


Figure S9.2 The XPS spectrum of copper wire following soaking of a copper coil in benzyl bromide (**1a**) for 24 hours, with characteristic spectrum for copper metal. Spectrum shown in red, fitted curved and residual in blue, and corrected baseline in green.

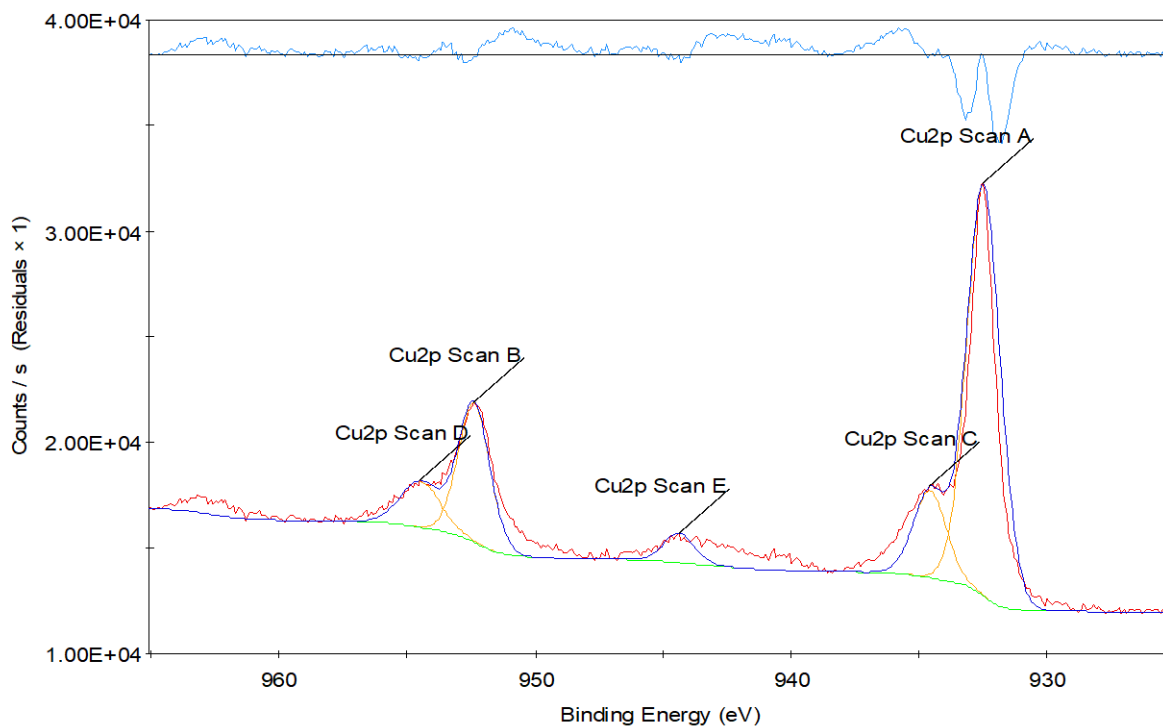


Figure S9.3 The XPS spectrum of copper wire following soaking of a copper coil in phenylacetylene (**1b**, 2 mL) for 24 hours, demonstrating characteristic spectrum for copper metal (scan A and B), copper (I) (A, B and E), and copper (II) (D, E and C). Spectrum shown in red, fitted curved and residual in blue and corrected baseline in green.

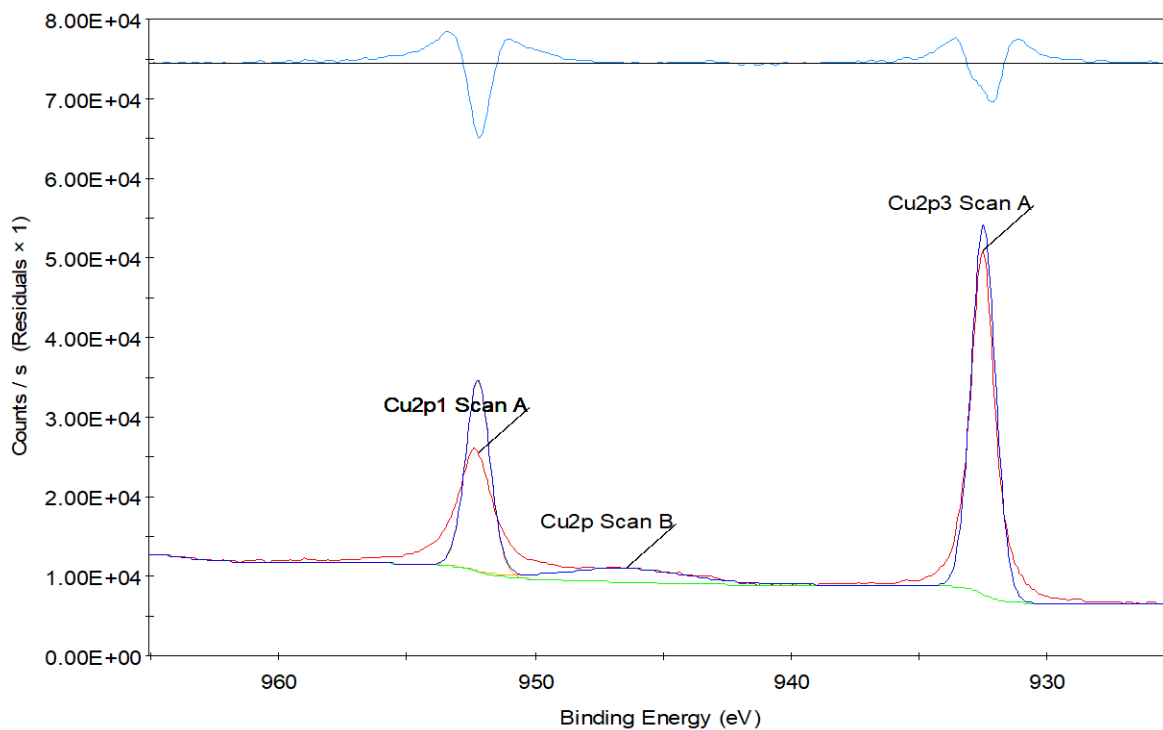


Figure S9.4 The XPS spectrum of copper wire following the copper coil-catalyzed reaction of **1a**, **2a**, NaN_3 in the presence of DMSO ($\eta = 0.5 \mu\text{L}/\text{mg}$) as a liquid additive, showing characteristic spectrum for Cu(I) species. Spectrum shown in red, fitted curved and residual in blue and corrected baseline in green.

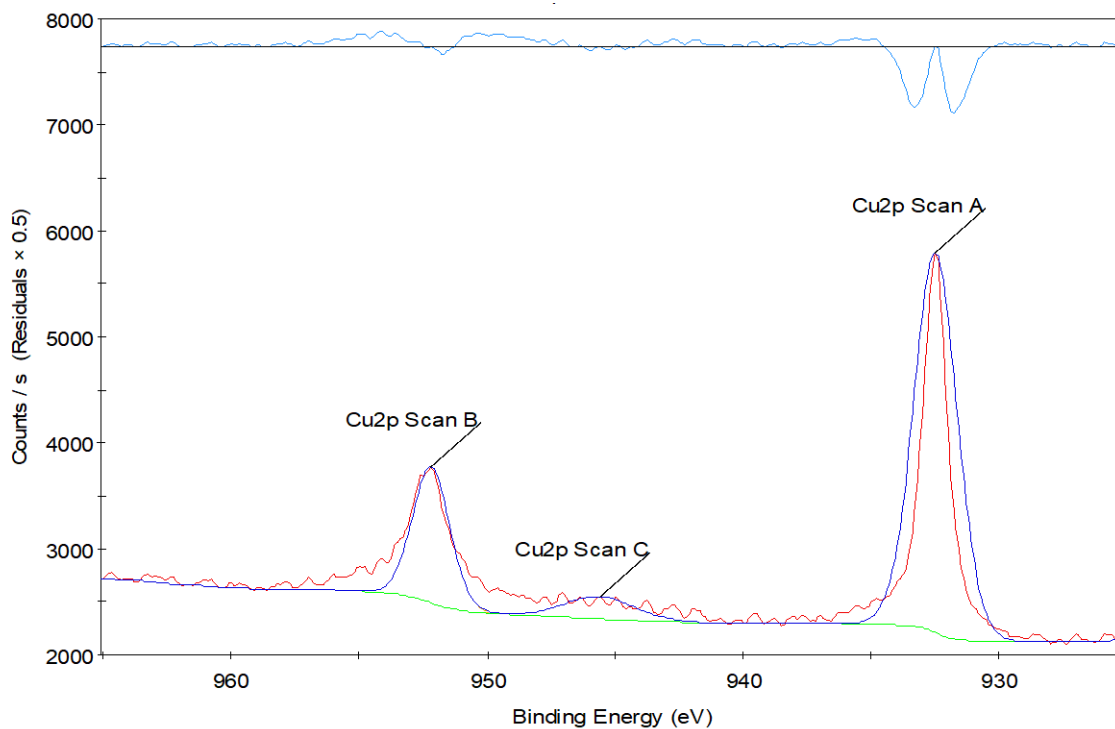


Figure S9.5 The XPS spectrum of copper wire following priming reaction with **2a** (2mmol), SiO_2 (300 mg) and DMSO ($\eta = 0.5 \mu\text{L}/\text{mg}$), showing spectrum for Cu(I). Spectrum shown in red, fitted curved and residuals in blue, and corrected baseline in green.

S10. ^1H -, ^{13}C -NMR spectra

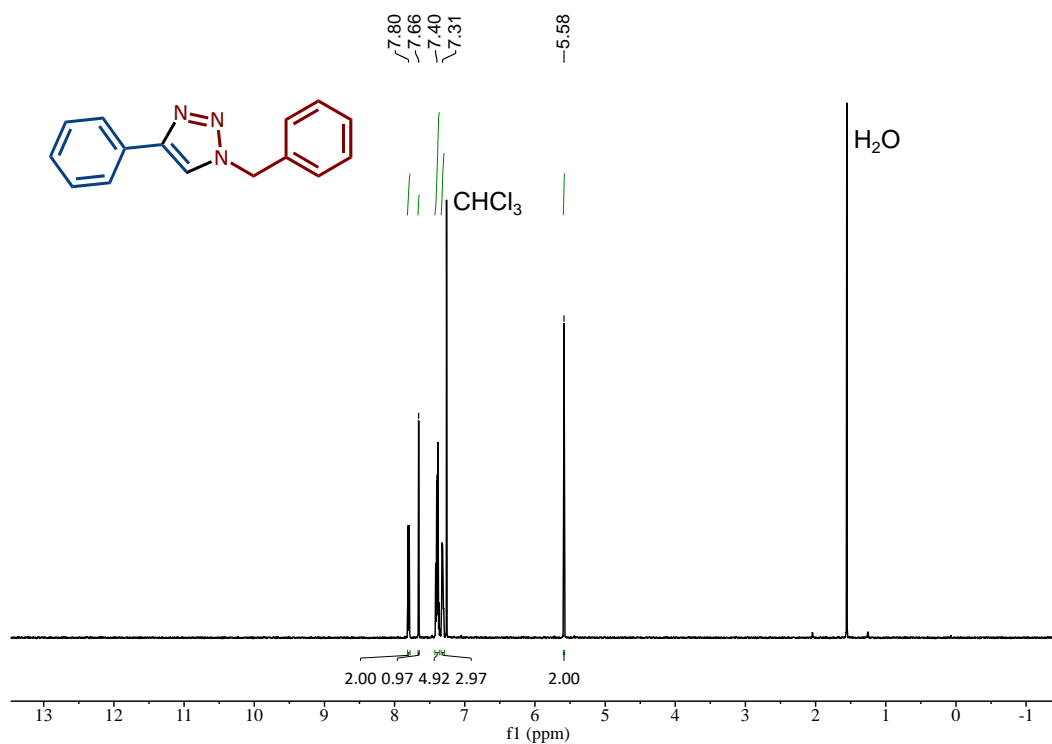


Figure S10.1 ^1H -NMR spectrum of **4a** made by RAM direct mechanocatalysis, recorded in CDCl_3 .

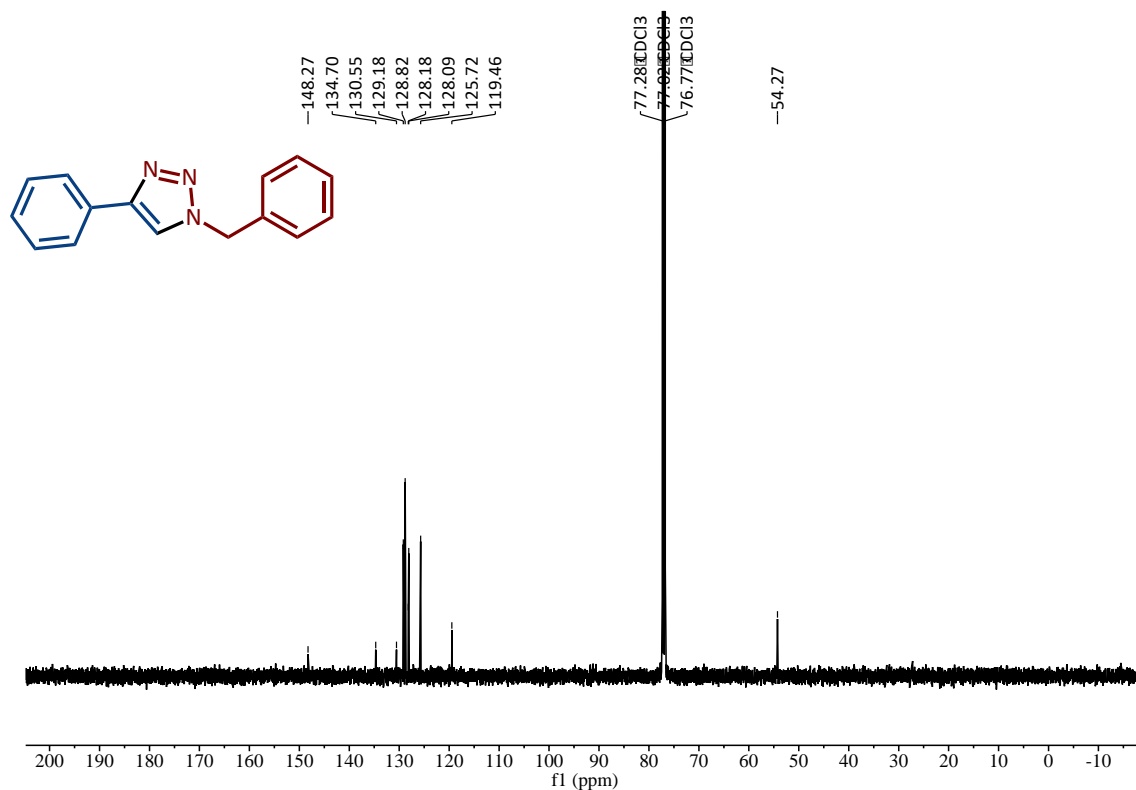


Figure S10.2 ^{13}C -NMR spectrum of **4a** made by RAM direct mechanocatalysis, recorded in CDCl_3 .

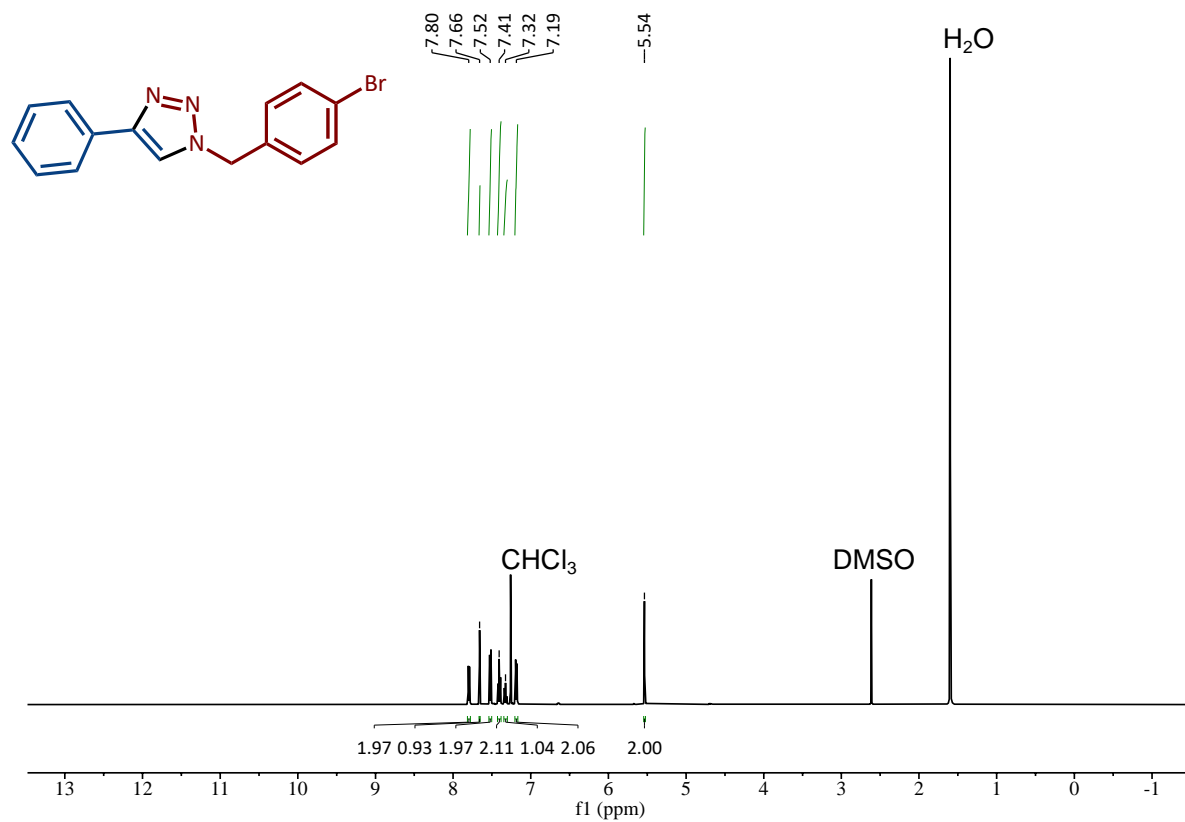


Figure S10.3 $^1\text{H-NMR}$ spectrum of **4b** made by RAM direct mechanocatalysis, recorded in CDCl_3 .

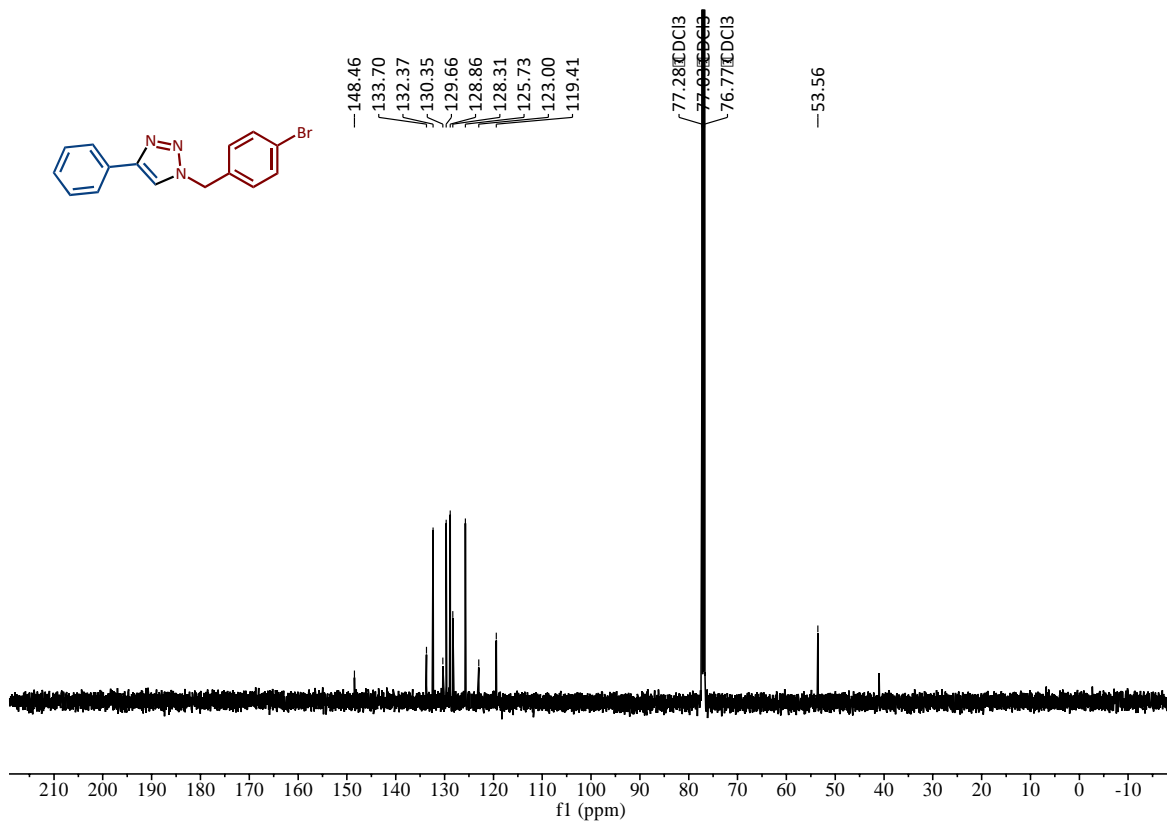


Figure S10.4 ¹³C-NMR spectrum of **4b** made by RAM direct mechanocatalysis, recorded in CDCl₃.

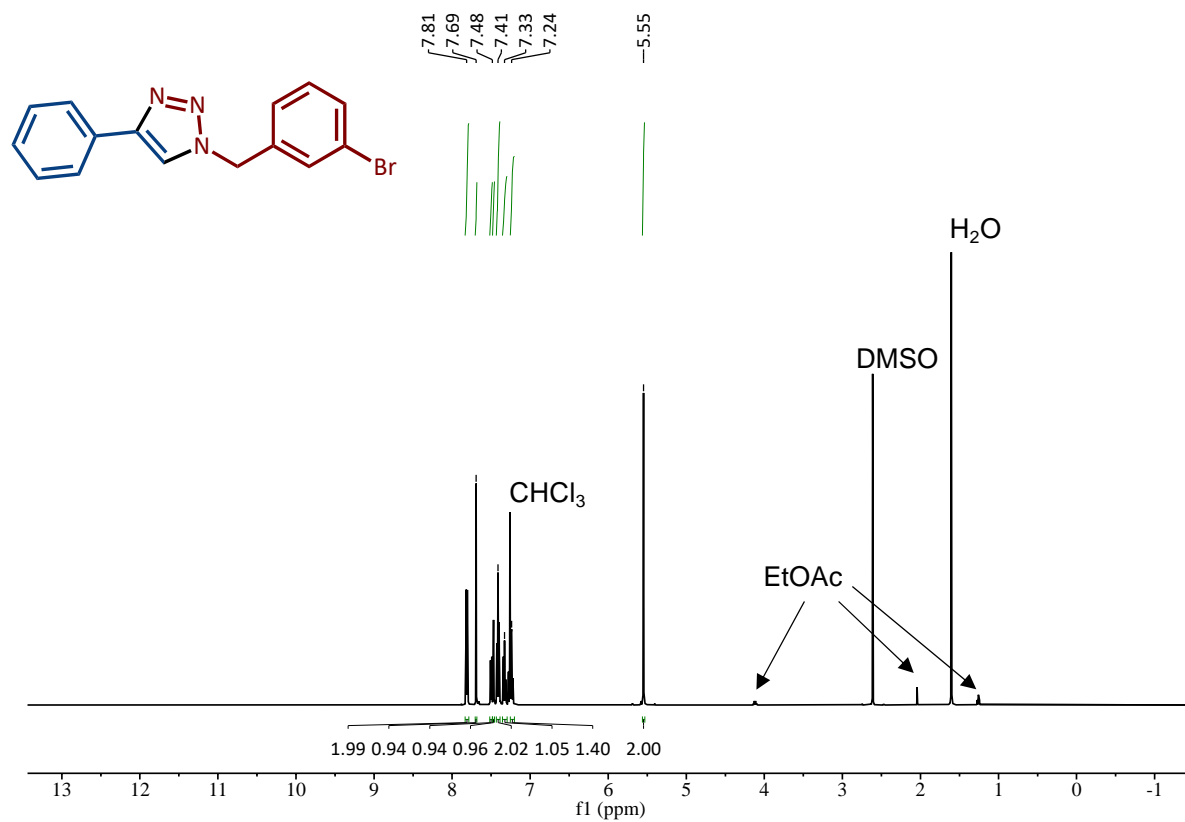


Figure S10.5 ¹H-NMR spectrum of 4c made by RAM direct mechanocatalysis, recorded in CDCl₃.

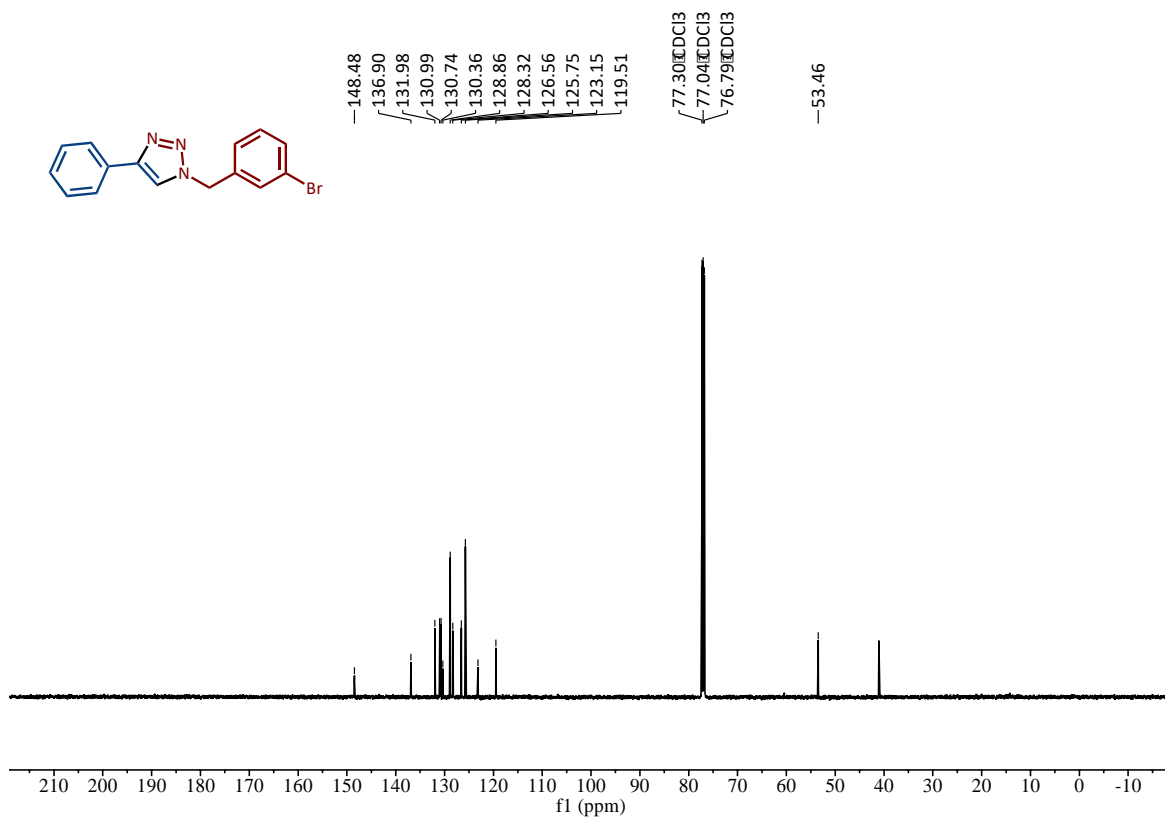


Figure S10.6 ¹³C-NMR spectrum of **4c** made by RAM direct mechanocatalysis, recorded in CDCl₃.

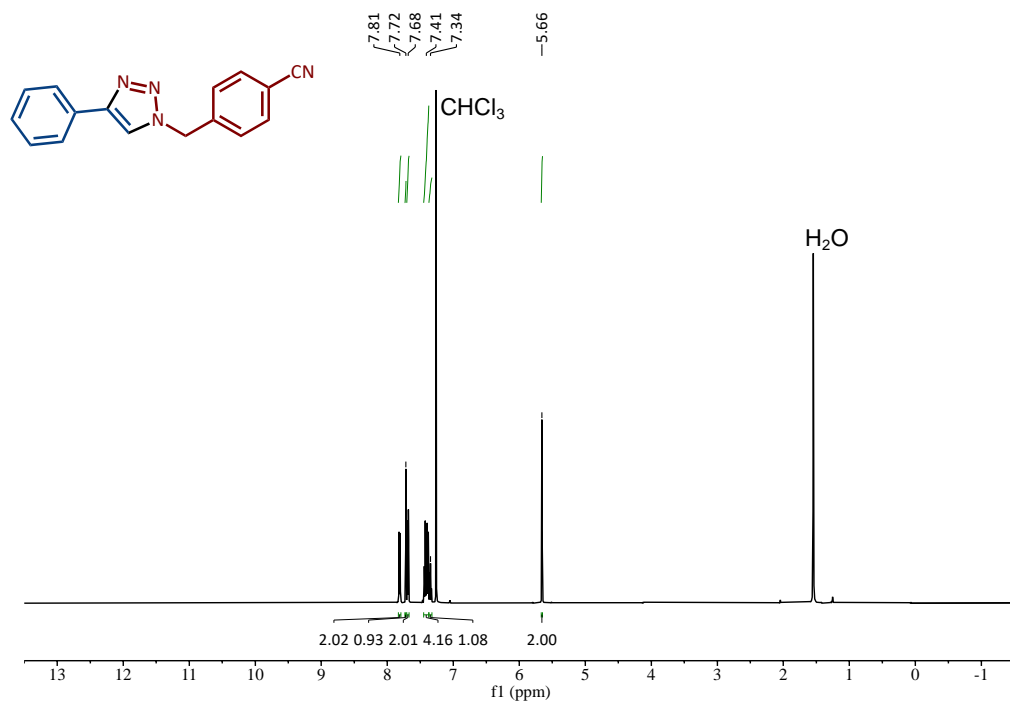


Figure S10.7 ¹H-NMR spectrum of **4d** made by RAM direct mechanocatalysis, recorded in CDCl₃.

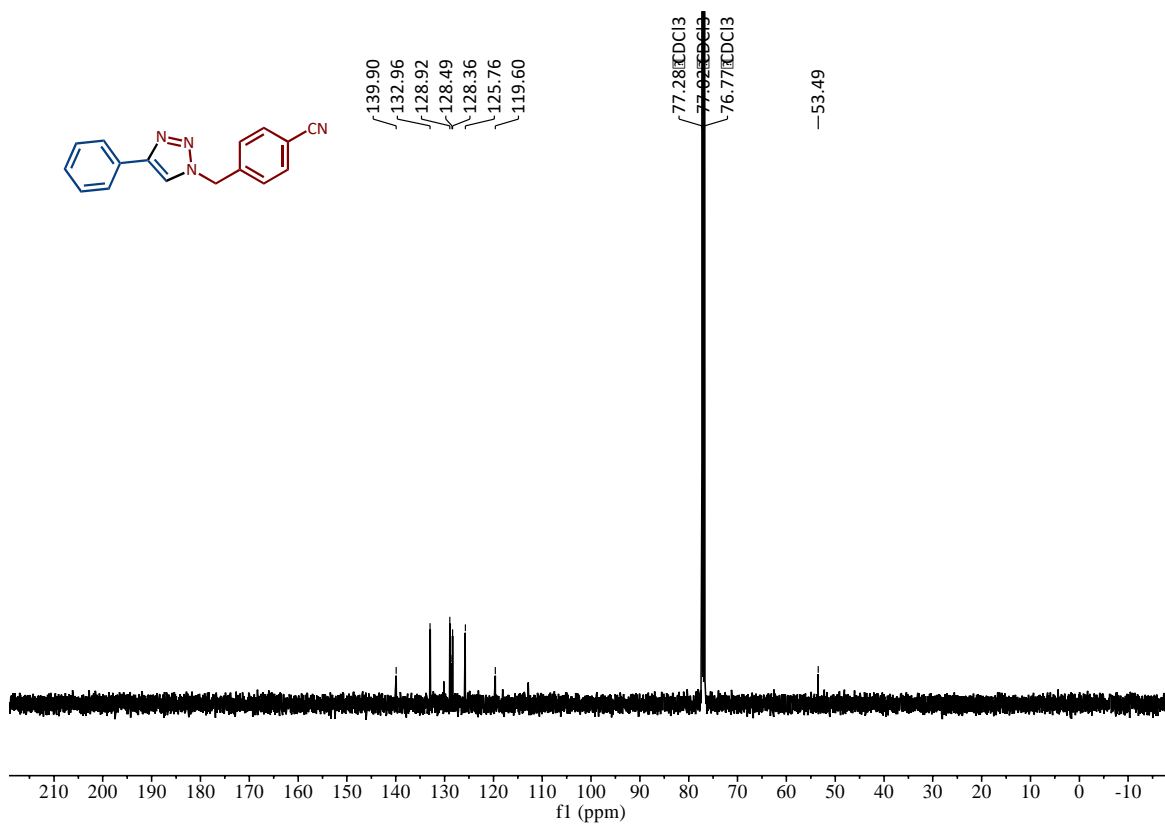


Figure S10.8 ¹³C-NMR spectrum of **4d** made by RAM direct mechanocatalysis, recorded in CDCl₃.

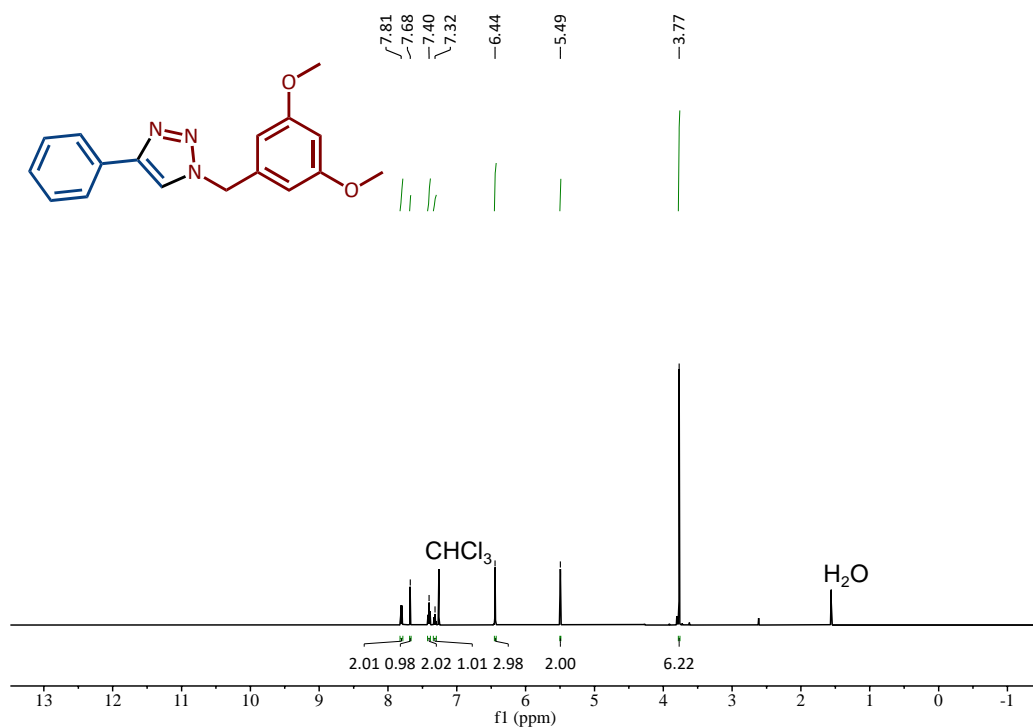


Figure S10.9 ¹H-NMR spectrum of 4e made by RAM direct mechanocatalysis, recorded in CDCl₃.

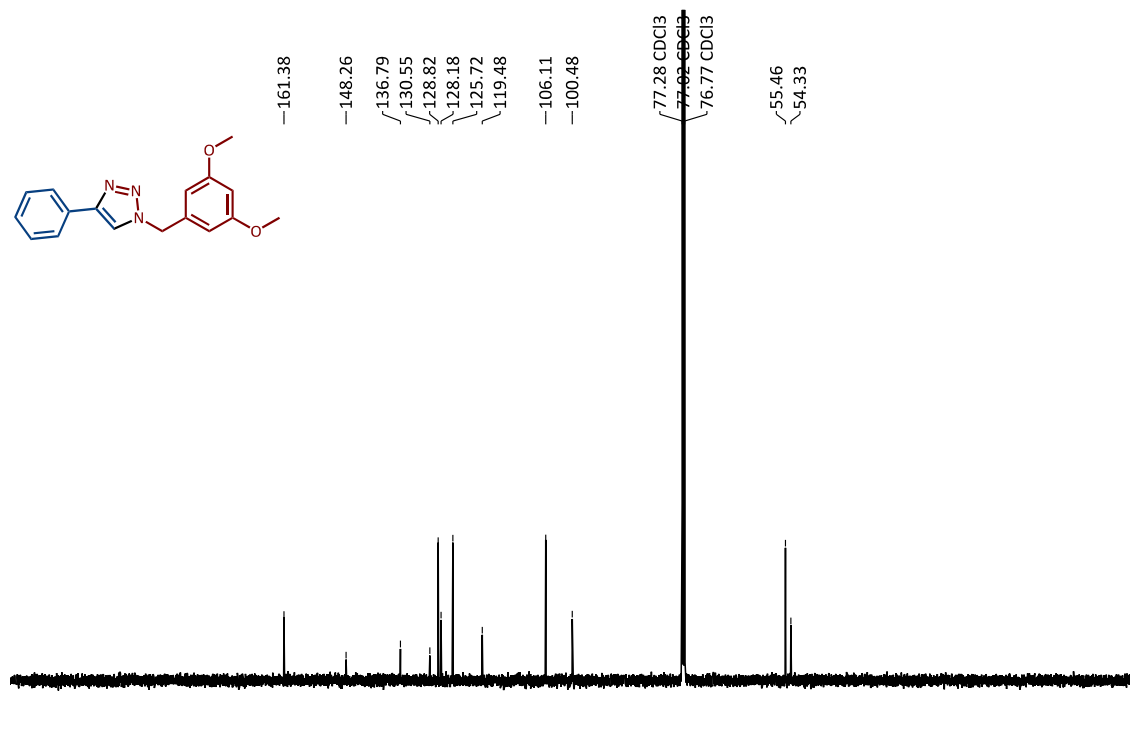


Figure S10.10 ¹³C-NMR spectrum of 4e made by RAM direct mechanocatalysis, recorded in CDCl₃.

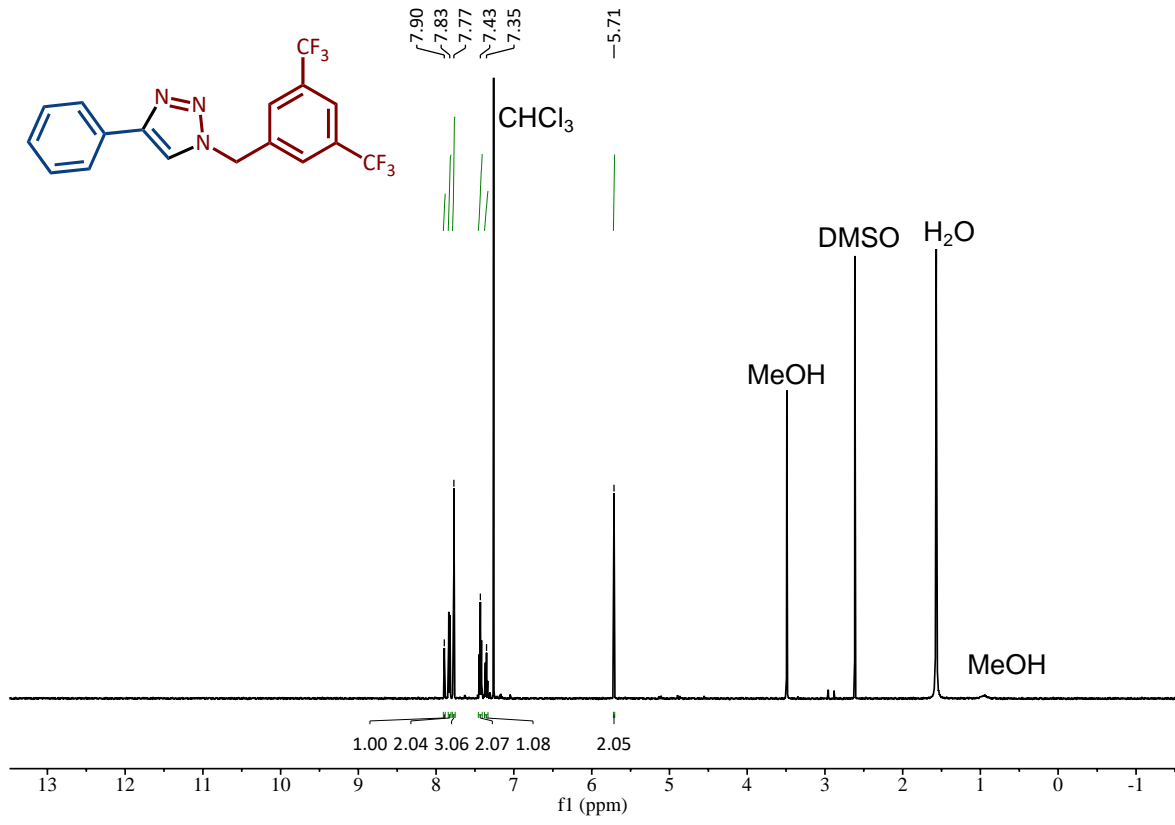


Figure S10.11 ¹H-NMR spectrum of **4f** made by RAM direct mechanocatalysis, recorded in CDCl₃.

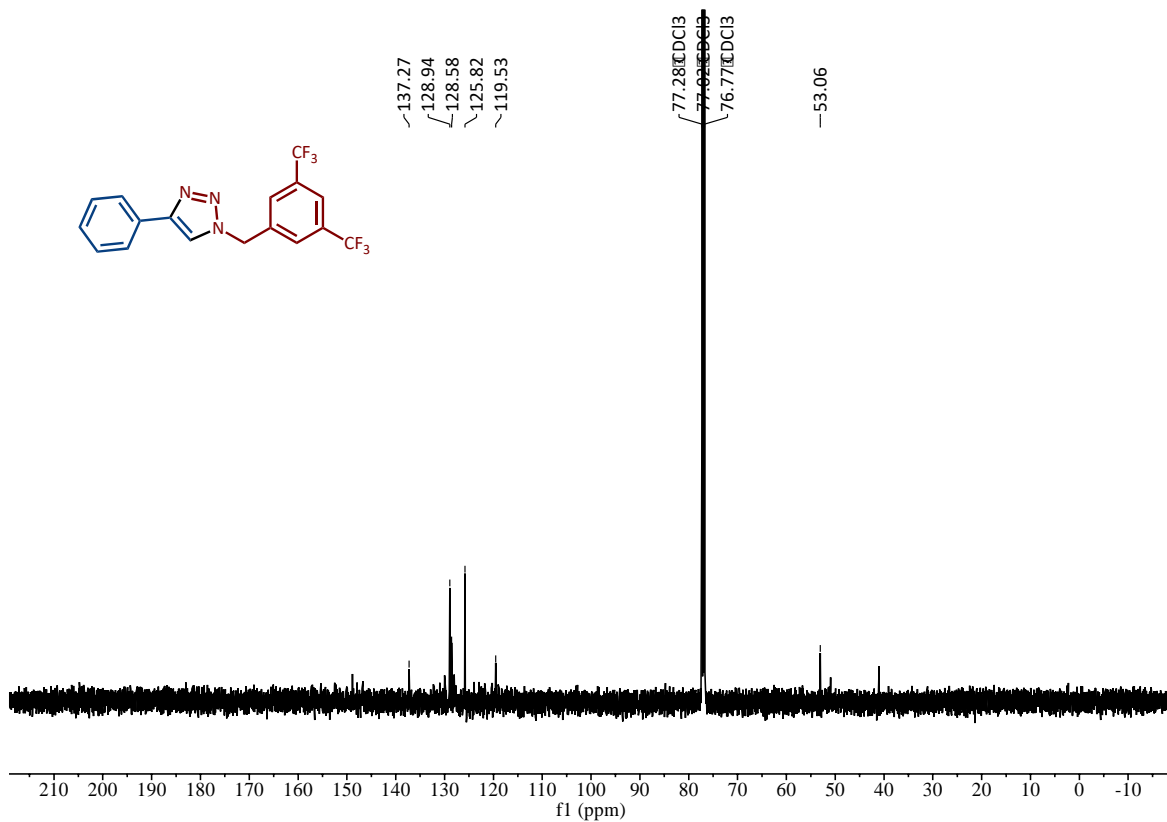


Figure S10.12 ^{13}C -NMR spectrum of **4f** made by RAM direct mechanocatalysis, recorded in CDCl_3 .

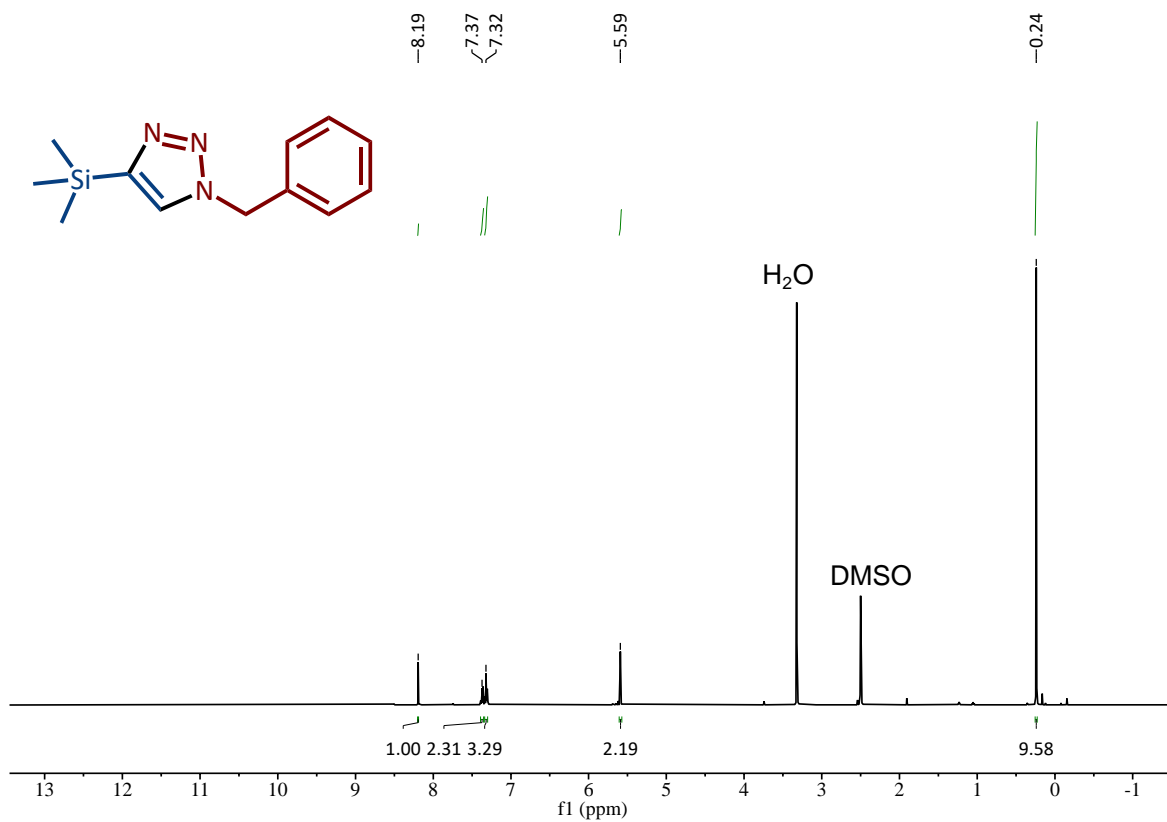


Figure S10.13 $^1\text{H-NMR}$ spectrum of **4g** made by RAM direct mechanocatalysis, recorded in $\text{d}_6\text{-DMSO}$.

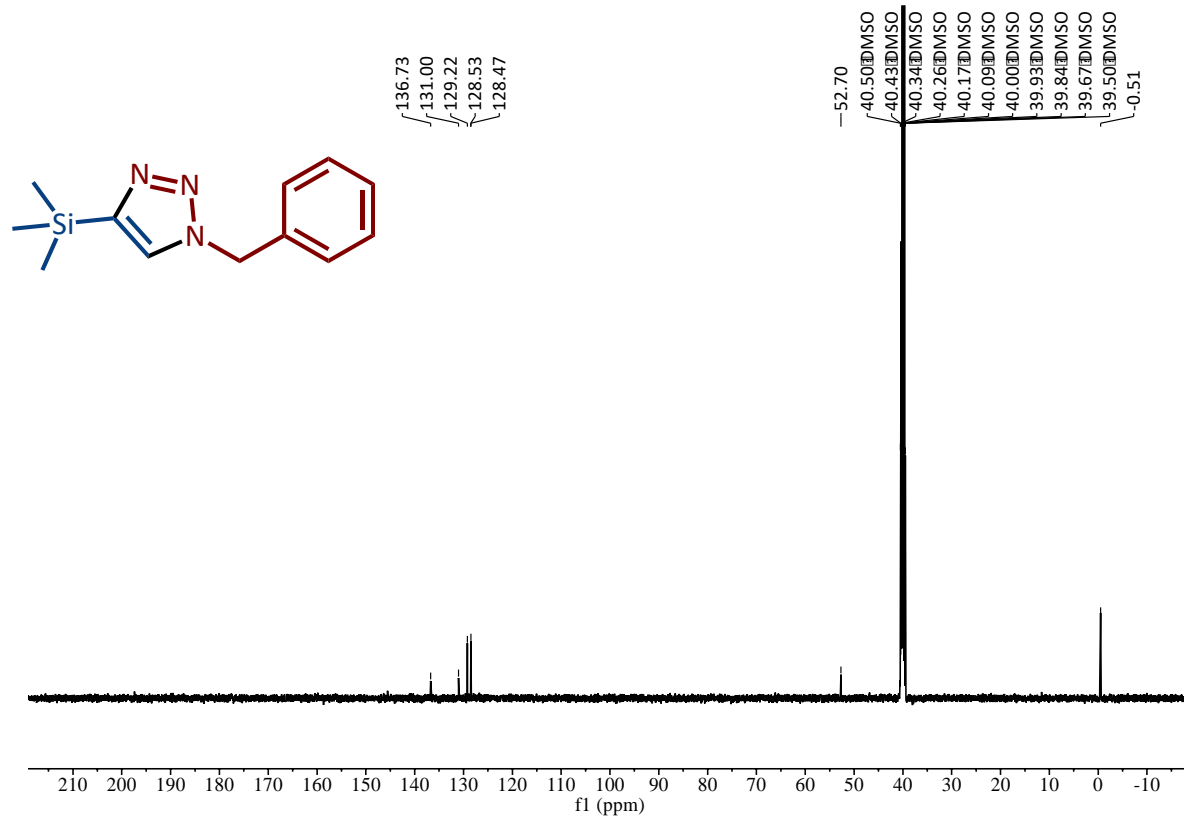


Figure S10.14 $^{13}\text{C-NMR}$ spectrum of **4g** made by RAM direct mechanocatalysis, recorded in CDCl_3 .

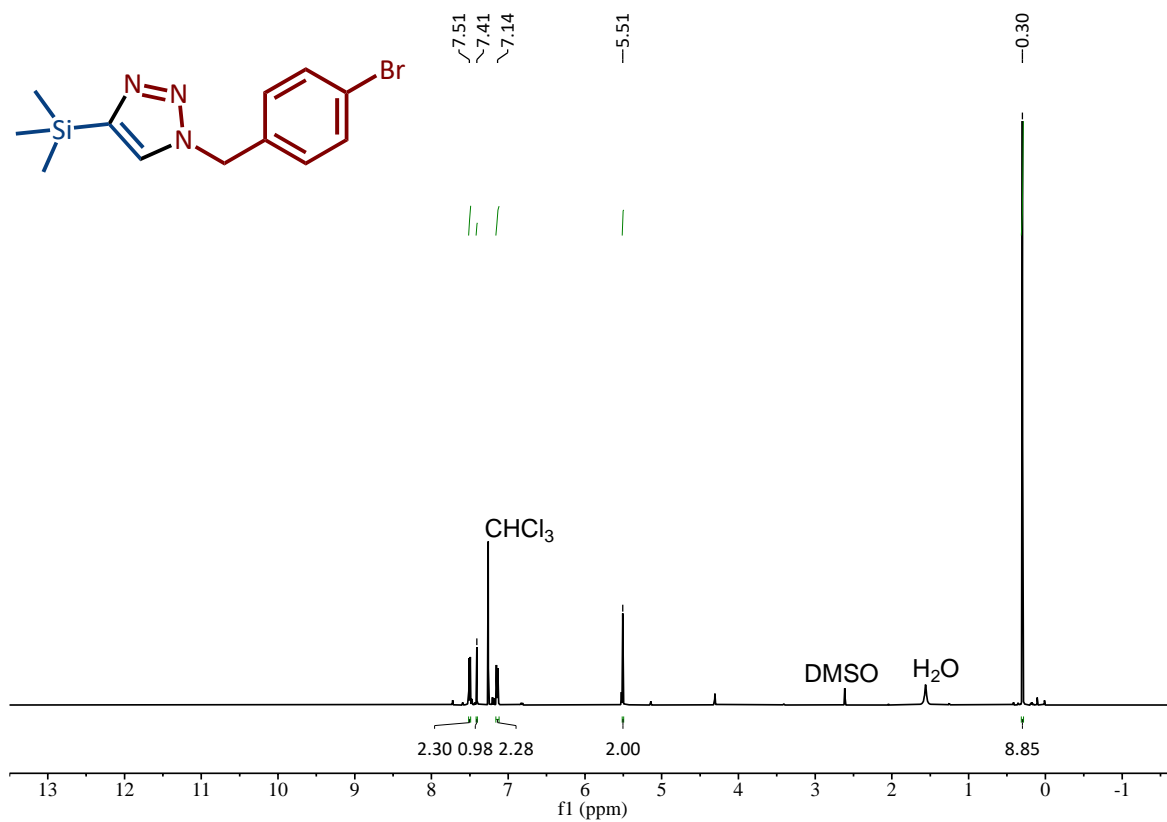


Figure S10.15 ¹H-NMR spectrum of **4h** made by RAM direct mechanocatalysis, recorded in CDCl₃.

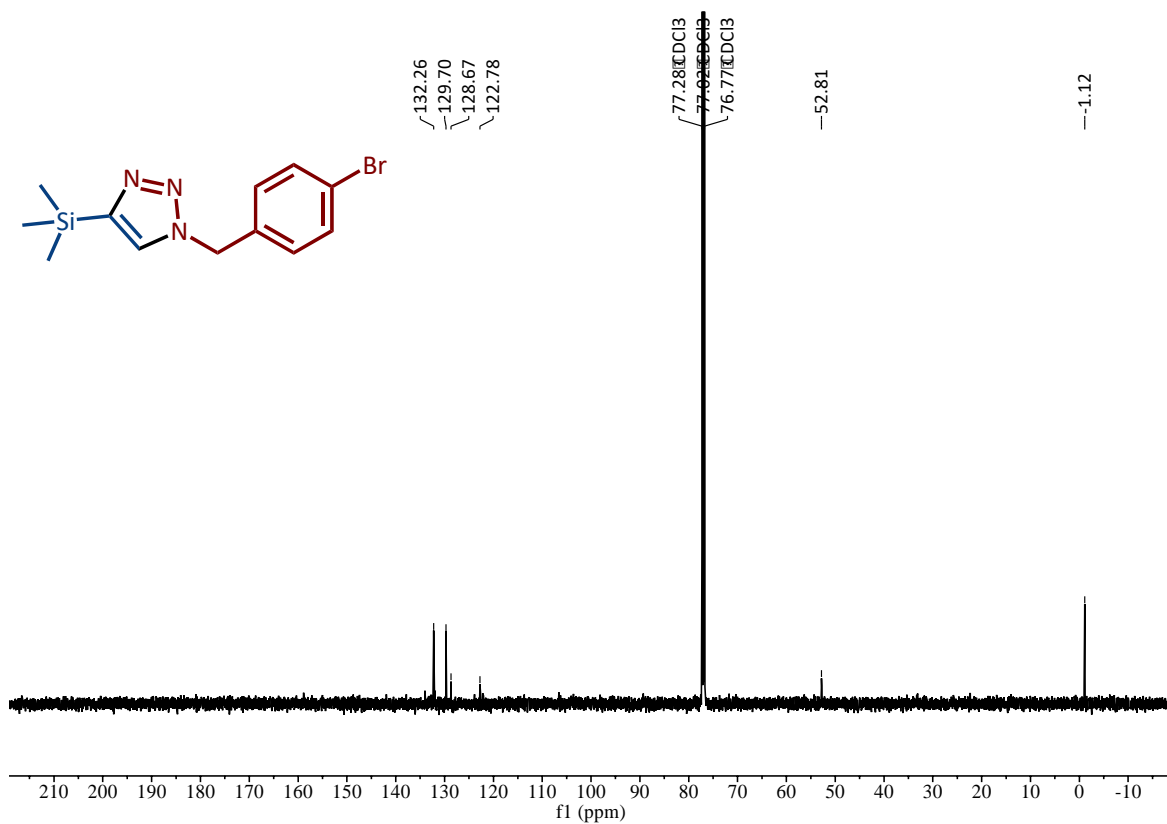


Figure S10.16 ^{13}C -NMR spectrum of 4h made by RAM direct mechanocatalysis, recorded in CDCl_3 .

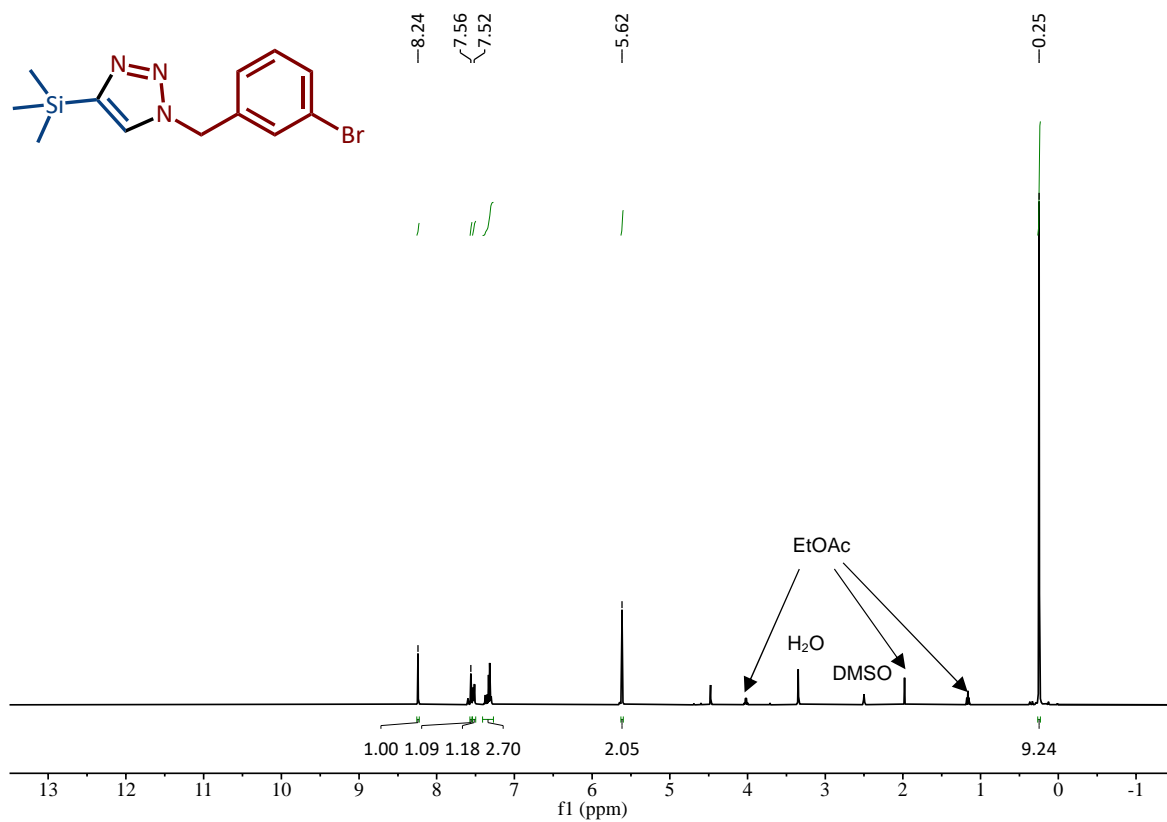


Figure S10.17 ¹H-NMR spectrum of **4i** made by RAM direct mechanocatalysis, recorded in d₆-DMSO.

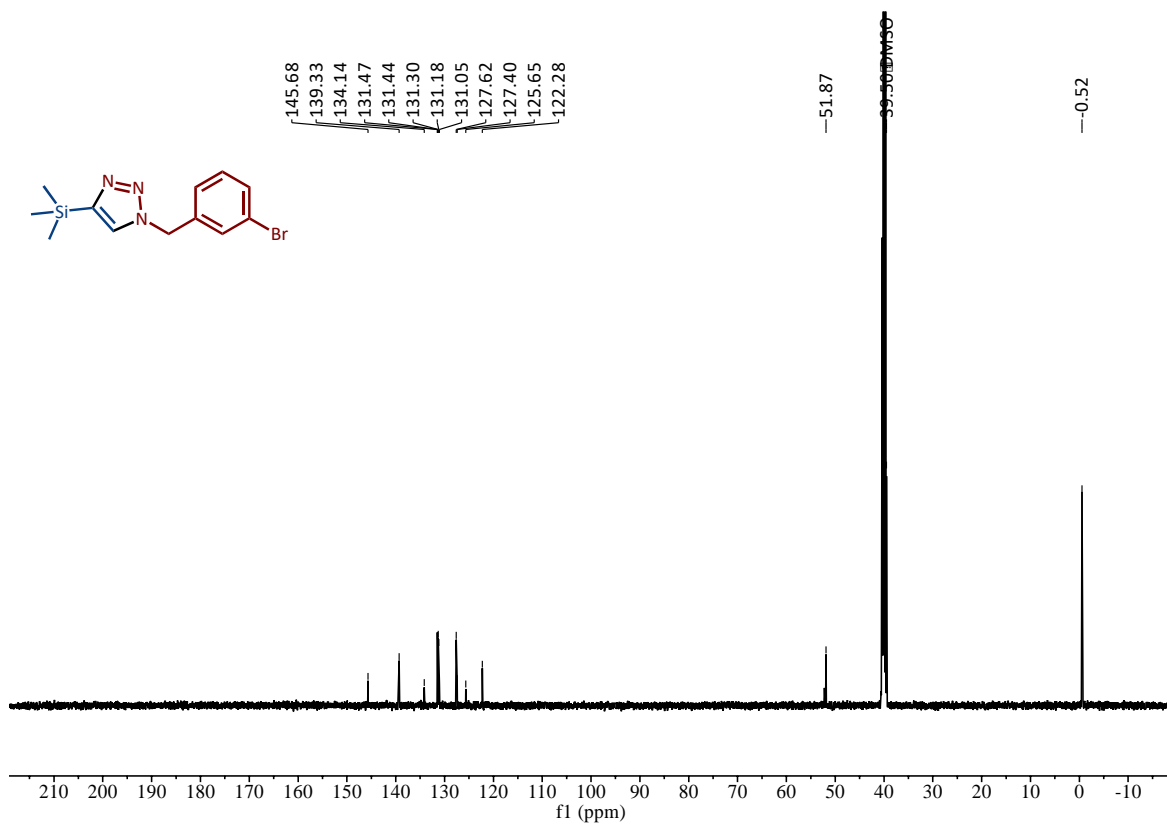


Figure S10.18 ¹³C-NMR spectrum of **4i** made by RAM direct mechanocatalysis, recorded in CDCl₃.

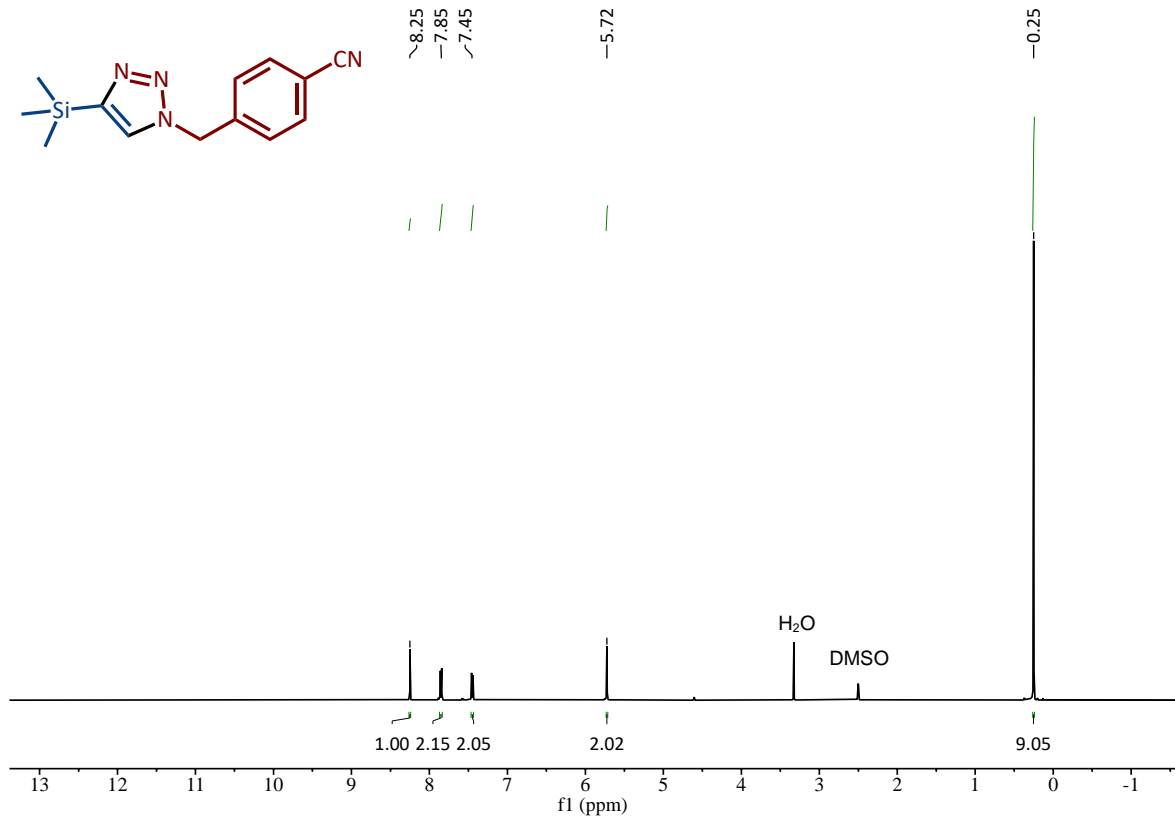


Figure S10.19 ¹H-NMR spectrum of **4j** made by RAM direct mechanocatalysis, recorded in d₆-DMSO.

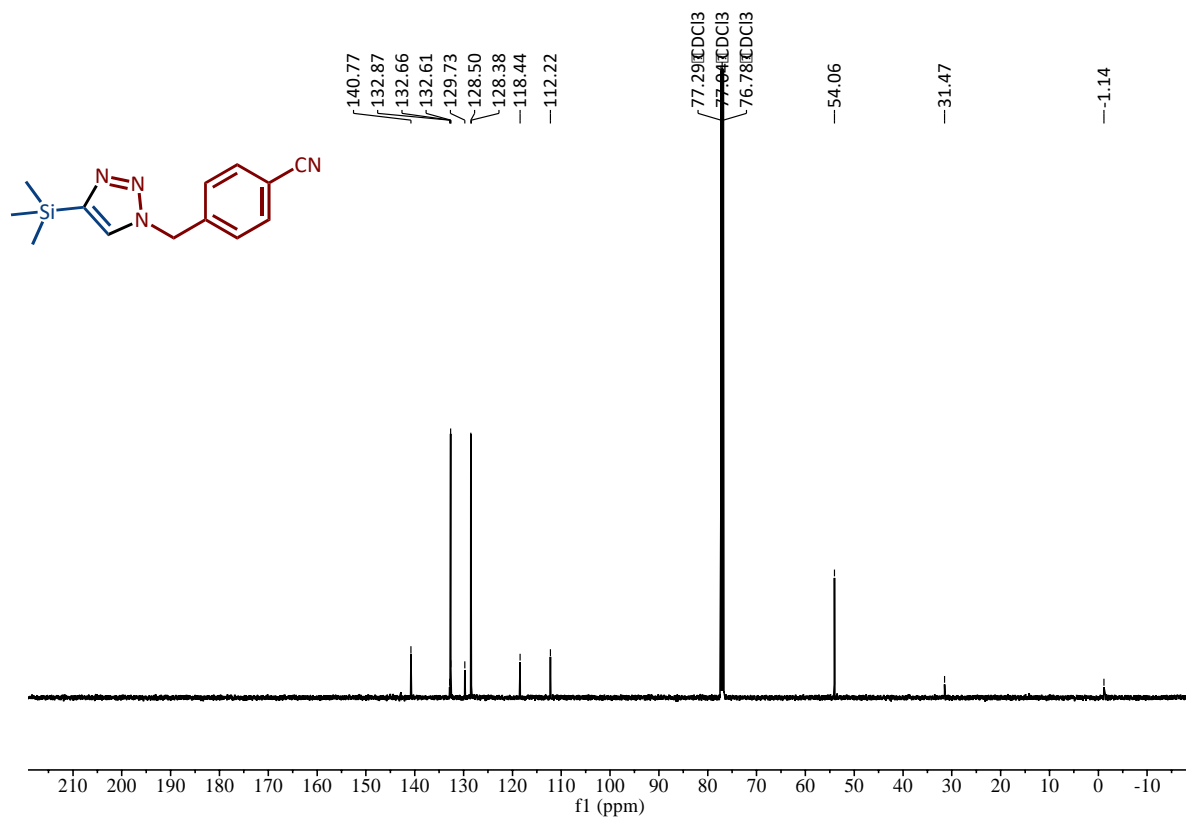


Figure S10.20 ¹³C-NMR spectrum of **4j** made by RAM direct mechanocatalysis, recorded in CDCl₃.

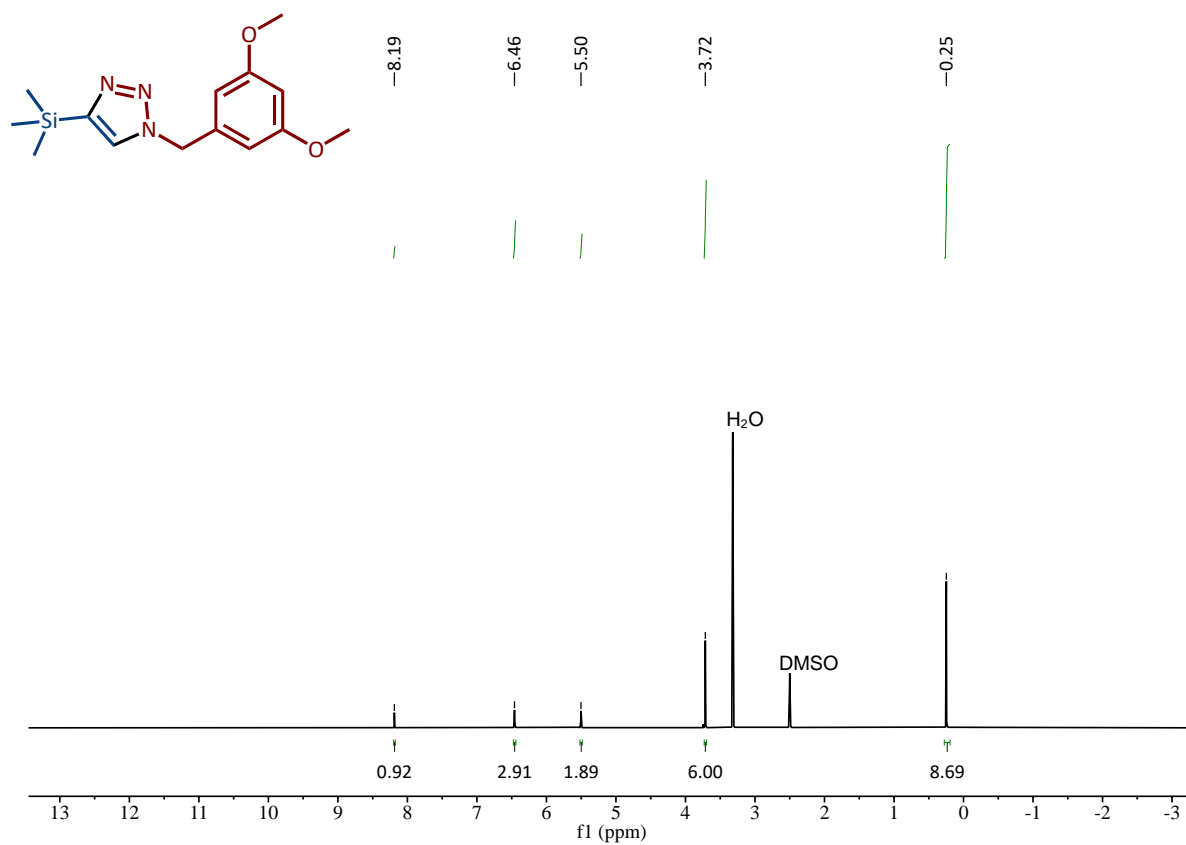


Figure S10.21 ¹H-NMR spectrum of **4k** made by RAM direct mechanocatalysis, recorded in d₆-DMSO.

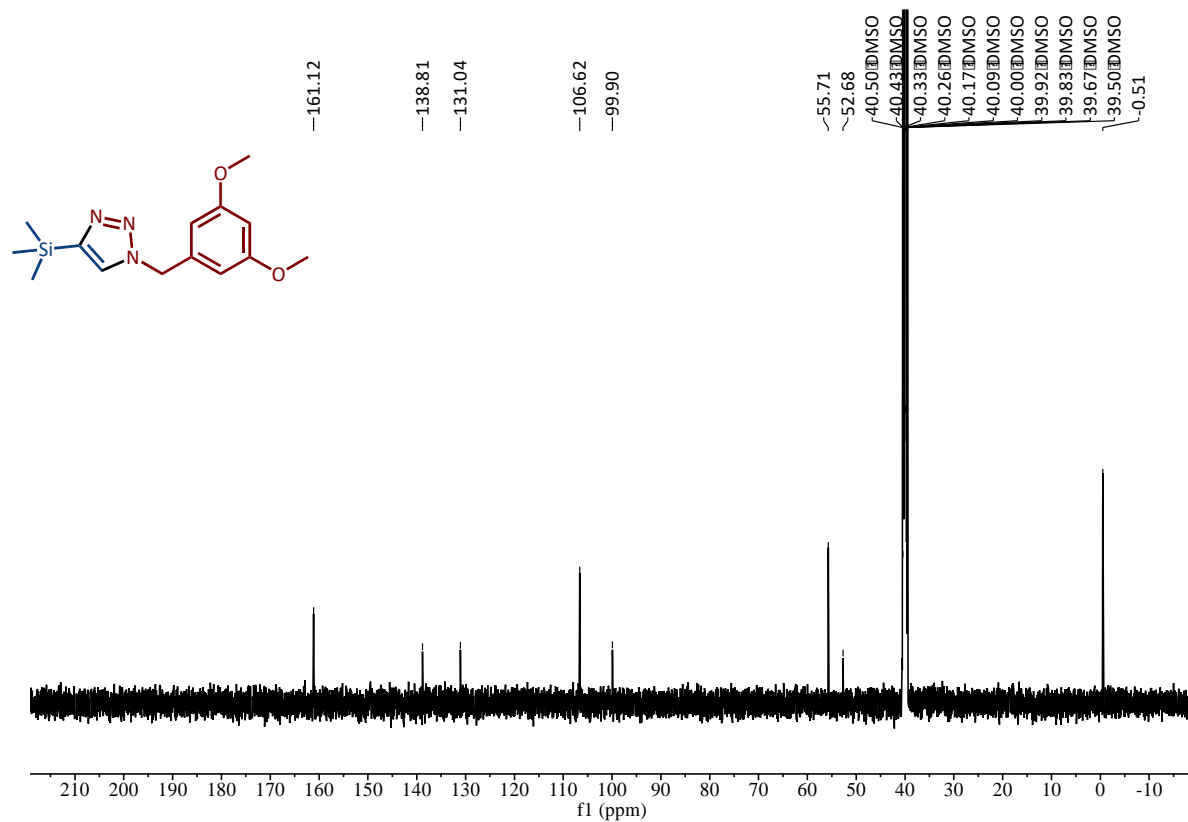


Figure S10.22 ¹³C-NMR spectrum of 4k made by RAM direct mechanocatalysis, recorded in d6-DMSO.

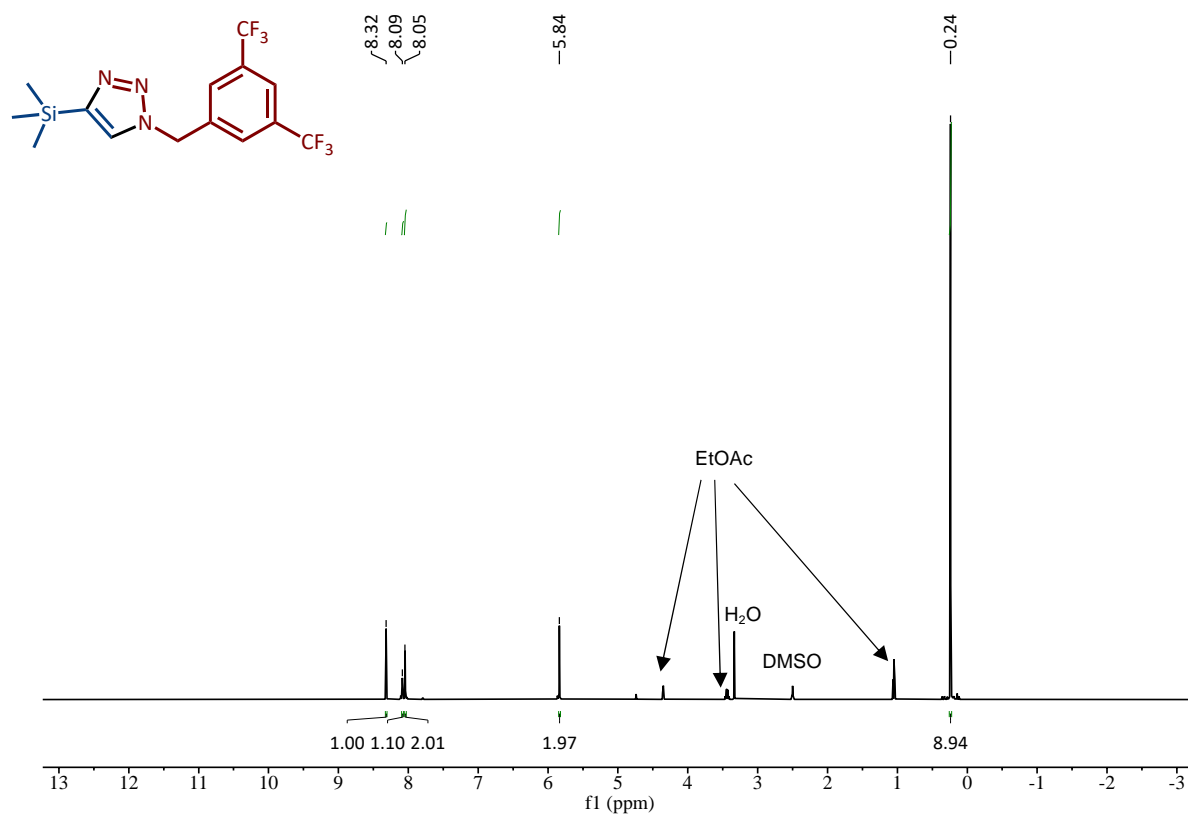


Figure S10.23 ¹H-NMR spectrum of **4I** made by RAM direct mechanocatalysis, recorded in d₆-DMSO.

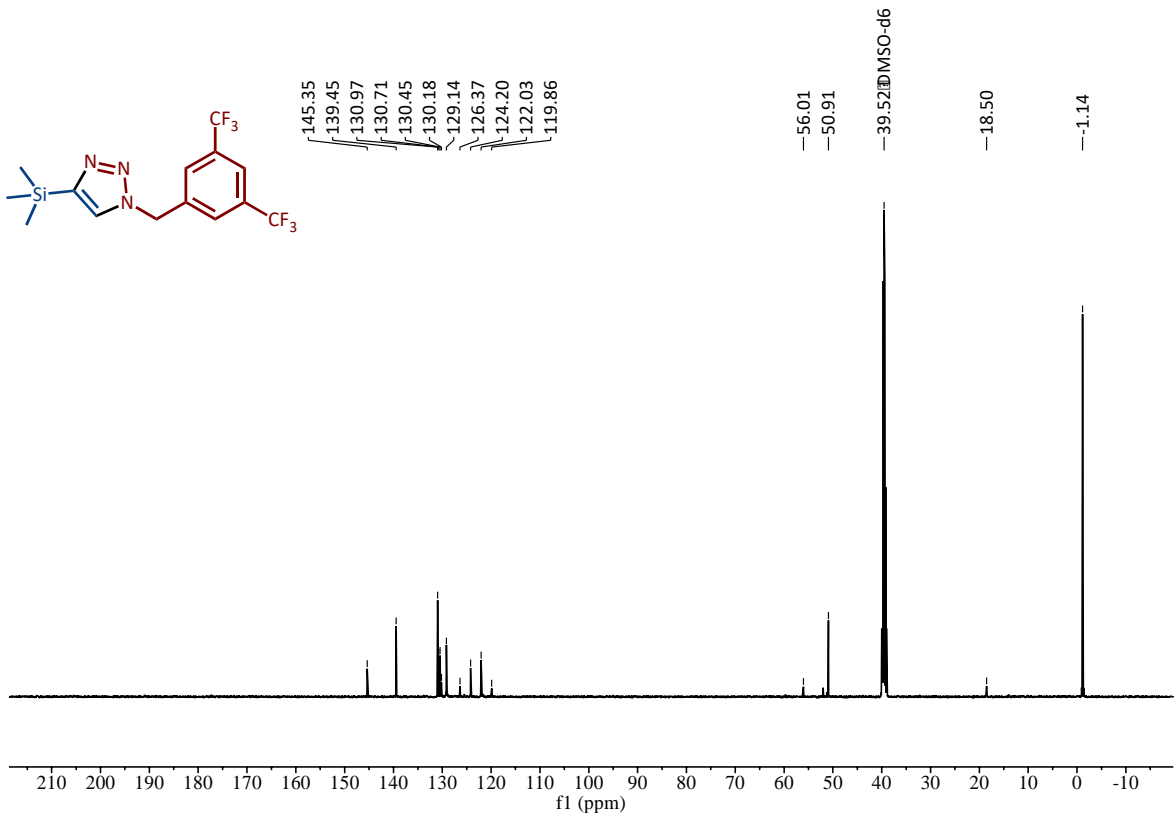


Figure S10.24 ¹³C-NMR spectrum of **4I** made by RAM direct mechanocatalysis, recorded in d6-DMSO.

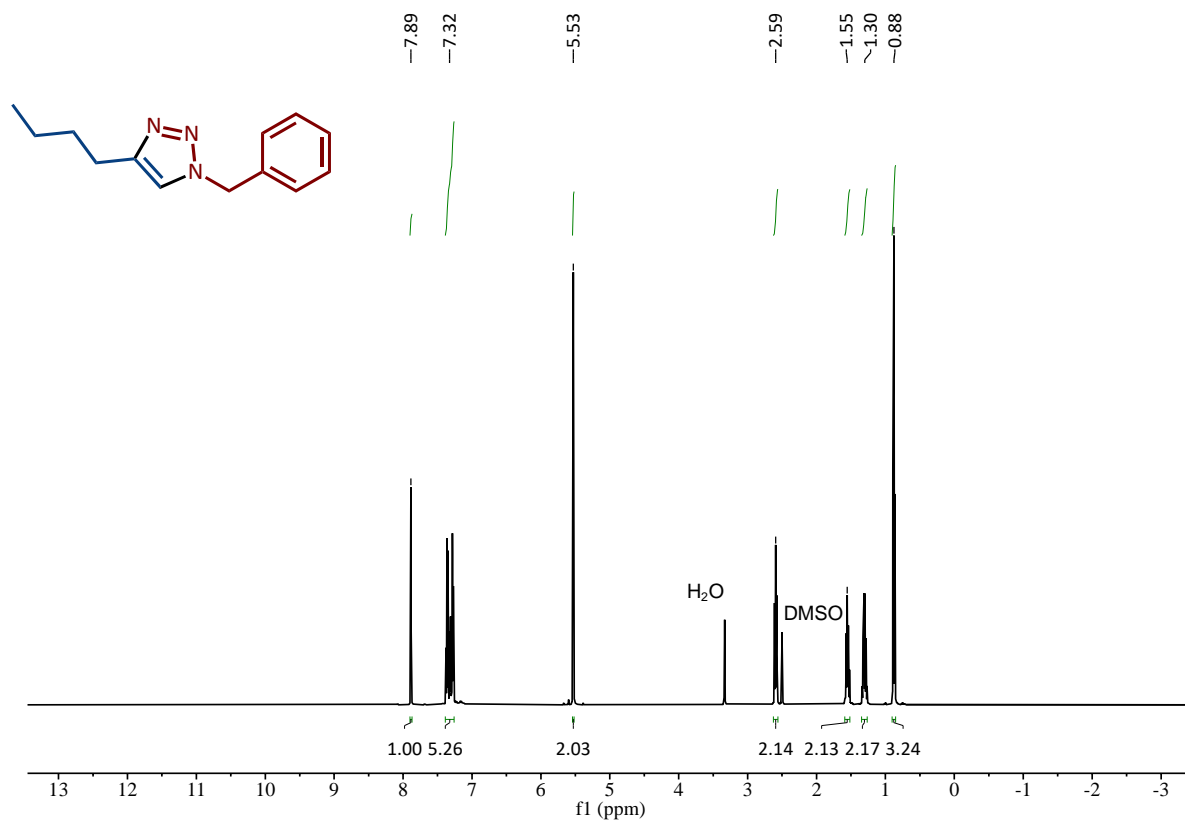


Figure S10.25 ¹H-NMR spectrum of **4m** made by RAM direct mechanocatalysis, recorded in d₆-DMSO.

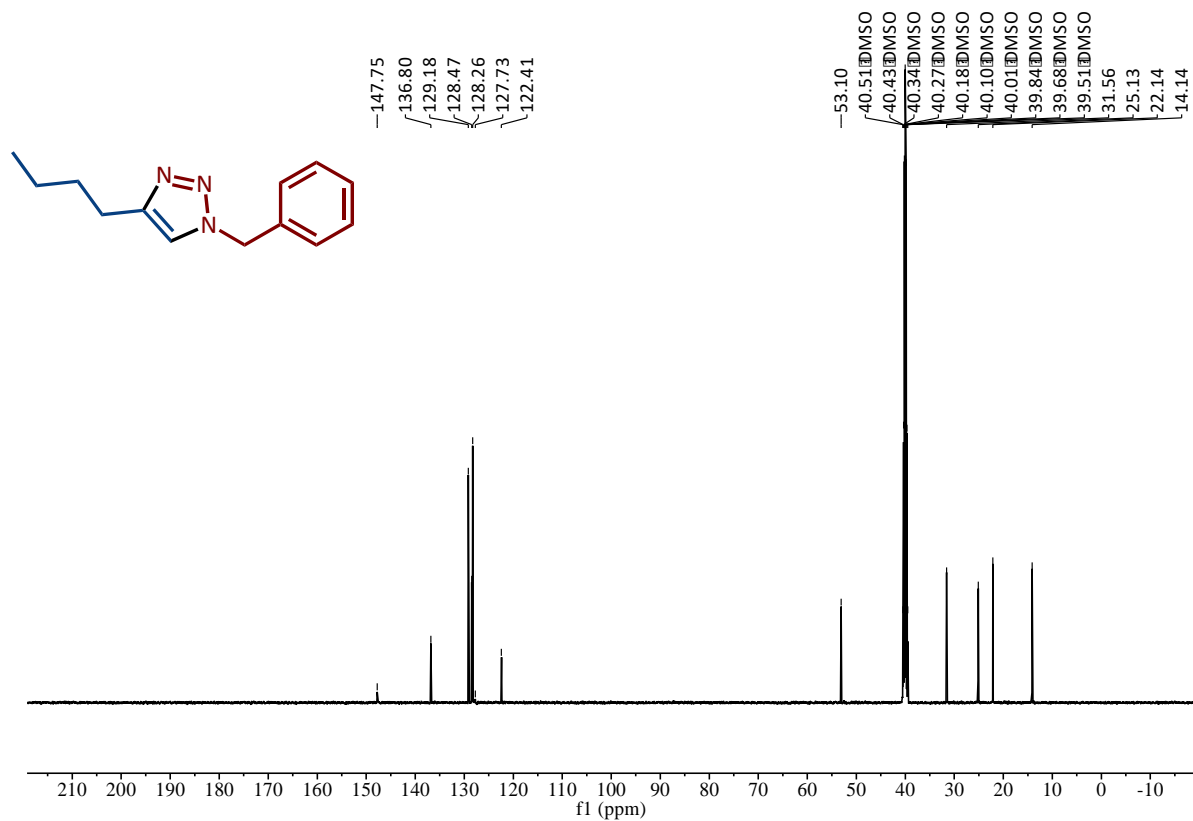


Figure S10.26 ^{13}C -NMR spectrum of **4m** made by RAM direct mechanocatalysis, recorded in d_6 -DMSO.

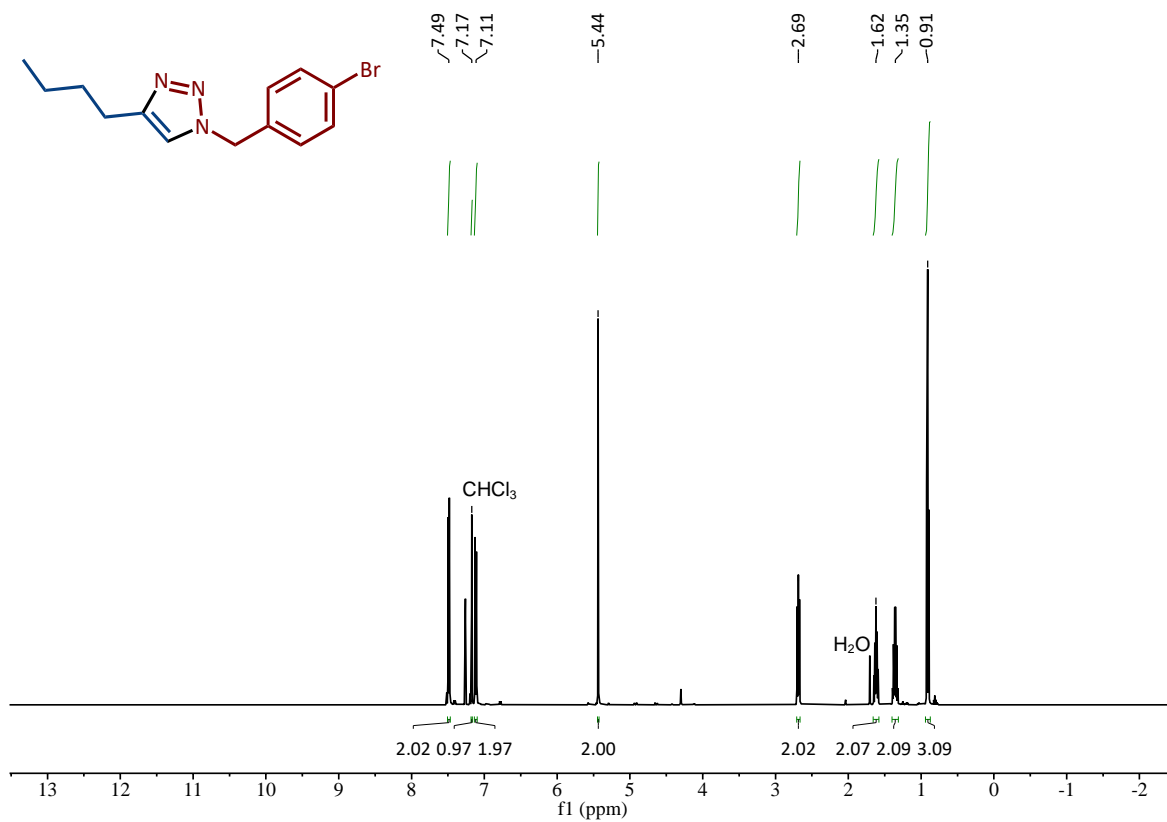


Figure S10.27 ¹H-NMR spectrum of **4n** made by RAM direct mechanocatalysis, recorded in CDCl₃.

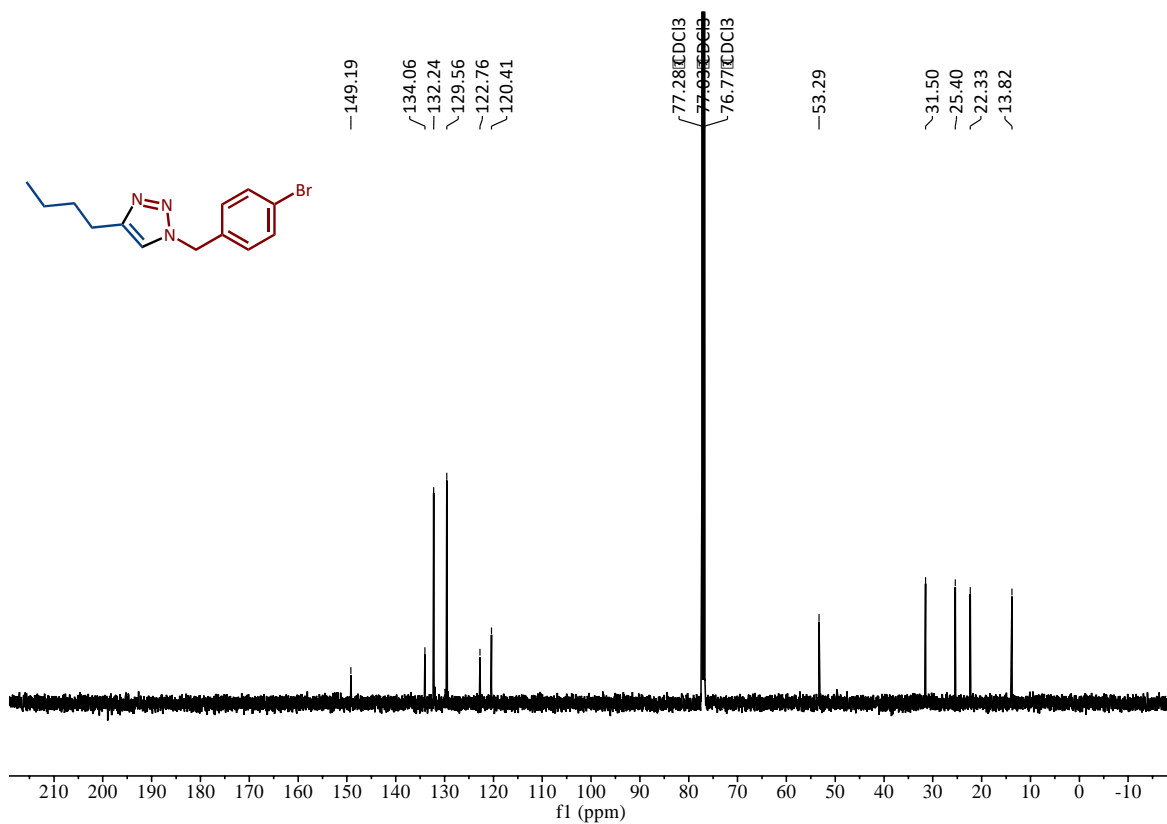


Figure S10.28 ^{13}C -NMR spectrum of **4n** made by RAM direct mechanocatalysis, recorded in d_6 -DMSO.

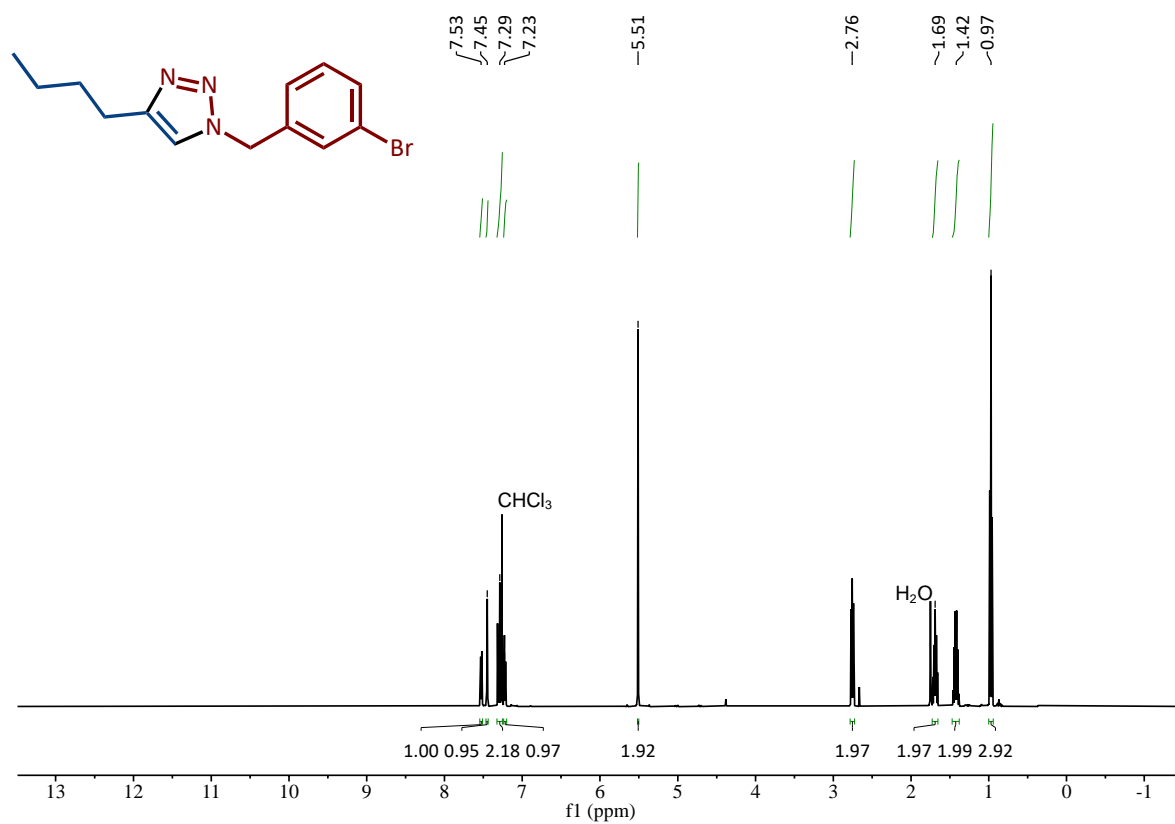


Figure S10.29 ¹H-NMR spectrum of **4o** made by RAM direct mechanocatalysis, recorded in CDCl₃.

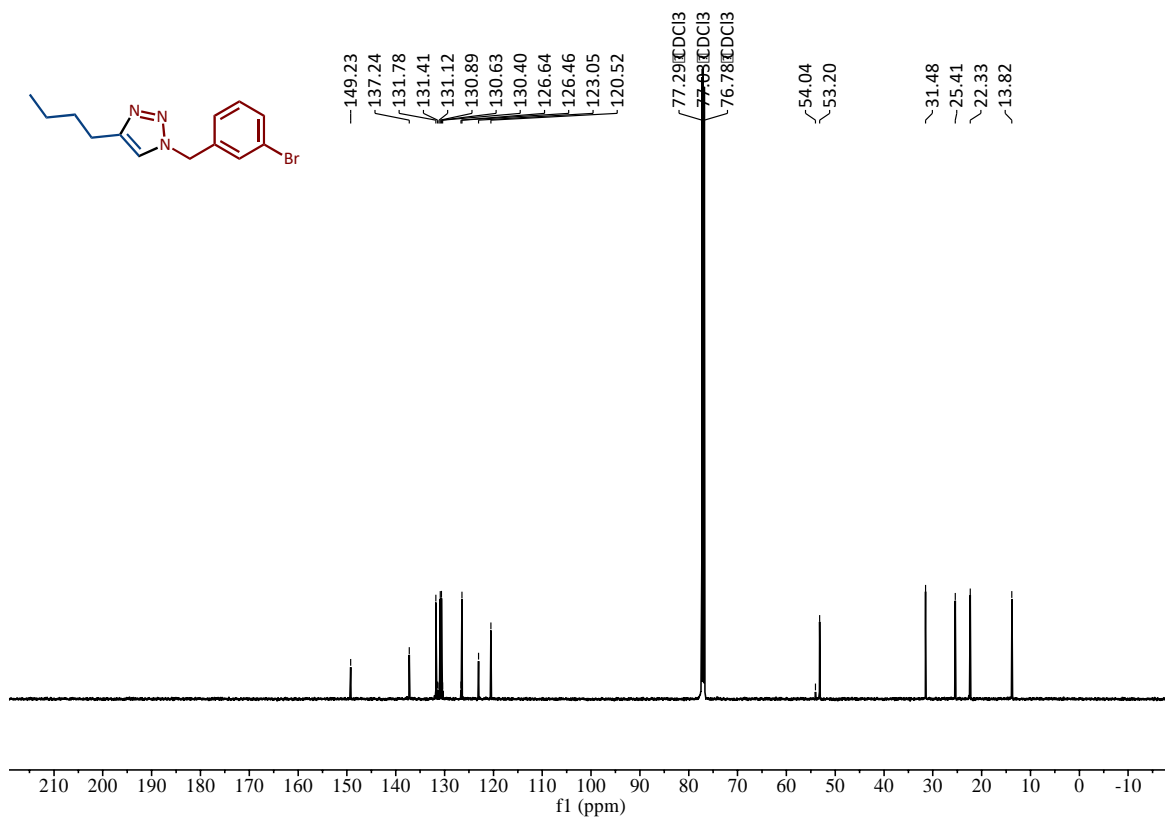


Figure S10.30 ¹³C-NMR spectrum of **4o** made by RAM direct mechanocatalysis, recorded in CDCl₃.

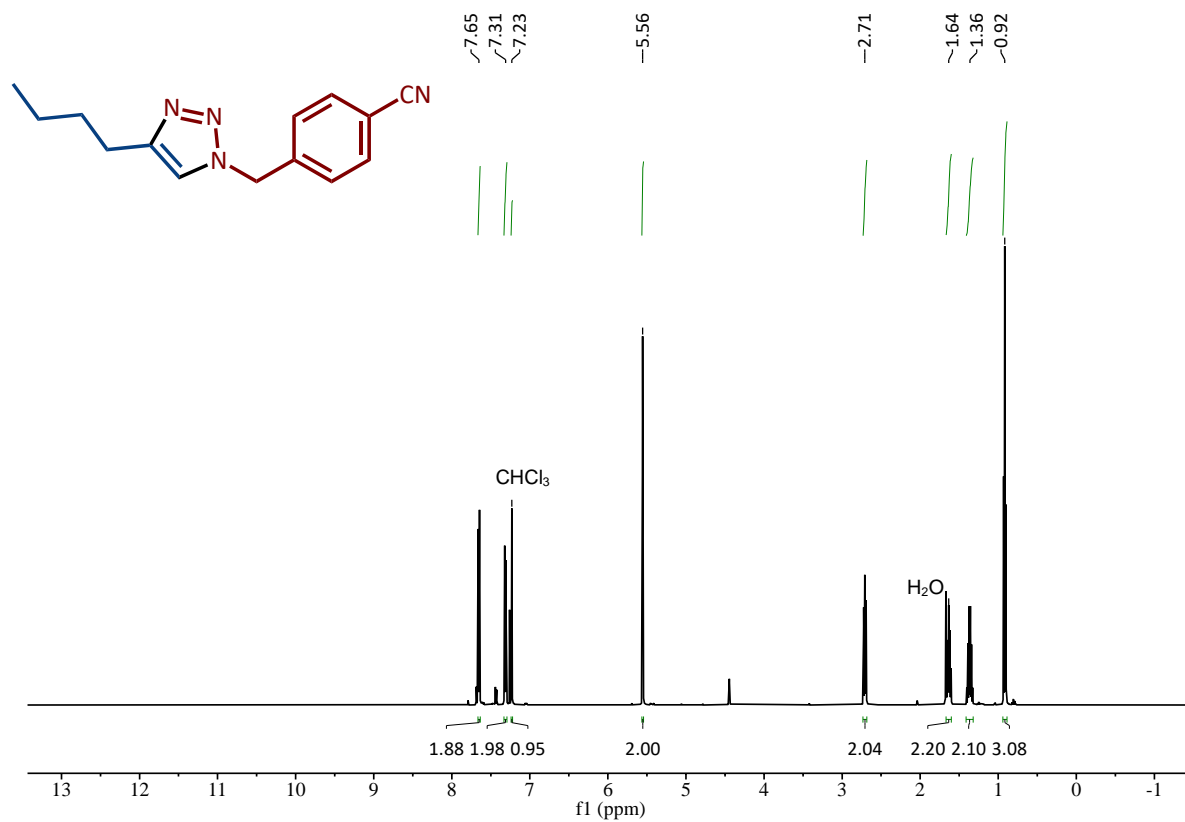


Figure S10.31 ¹H-NMR spectrum of **4p** made by RAM direct mechanocatalysis, recorded in CDCl₃.

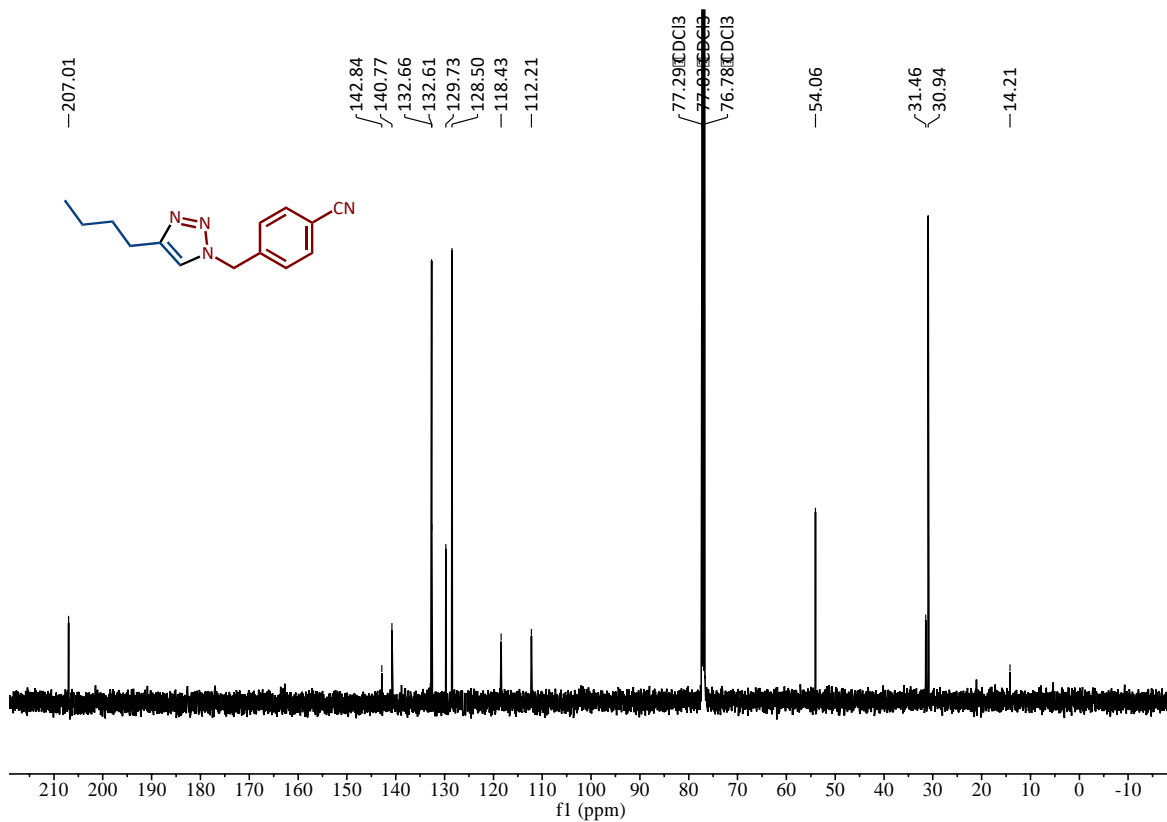


Figure S10.32 ¹³C-NMR spectrum of **4p** made by RAM direct mechanocatalysis, recorded in CDCl₃.

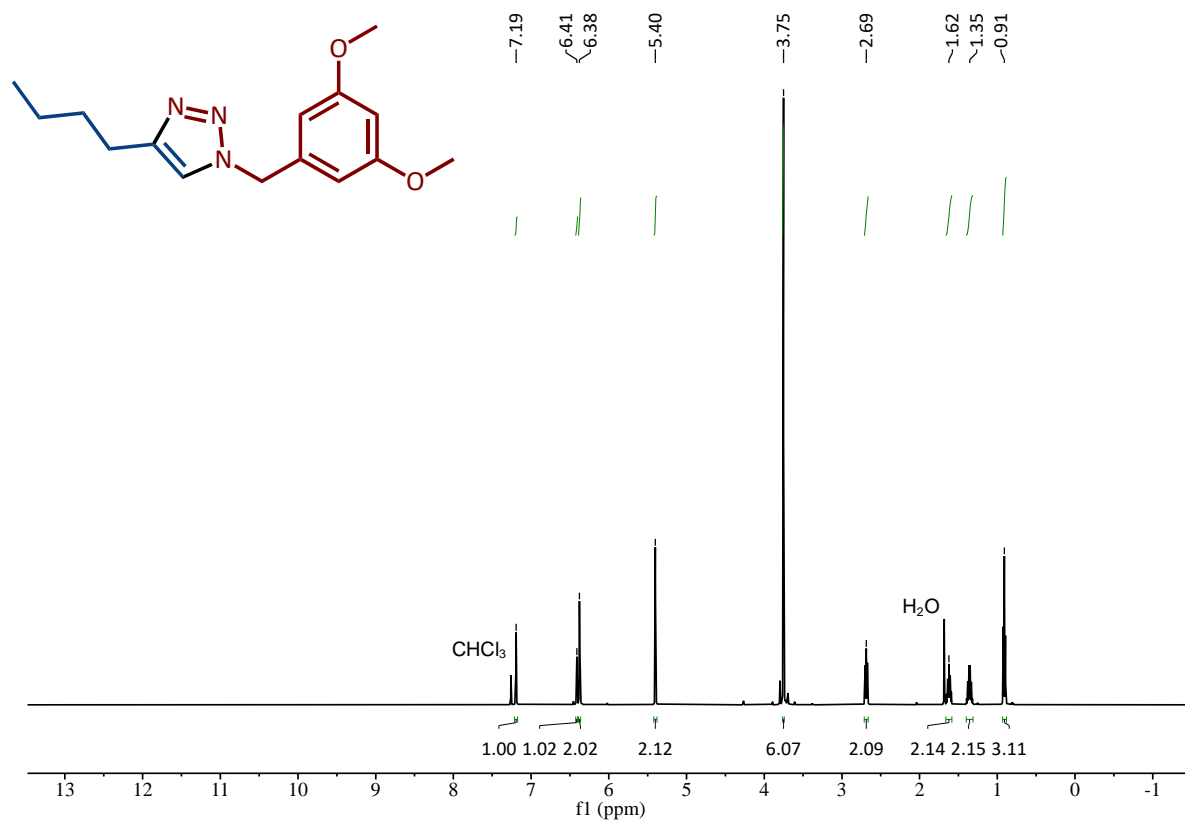


Figure S10.33 $^1\text{H-NMR}$ spectrum of **4q** made by RAM direct mechanocatalysis, recorded in CDCl_3 .

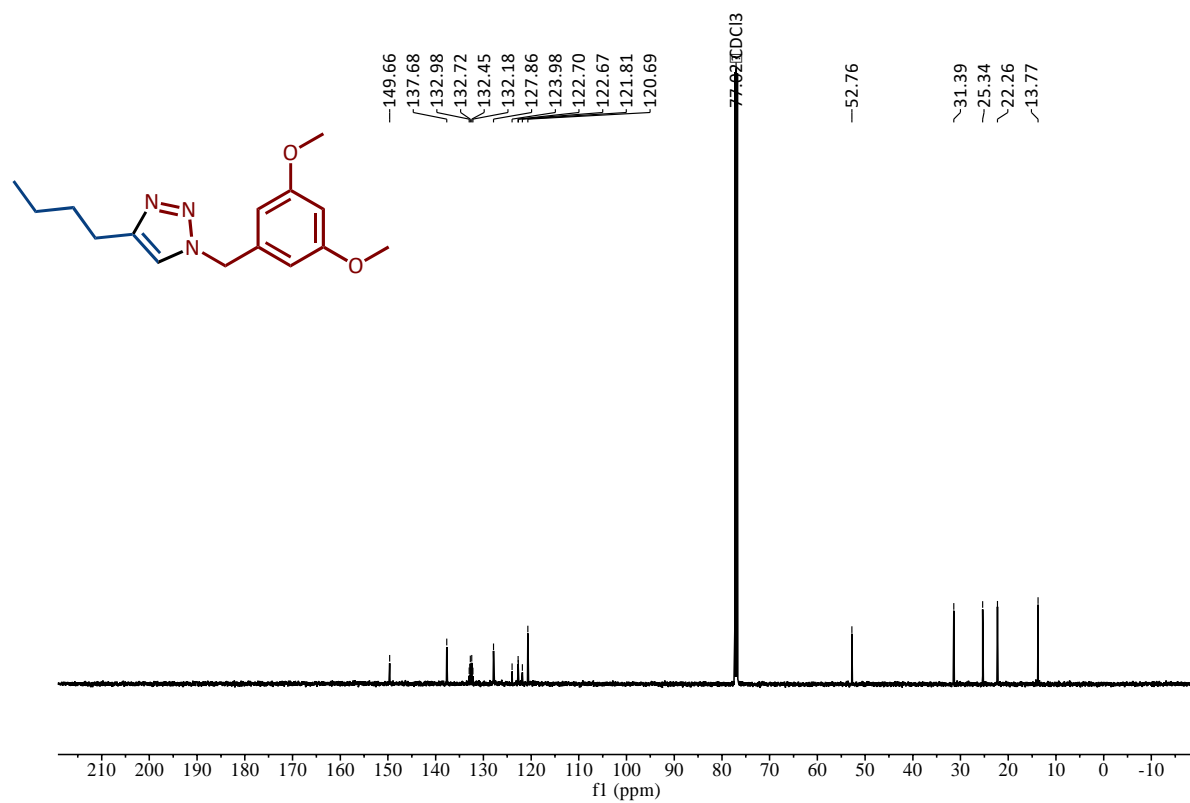


Figure S10.34 ¹³C-NMR spectrum of **4q** made by RAM direct mechanocatalysis, recorded in CDCl₃.

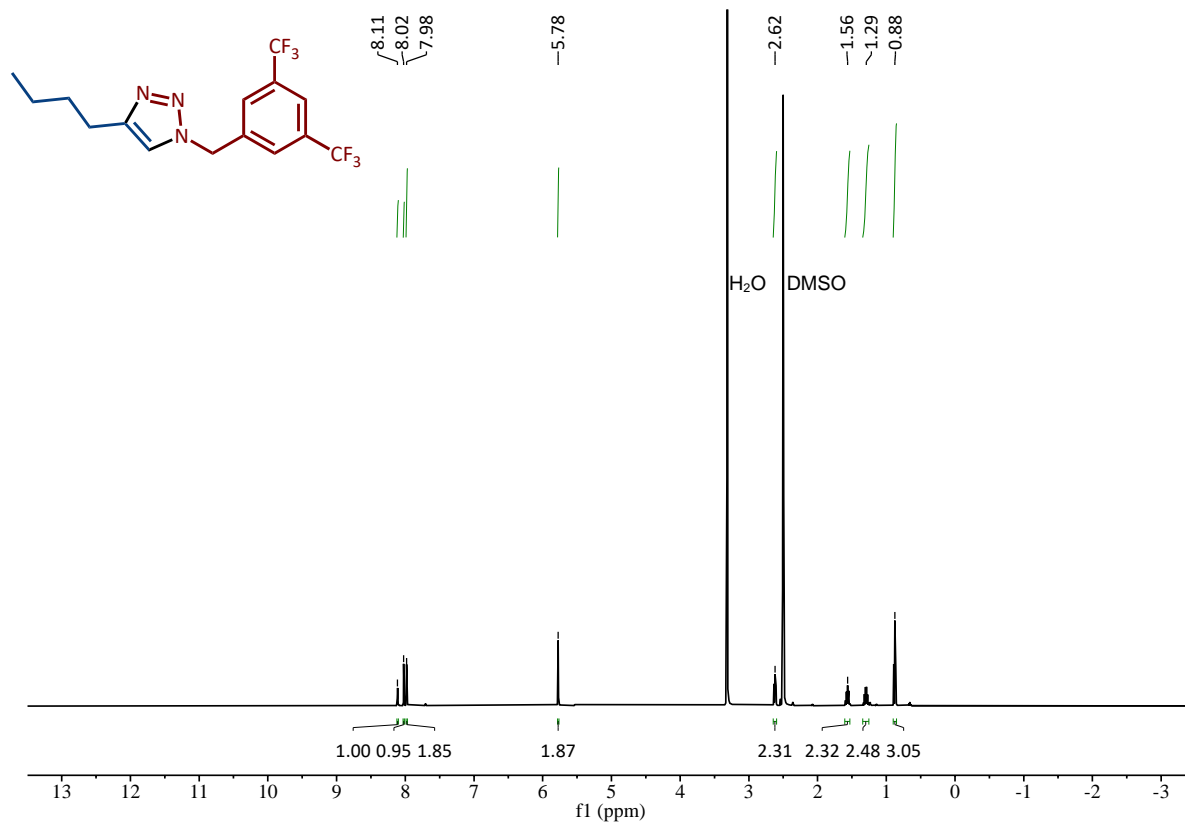


Figure S10.35 ¹H-NMR spectrum of **4r** made by RAM direct mechanocatalysis, recorded in d₆-DMSO.

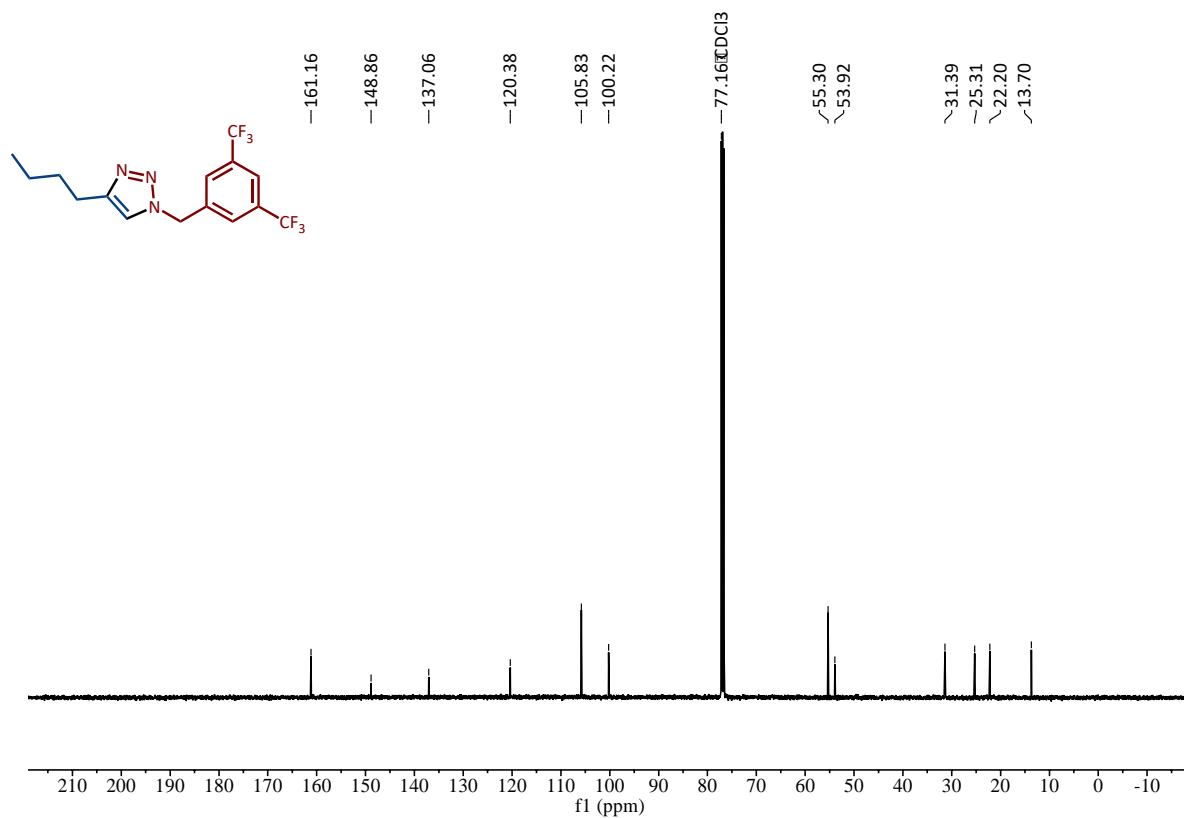


Figure S10.36 ^{13}C -NMR spectrum of 4r made by RAM direct mechanocatalysis, recorded in CDCl_3 .

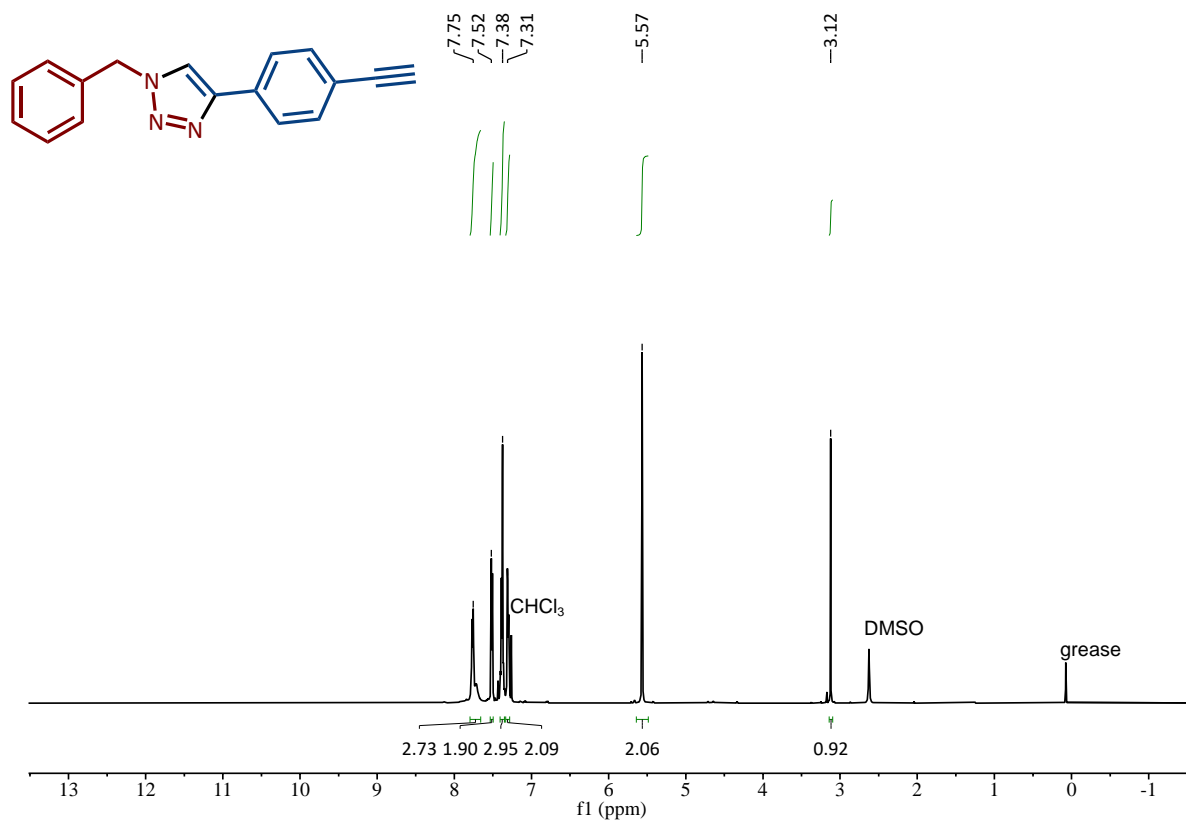


Figure S10.37 ¹H-NMR spectrum of **4s** made by RAM direct mechanocatalysis, recorded in CDCl₃.

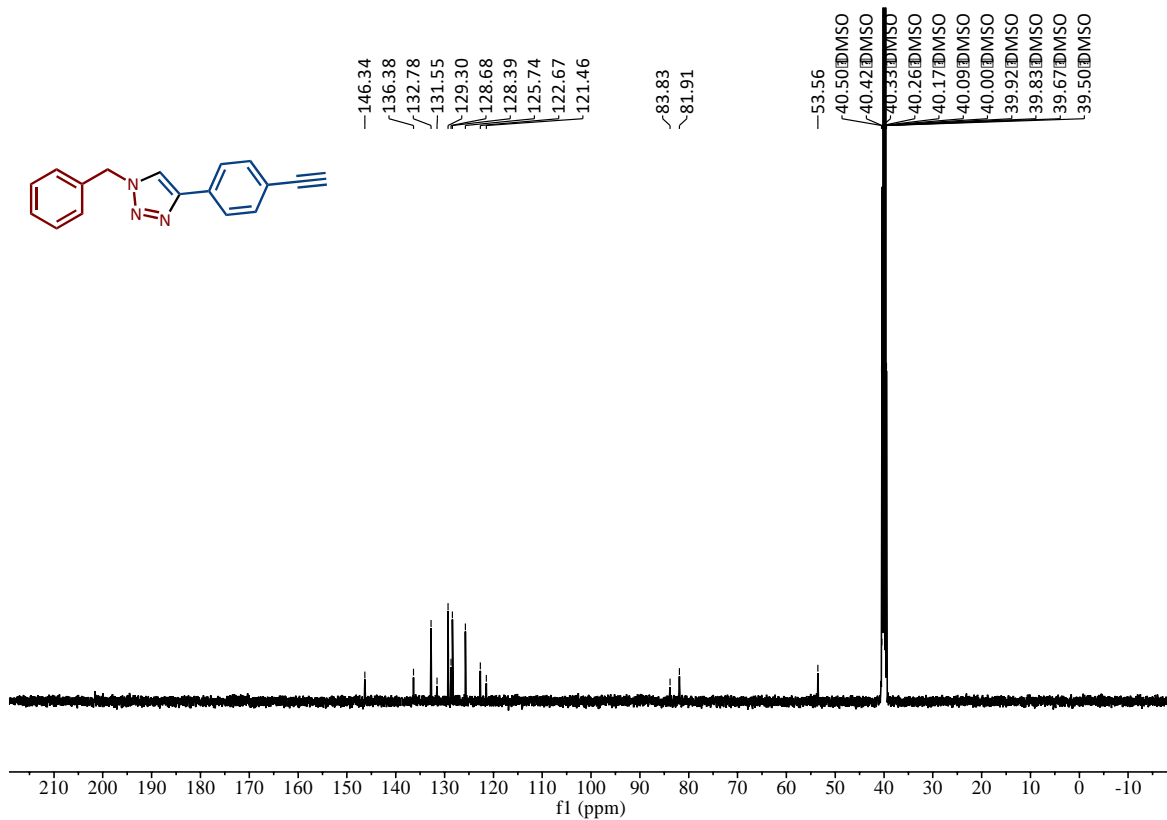


Figure S10.38 ¹³C-NMR spectrum of 4s made by RAM direct mechanocatalysis, recorded in CDCl₃.

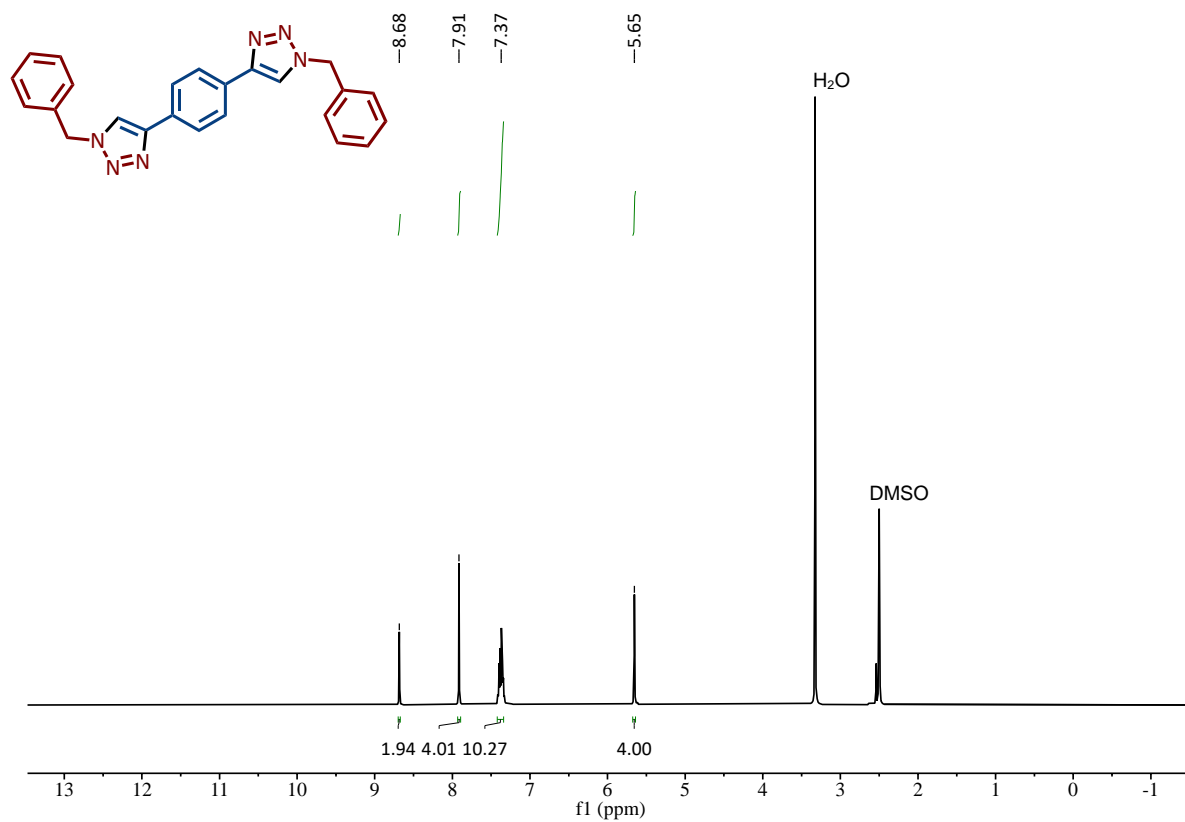


Figure S10.39 ¹H-NMR spectrum of **4t** made by RAM direct mechanocatalysis, recorded in d₆-DMSO.

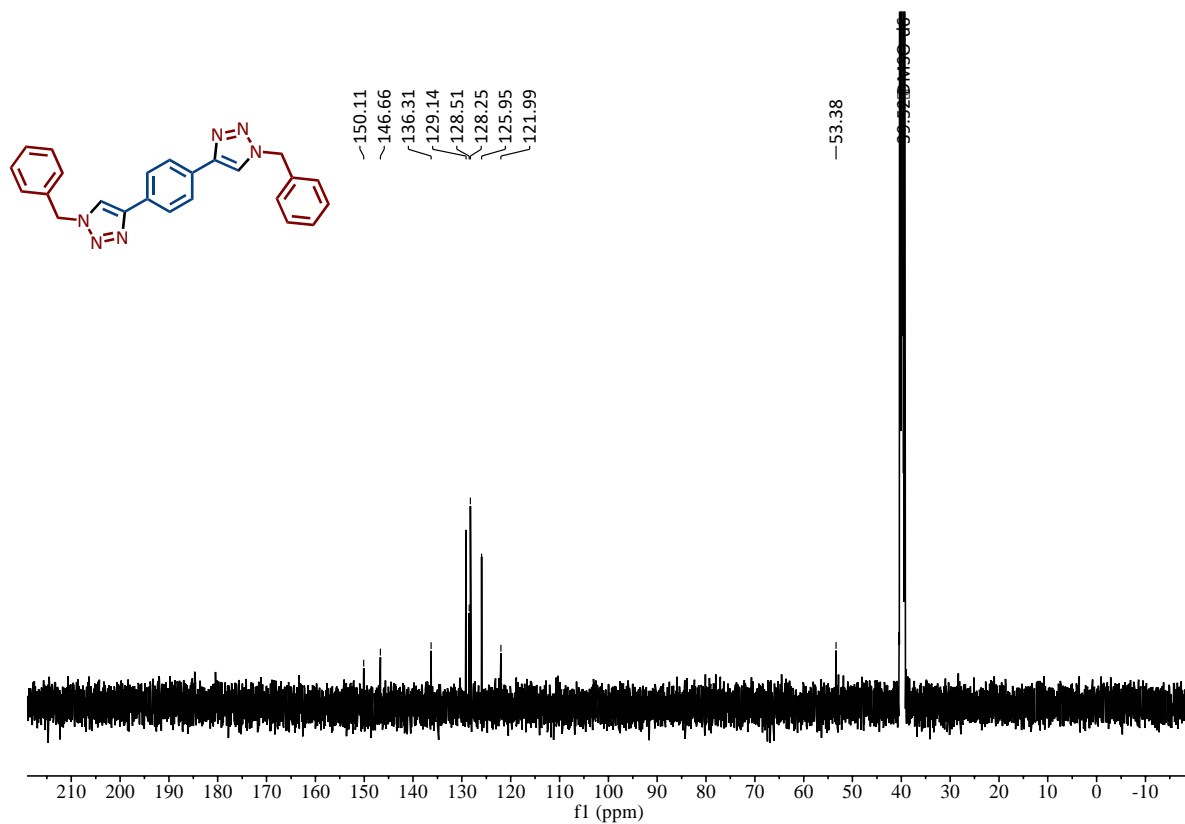


Figure S10.40 ¹³C-NMR spectrum of **4t** made by RAM direct mechanocatalysis, recorded in d₆-DMSO.

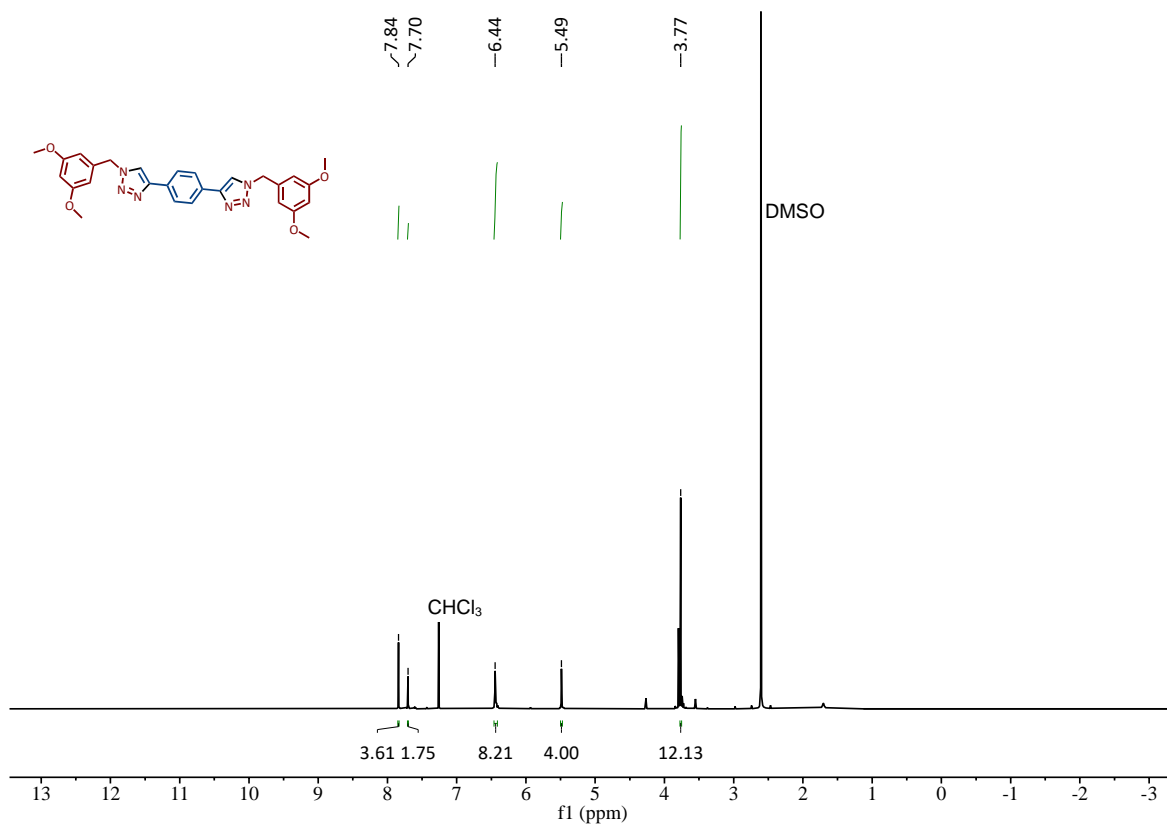


Figure S10.41 **4u** ¹H-NMR spectrum of **4u** made by RAM direct mechanocatalysis, recorded in CDCl₃.

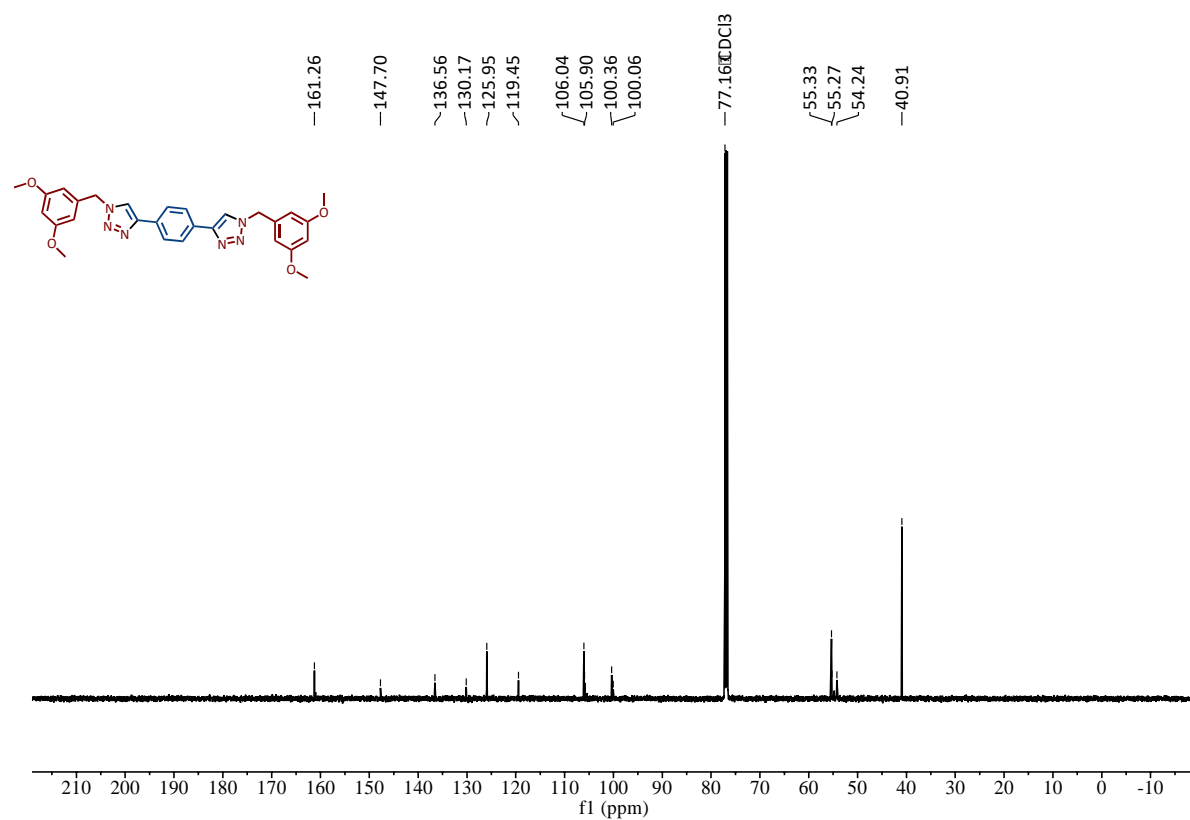


Figure S10.42 ^{13}C -NMR spectrum of 4u made by RAM direct mechanocatalysis, recorded in CDCl_3 .

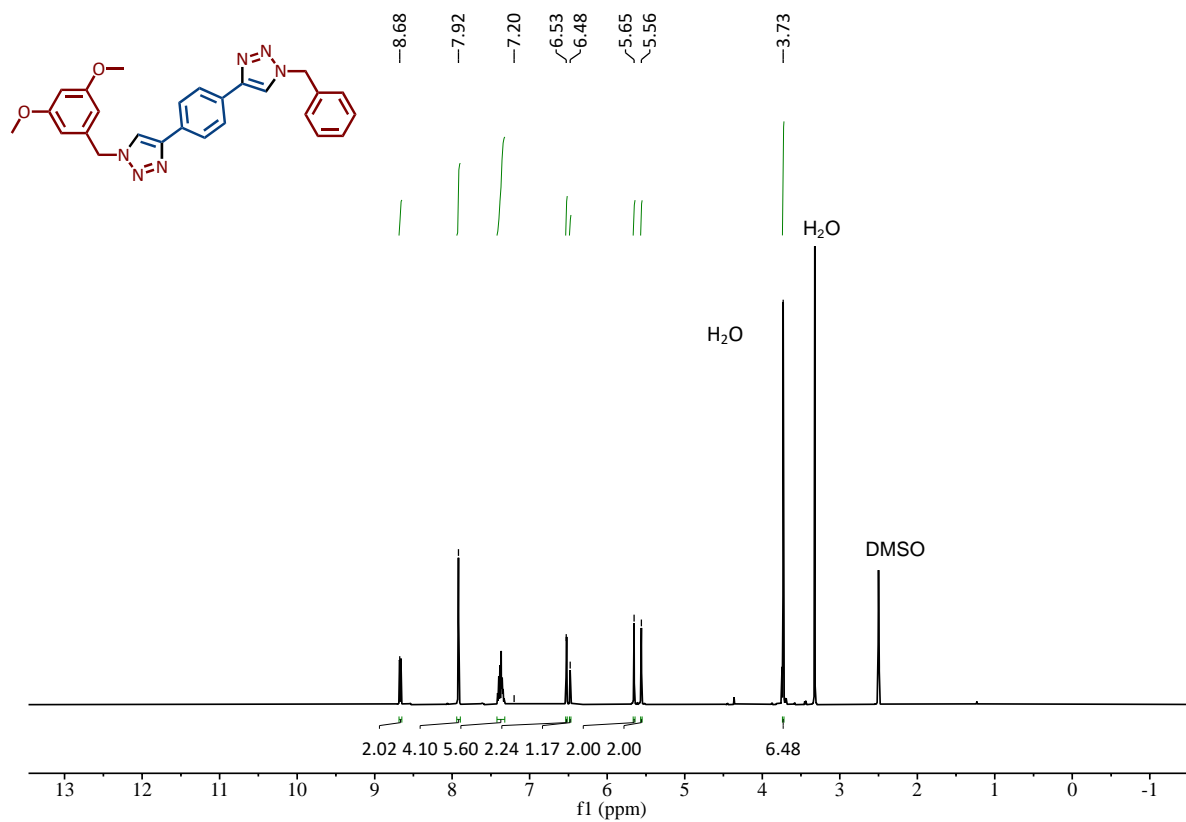


Figure S10.45 **4v** ¹H-NMR spectrum of **4v** made by RAM direct mechanocatalysis, recorded in d₆-DMSO.

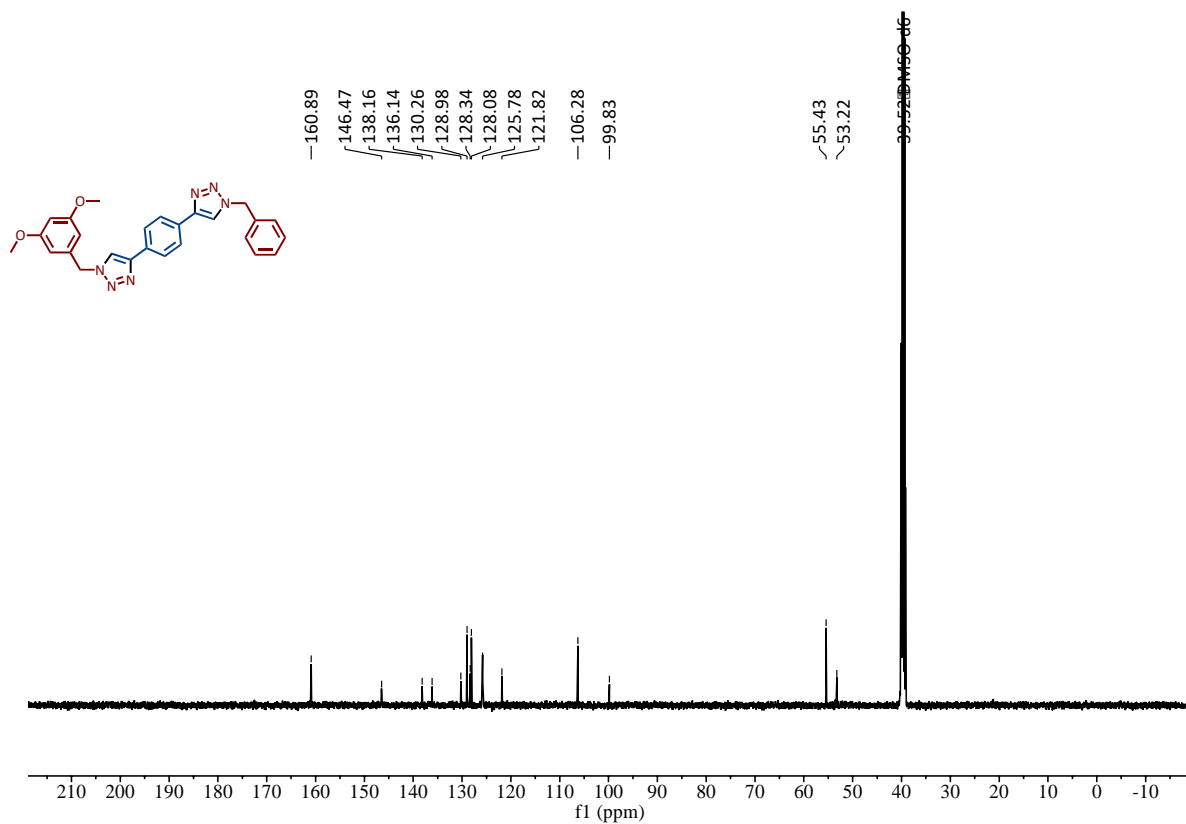


Figure S10.46 ¹³C-NMR spectrum of 4v made by RAM direct mechanocatalysis, recorded in d₆-DMSO.

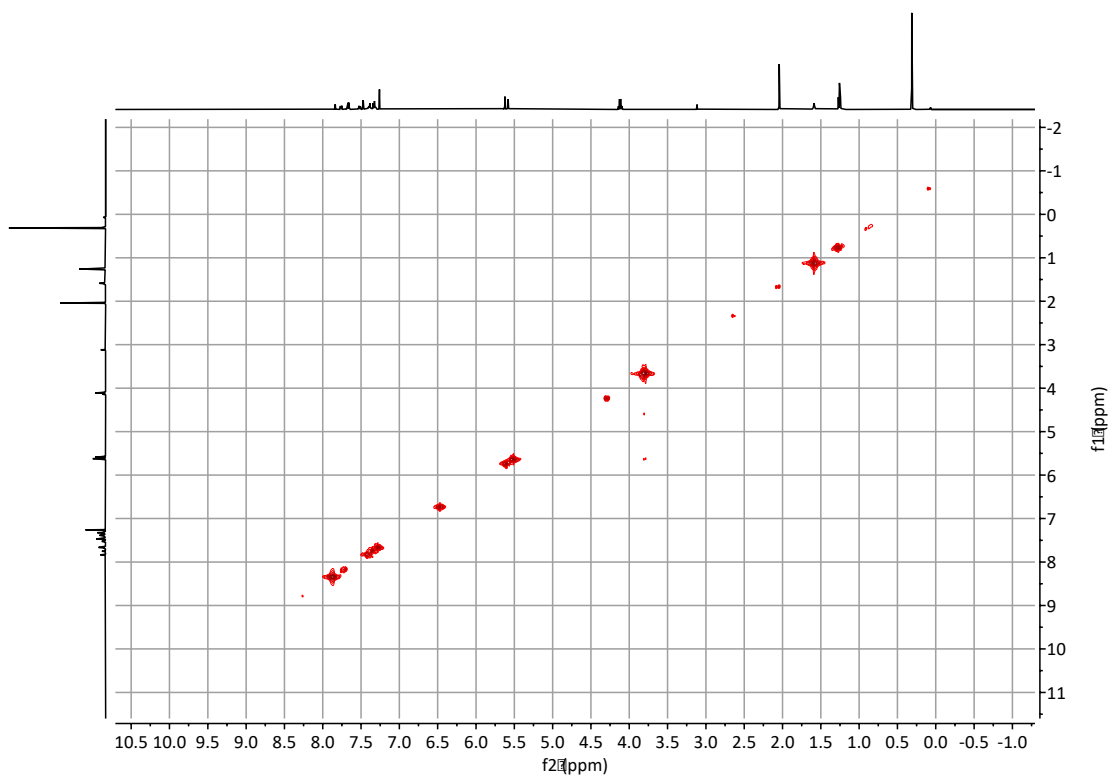


Figure S10.47 ¹H-¹H COSY-NMR of 4v made by RAM direct mechanocatalysis, recorded in d₆-DMSO.

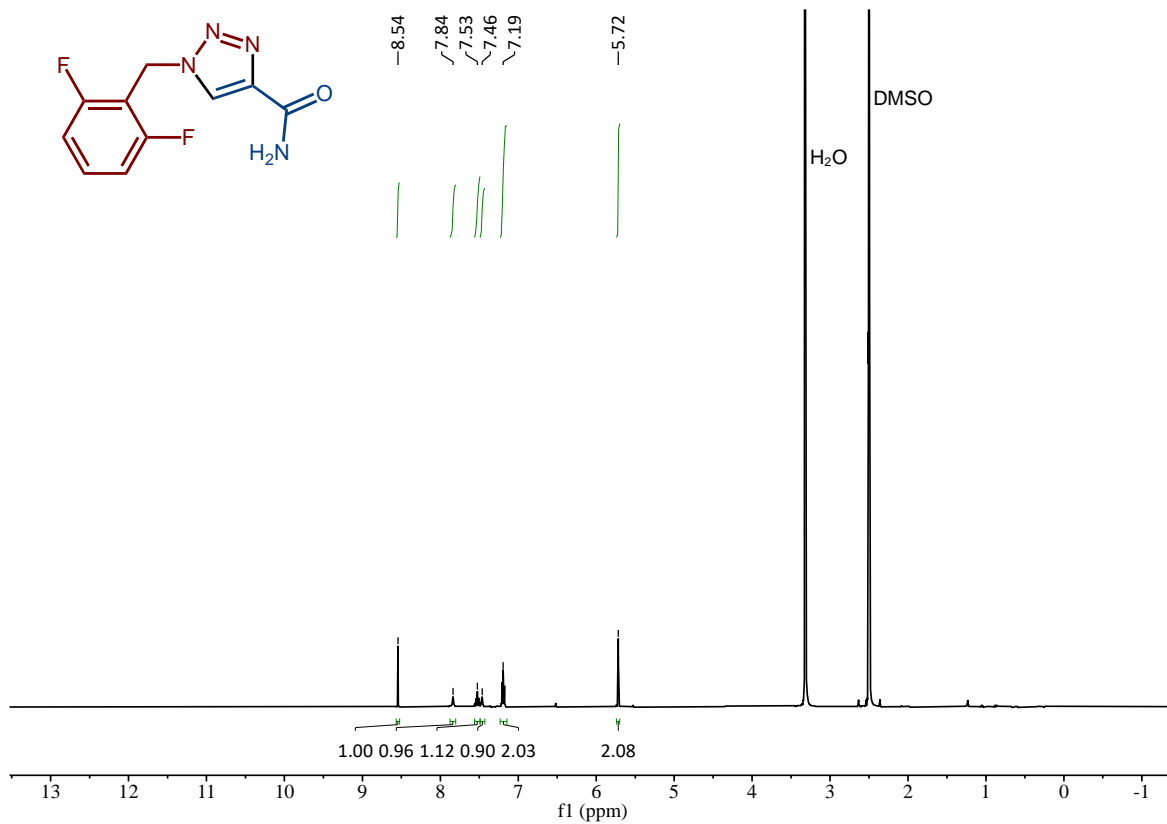


Figure S10.48 ¹H-NMR spectrum of Rufinamide made by RAM direct mechanocatalysis, recorded in d₆-DMSO.

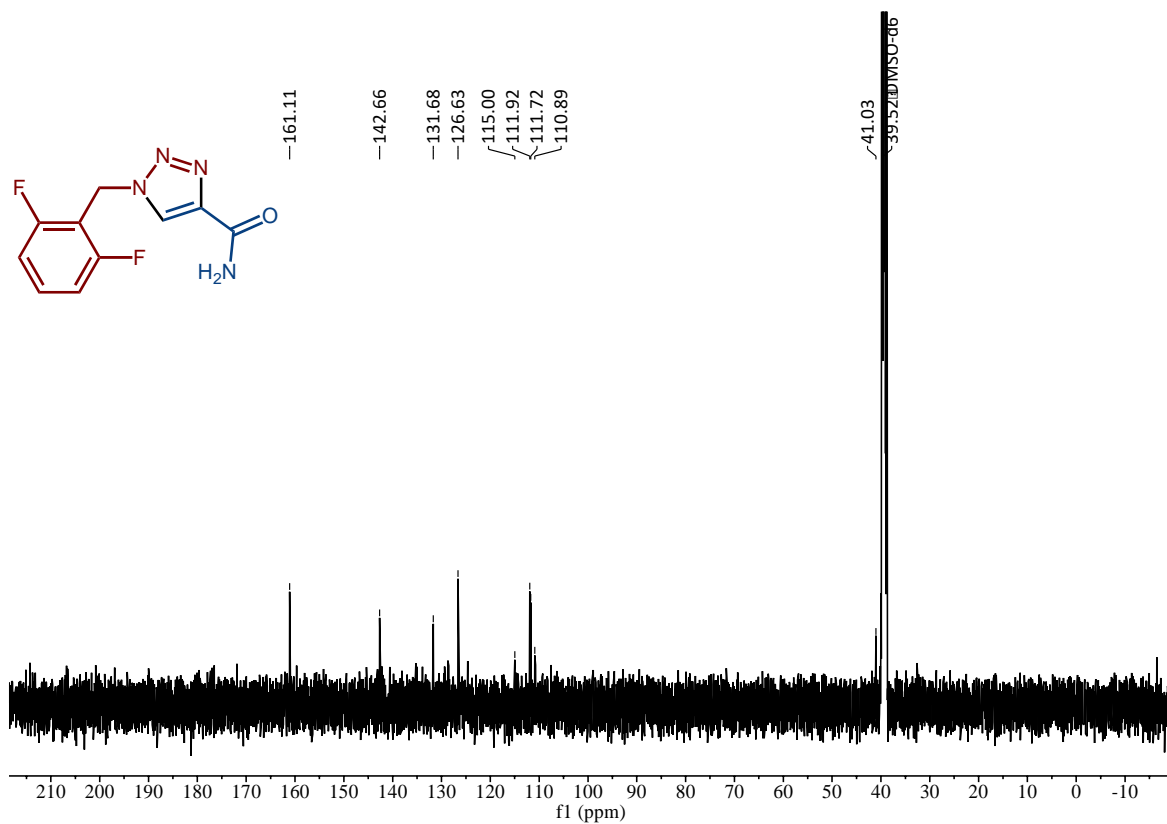


Figure S10.49 ¹³C-NMR spectrum of Rufinamide made by RAM direct mechanocatalysis, recorded in d₆-DMSO.

S11. Fourier-transform infrared attenuated total reflectance (FTIR-ATR) spectra of isolated products

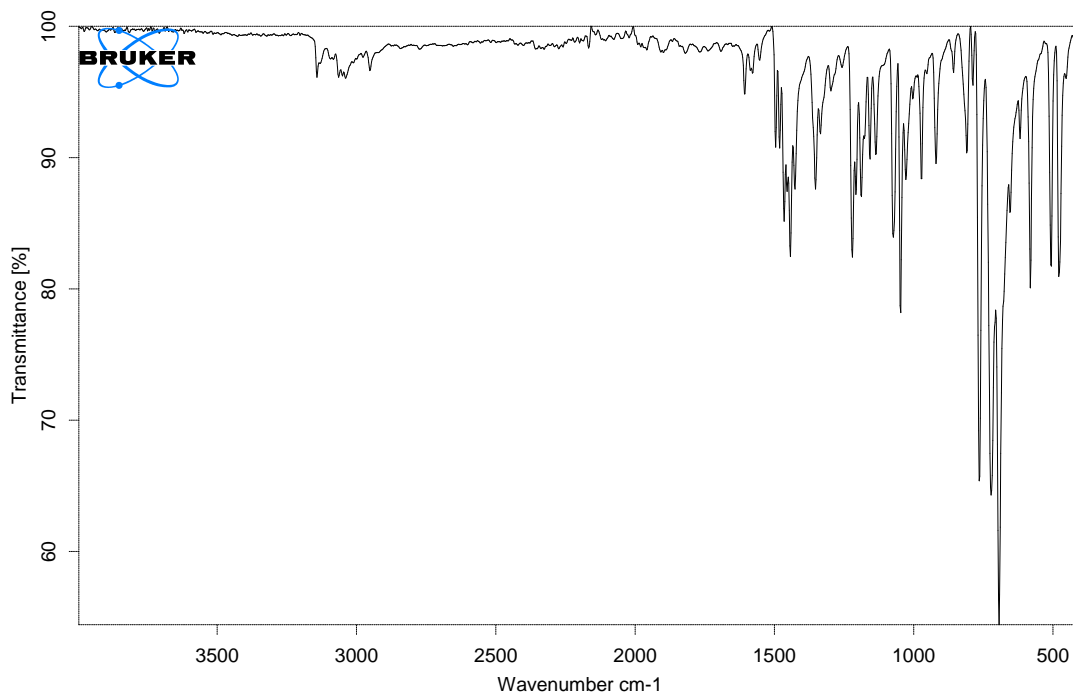


Figure S11.1 FTIR-ATR spectrum of isolated **4a**, synthesised by RAM direct mechanocatalysis.

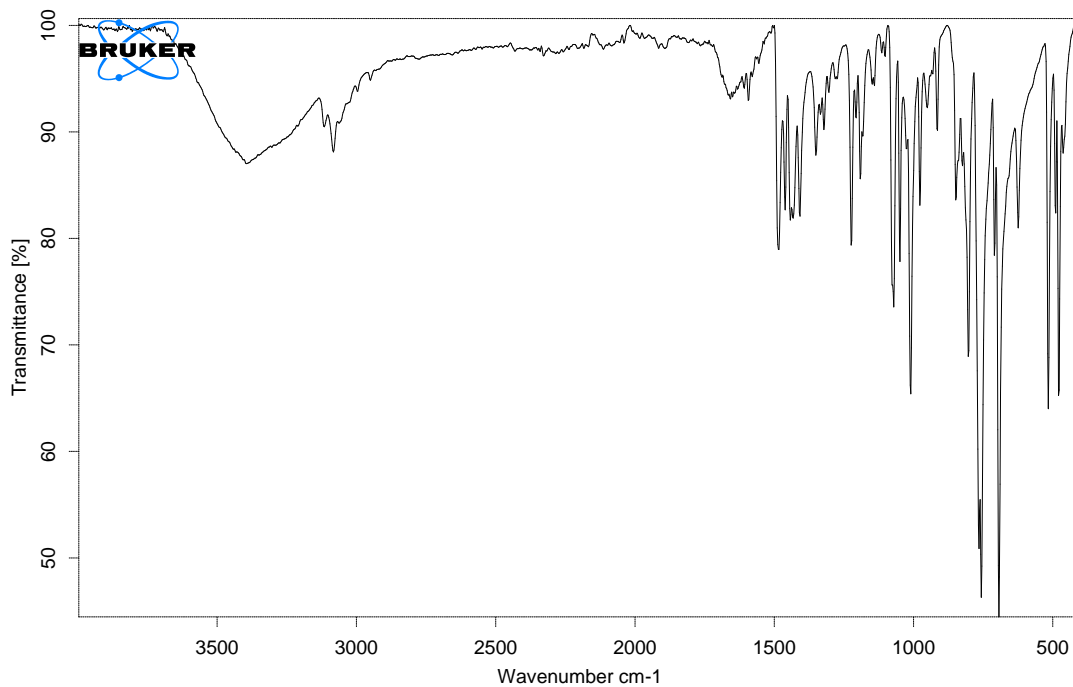


Figure S11.2 FTIR-ATR spectrum of isolated **4b**, synthesised by RAM direct mechanocatalysis.

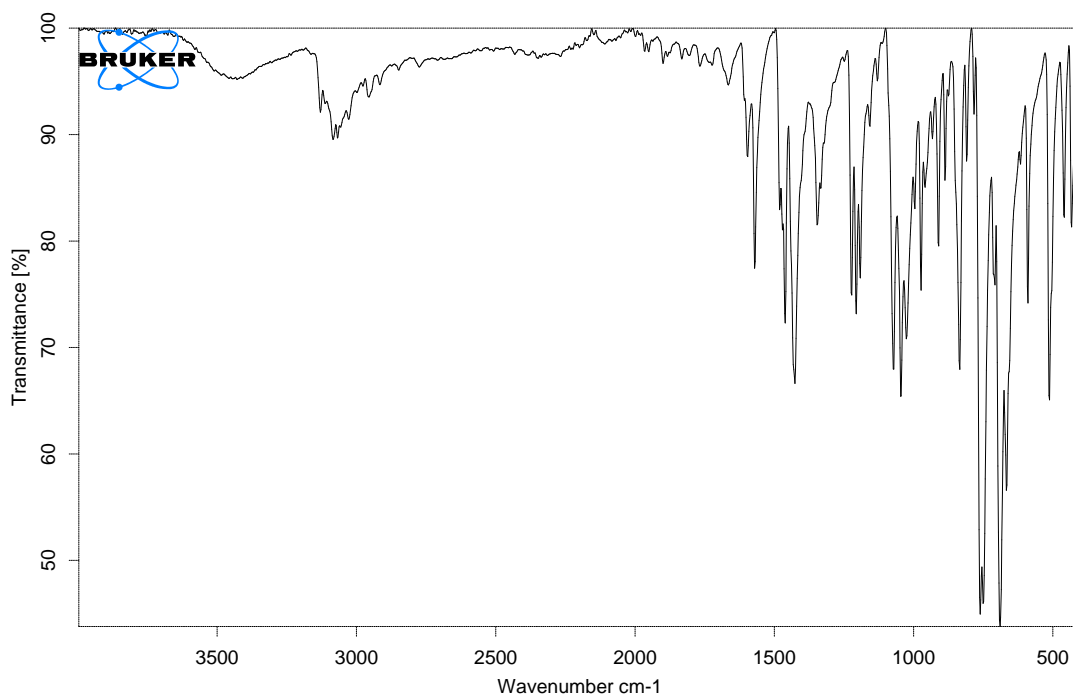


Figure S11.3 FTIR-ATR spectrum of isolated **4c**, synthesised by RAM direct mechanocatalysis.

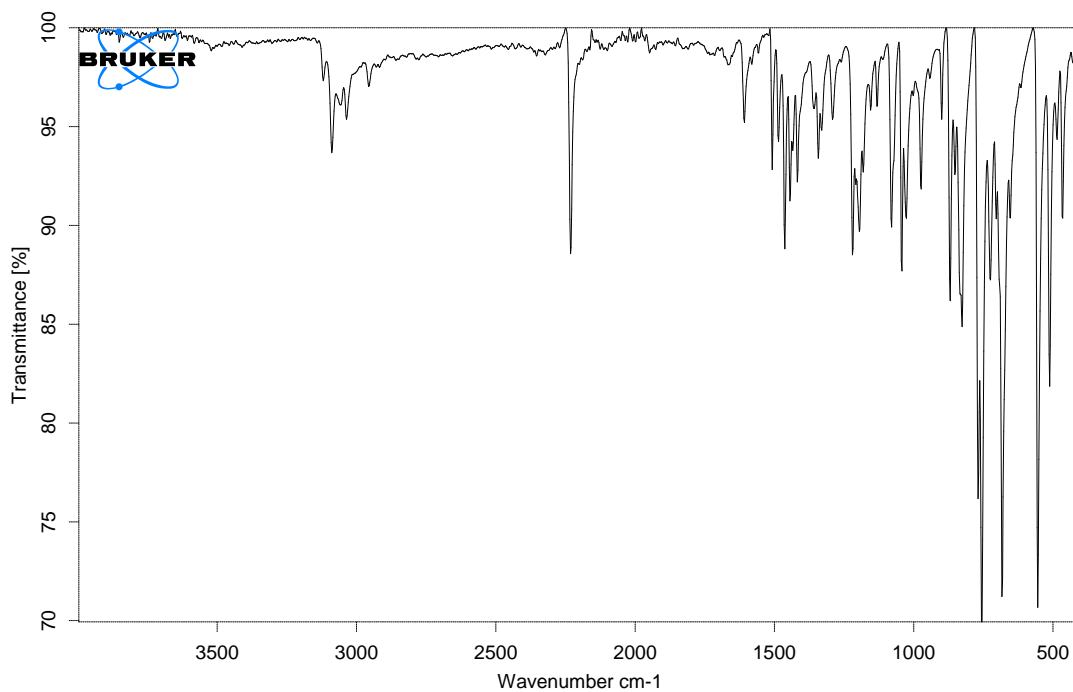


Figure S11.4 FTIR-ATR spectrum of isolated **4d**, synthesised by RAM direct mechanocatalysis.

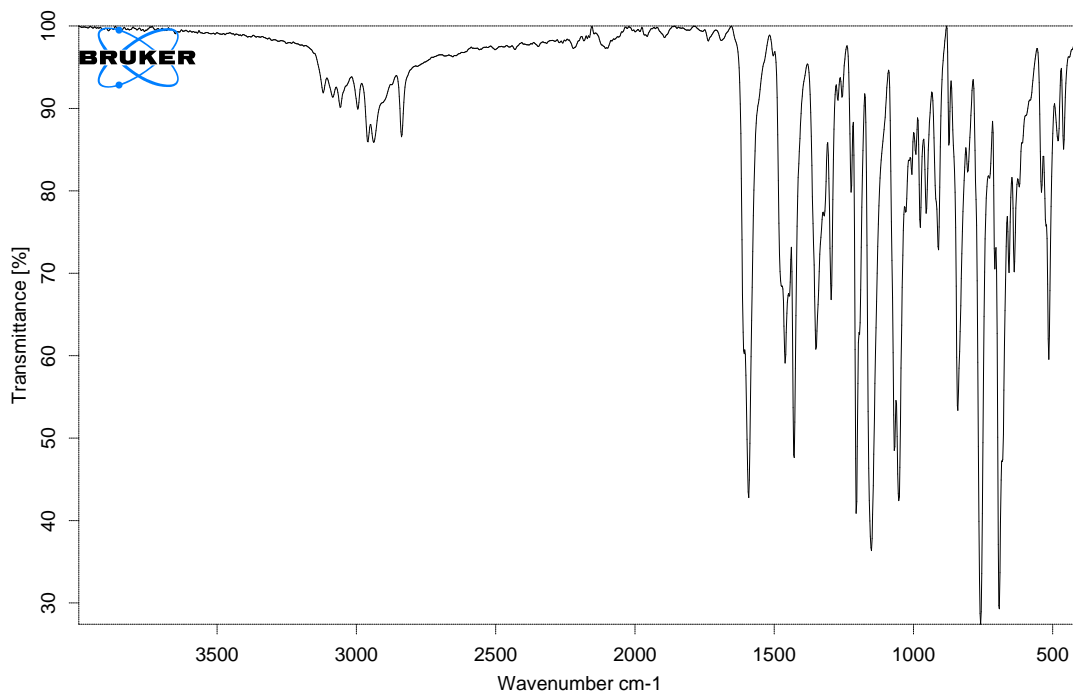


Figure 11.5 FTIR-ATR spectrum of isolated **4e**, synthesised by RAM direct mechanocatalysis.

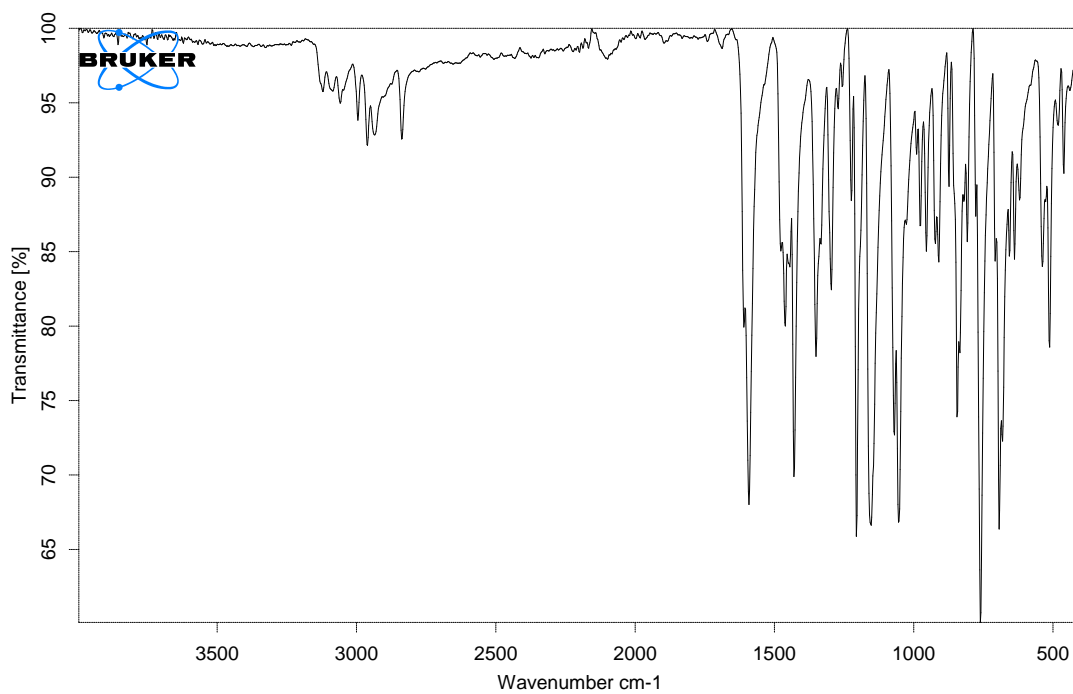


Figure S11.6 FTIR-ATR spectrum of isolated **4f**, synthesised by RAM direct mechanocatalysis.

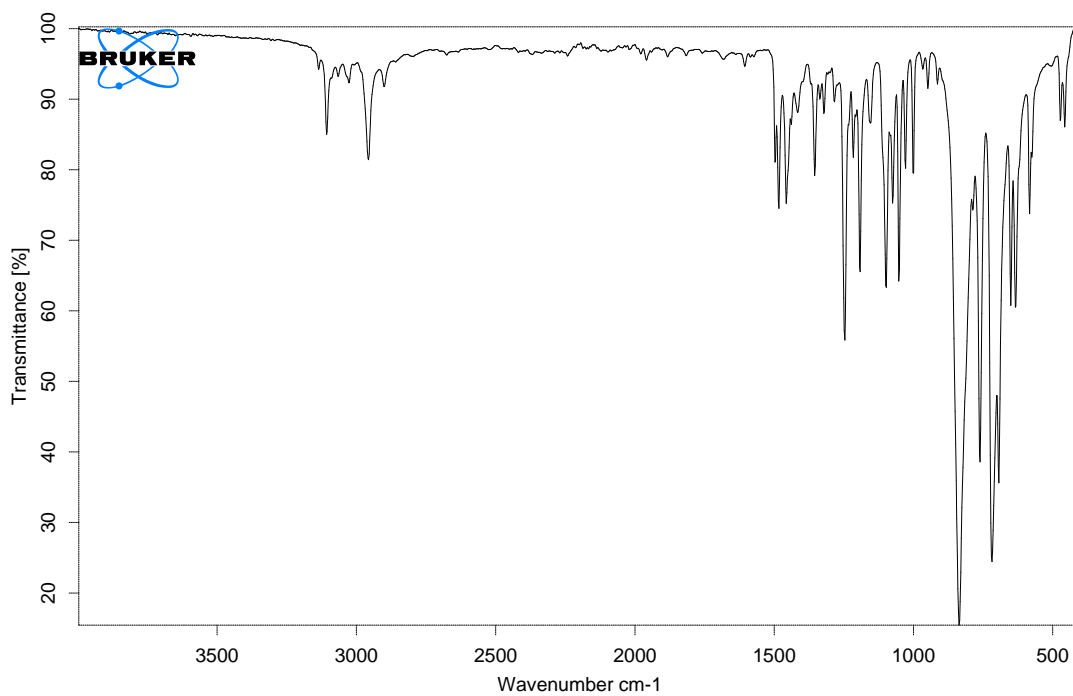


Figure S11.7 FTIR-ATR spectrum of isolated **4g**, synthesised by RAM direct mechanocatalysis.

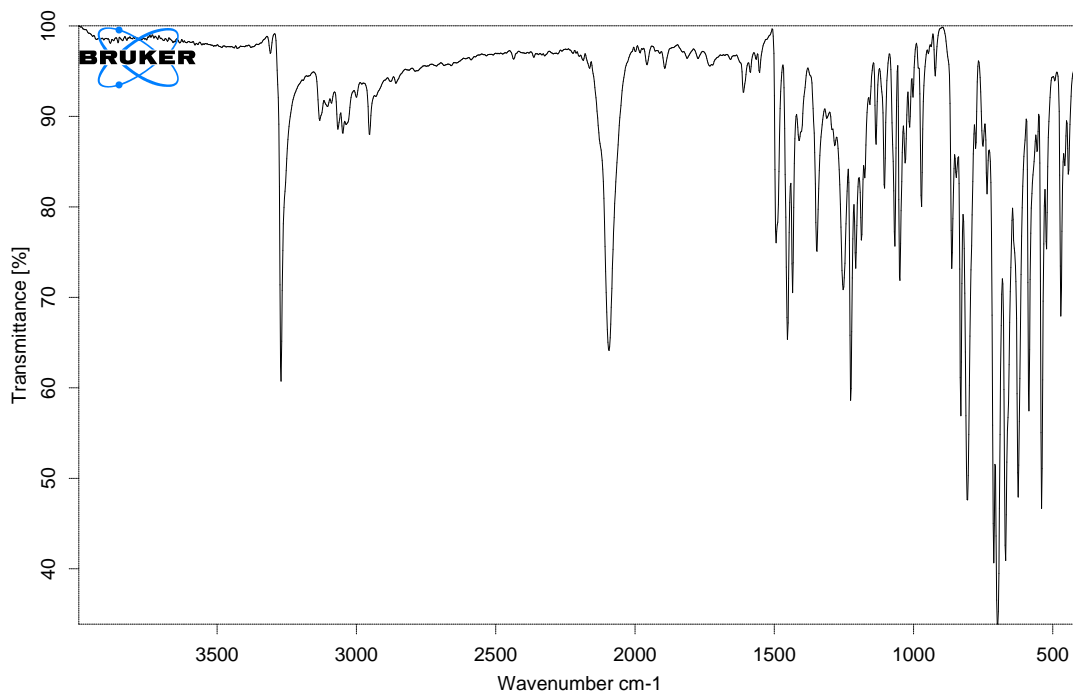


Figure S11.8 FTIR-ATR spectrum of isolated **4h**, synthesised by RAM direct mechanocatalysis.

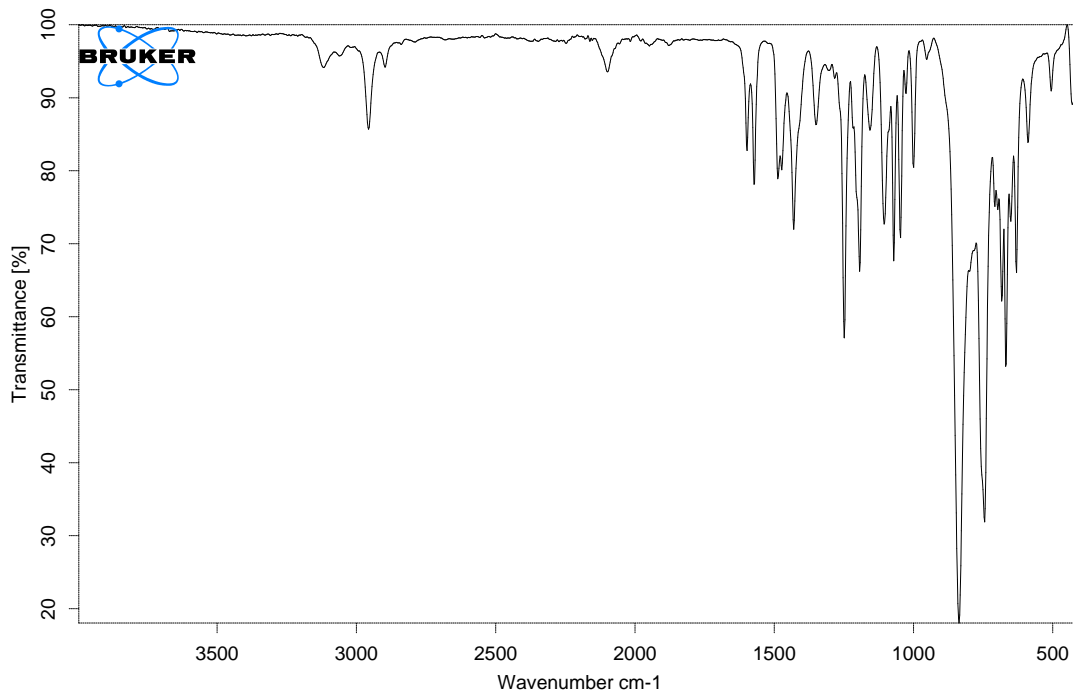


Figure S11.9 FTIR-ATR spectrum of isolated **4i**, synthesised by RAM direct mechanocatalysis.

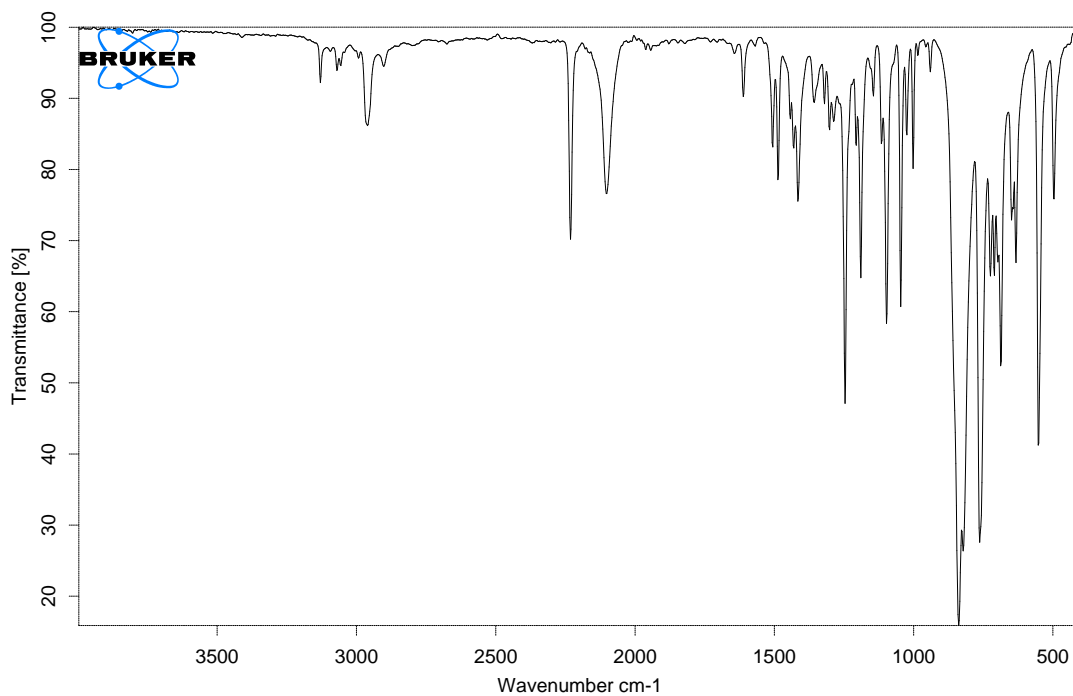


Figure S11.10 FTIR-ATR spectrum of isolated **4j**, synthesised by RAM direct mechanocatalysis.

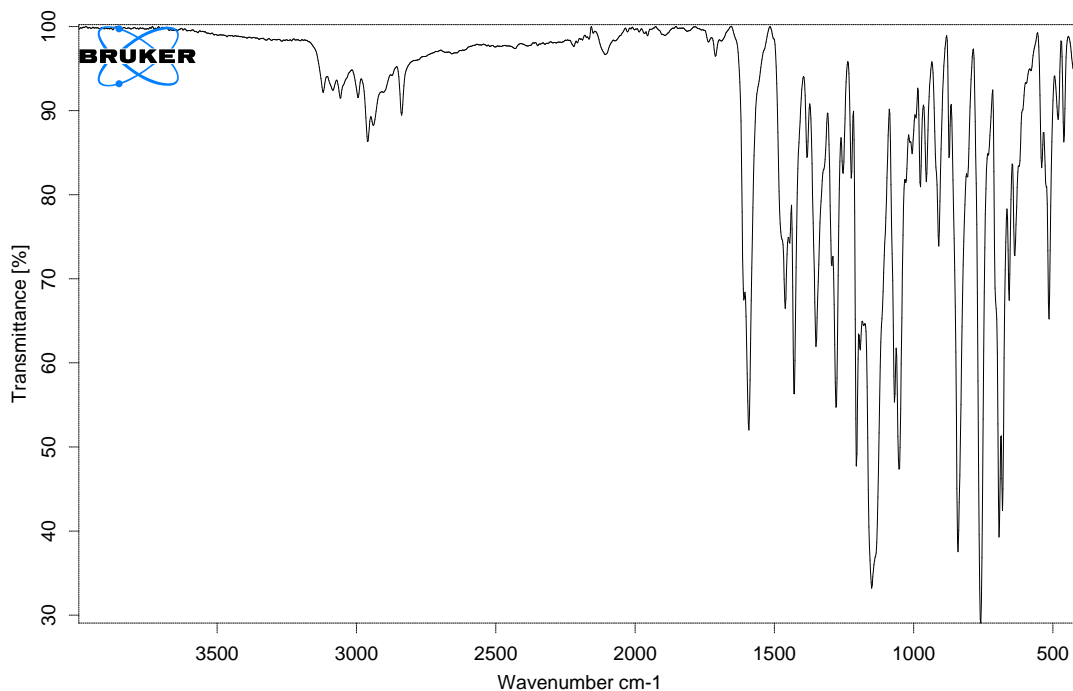


Figure S11.11 FTIR-ATR spectrum of isolated **4k**, synthesised by RAM direct mechanocatalysis.

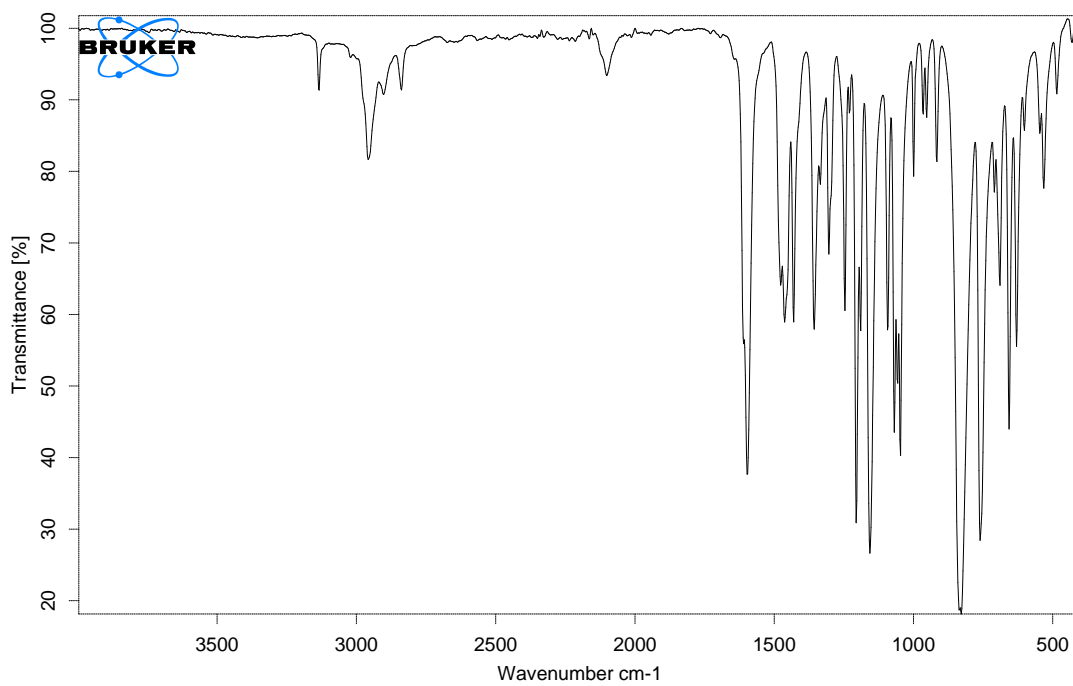


Figure S11.12 FTIR-ATR spectrum of isolated **4l**, synthesised by RAM direct mechanocatalysis.

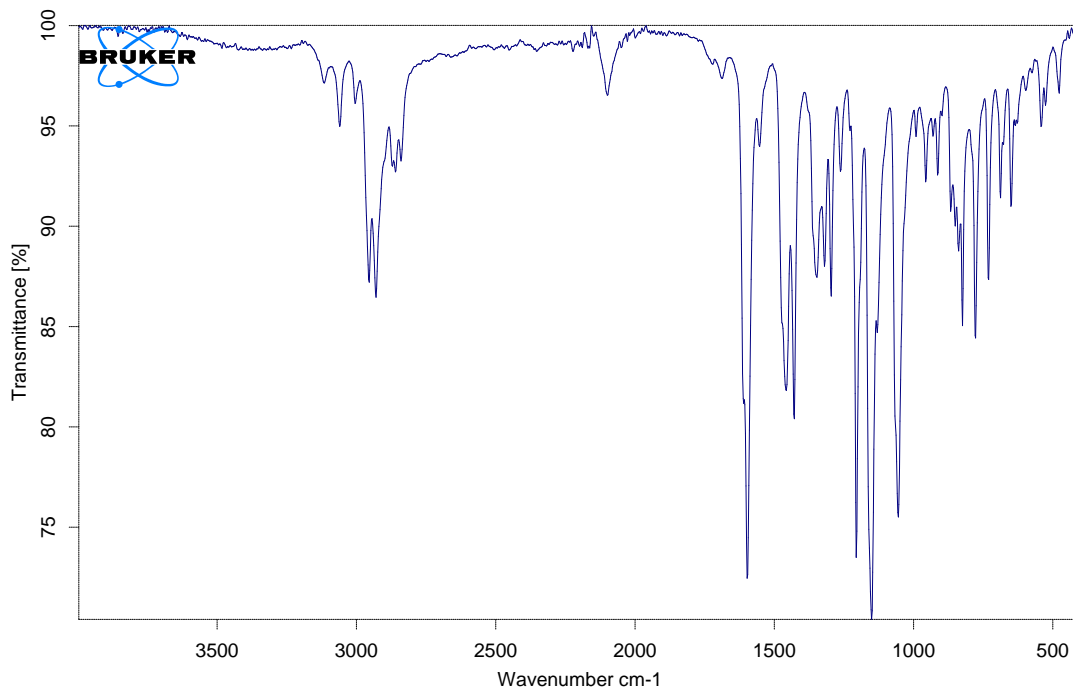


Figure S11.13 FTIR-ATR spectrum of isolated **4m**, synthesised by RAM direct mechanocatalysis.

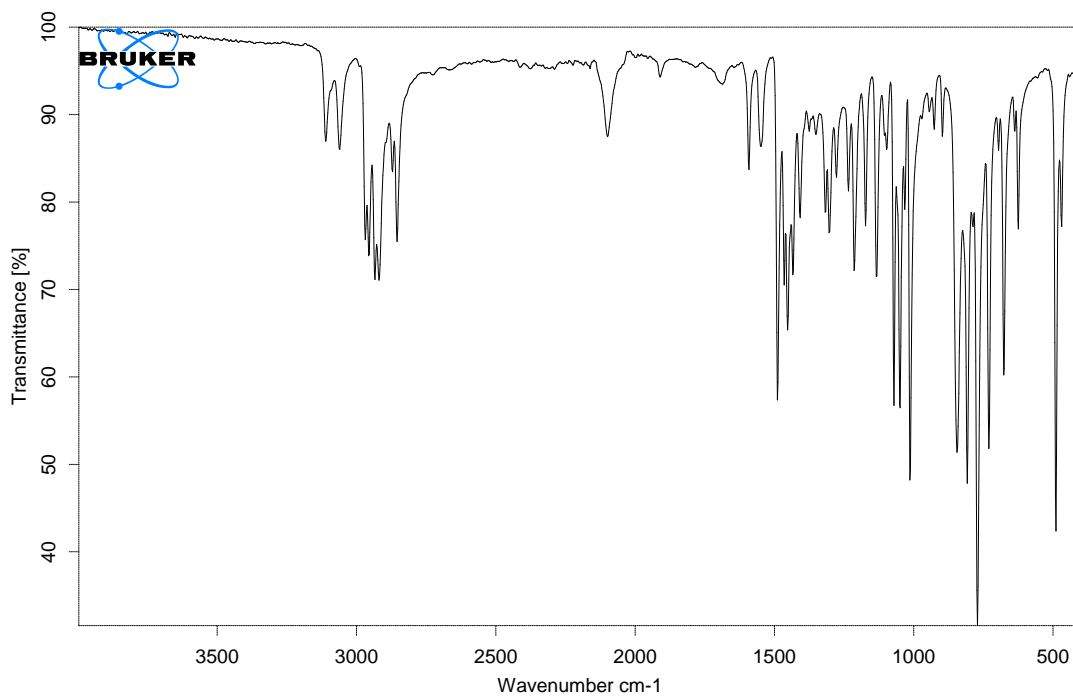


Figure S11.14 FTIR-ATR spectrum of isolated **4n**, synthesised by RAM direct mechanocatalysis.

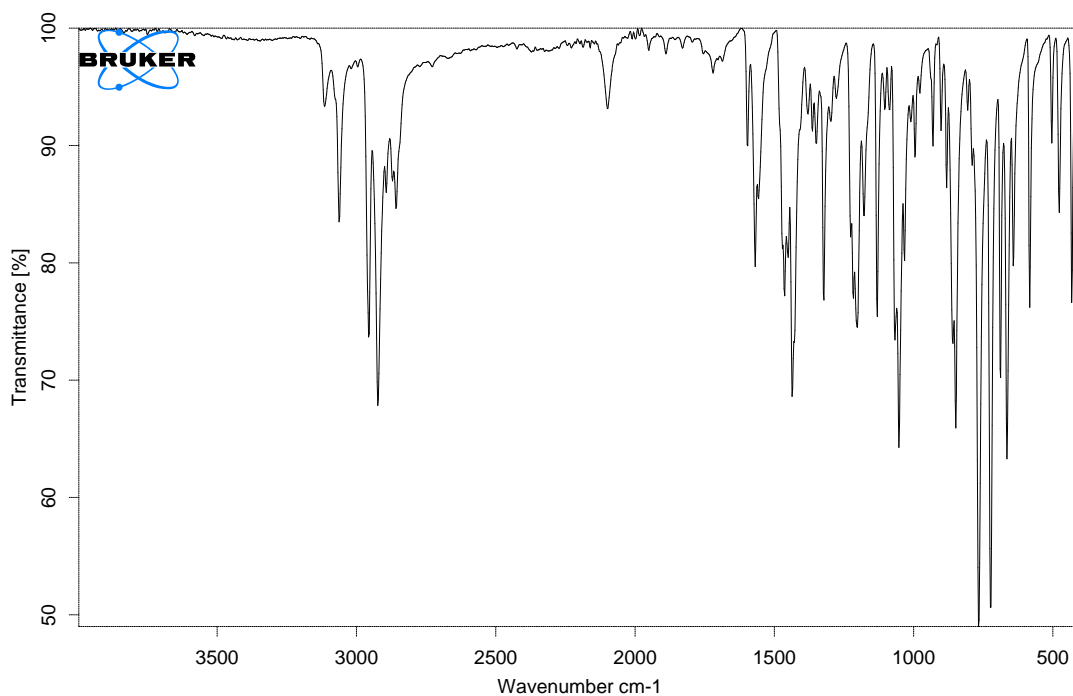


Figure S11.15 FTIR-ATR spectrum of isolated **4o**, synthesised by RAM direct mechanocatalysis.

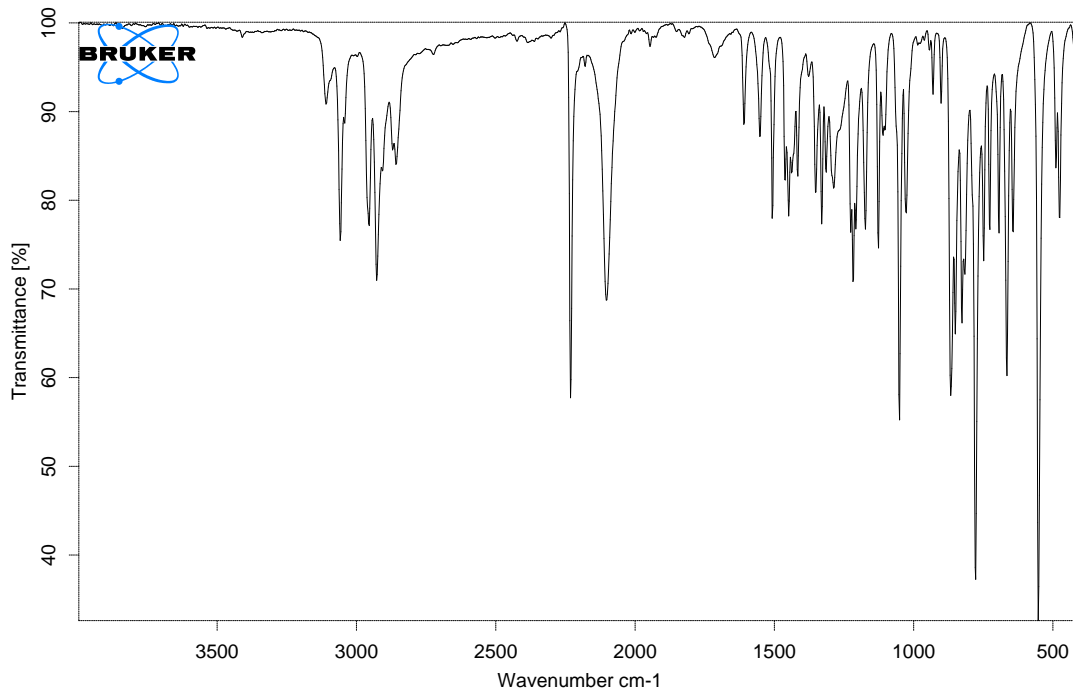


Figure S11.16 FTIR-ATR spectrum of isolated **4p**, synthesised by RAM direct mechanocatalysis.

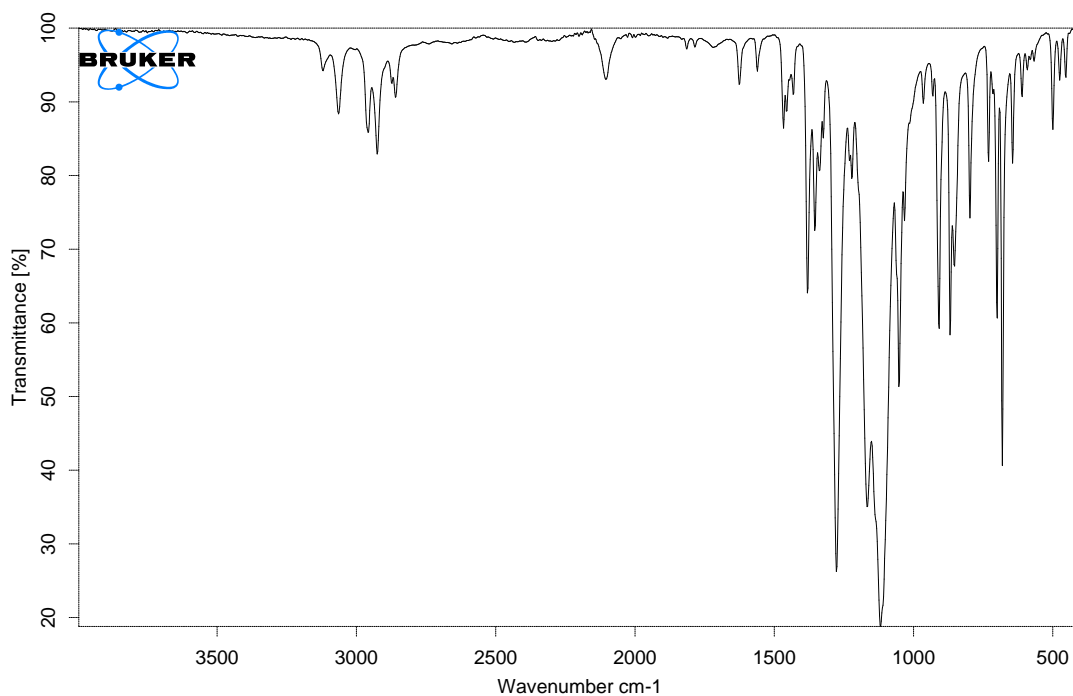


Figure S11.17 FTIR-ATR spectrum of isolated **4q**, synthesised by RAM direct mechanocatalysis.

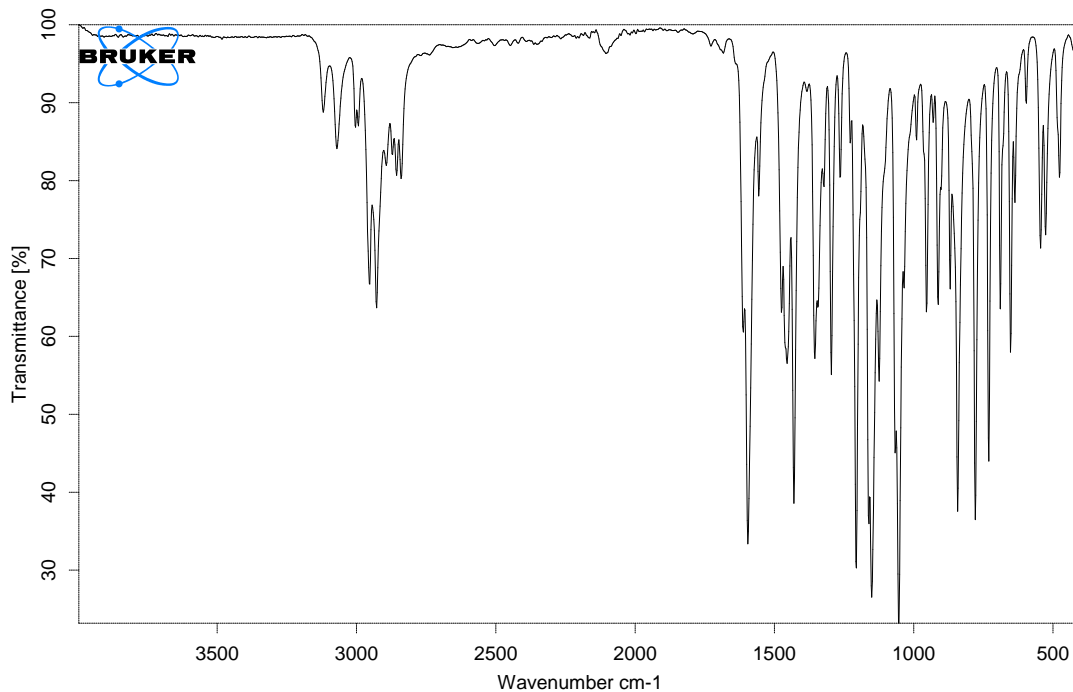


Figure S11.18 FTIR-ATR spectrum of isolated **4r**, synthesised by RAM direct mechanocatalysis.

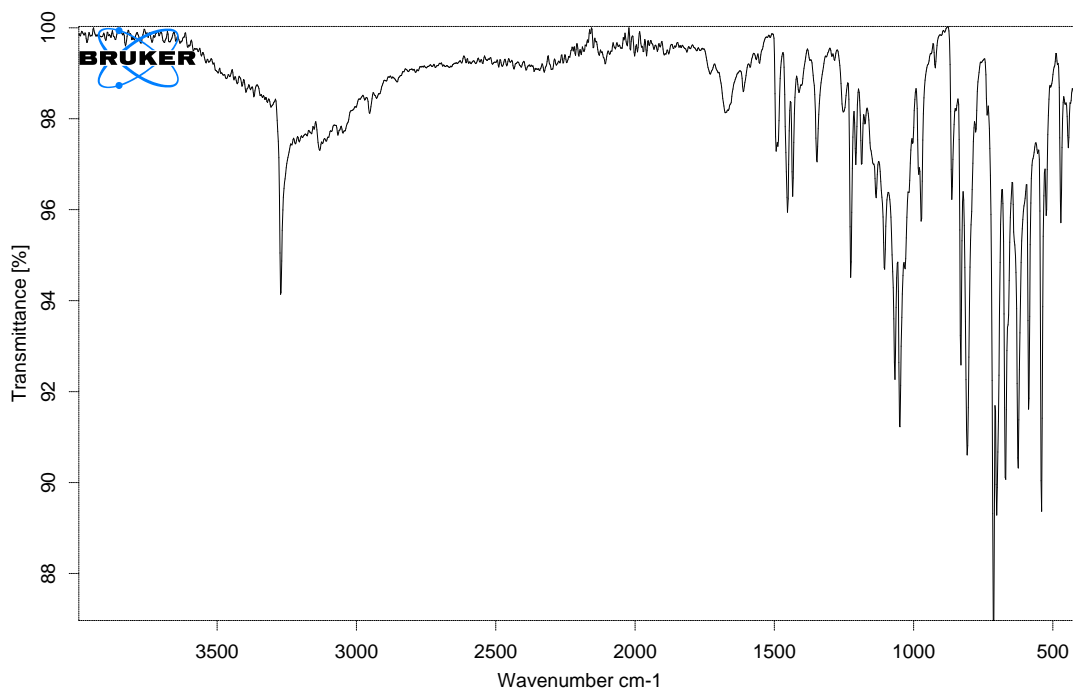


Figure S11.19 FTIR-ATR spectrum of isolated **4s**, synthesised by RAM direct mechanocatalysis.

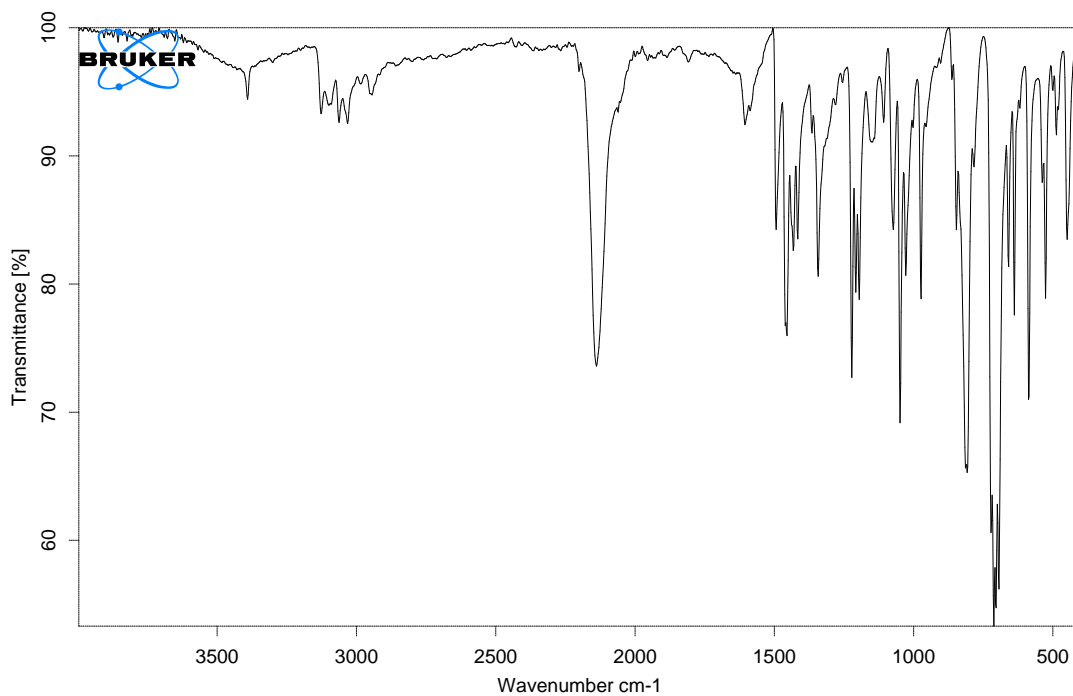


Figure S11.20 FTIR-ATR spectrum of isolated **4t**, synthesised by RAM direct mechanocatalysis.

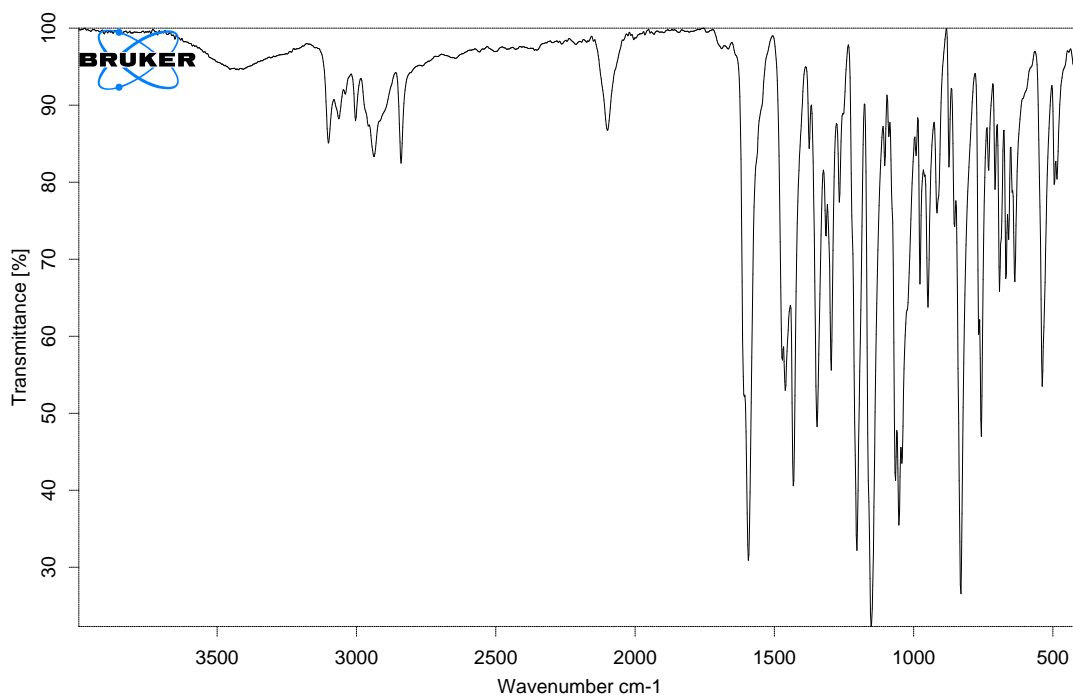


Figure S11.21 FTIR-ATR spectrum of isolated **4u**, synthesised by RAM direct mechanocatalysis.

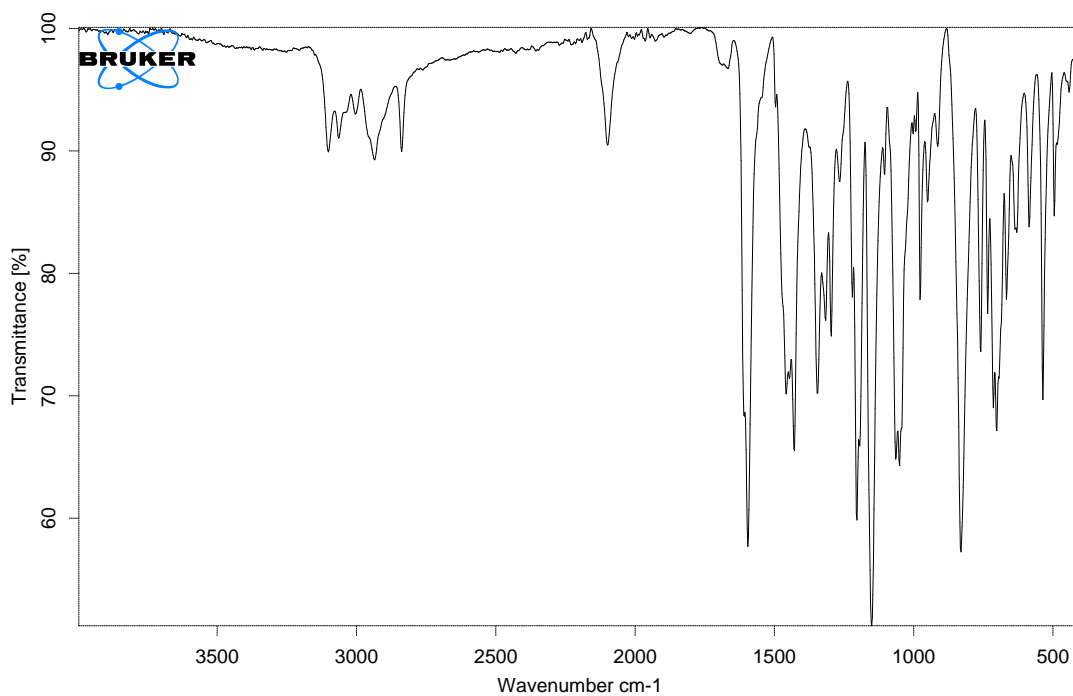


Figure S11.22 FTIR-ATR spectrum of isolated **4v**, synthesised by RAM direct mechanocatalysis.

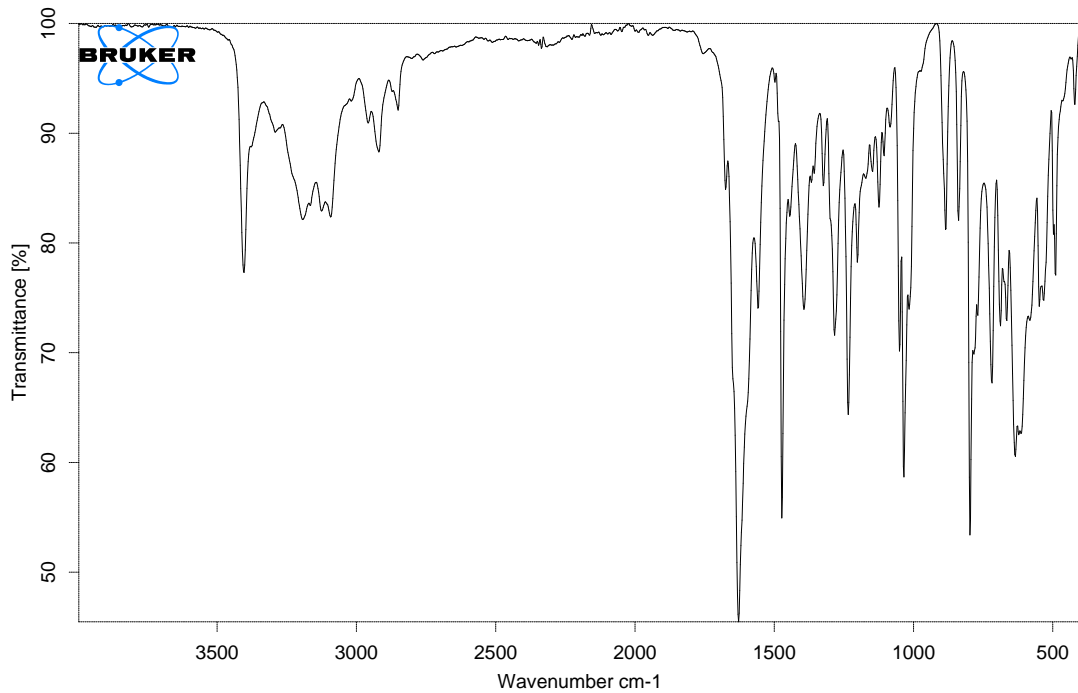


Figure S11.23 FTIR-ATR spectrum of isolated Rufinamide, synthesised by RAM direct mechanocatalysis.

S12. In situ Raman measurements

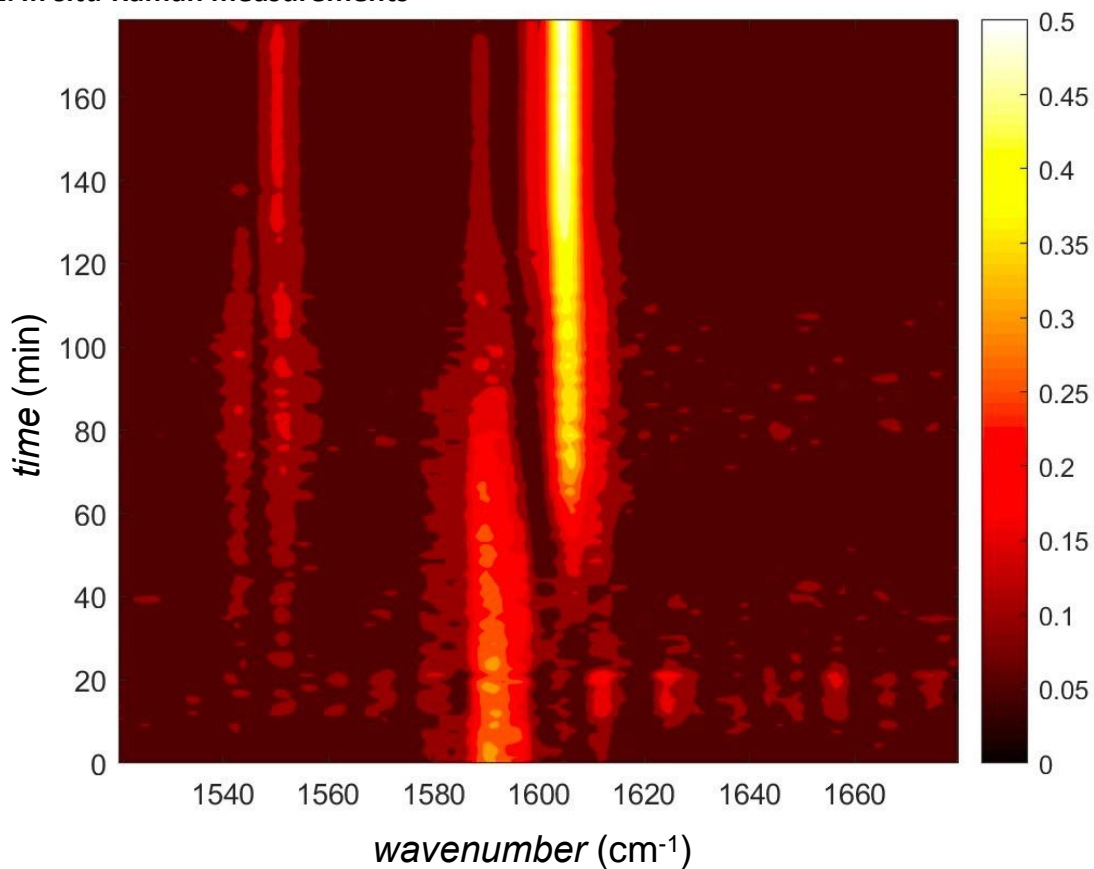


Figure S12.1 Contour plots of Raman absorbance bands over time, following the formation of **4e** during RAM direct mechanocatalysis demonstrating the disappearance of reactants **1e** and **2a**, and the formation of **4e**.

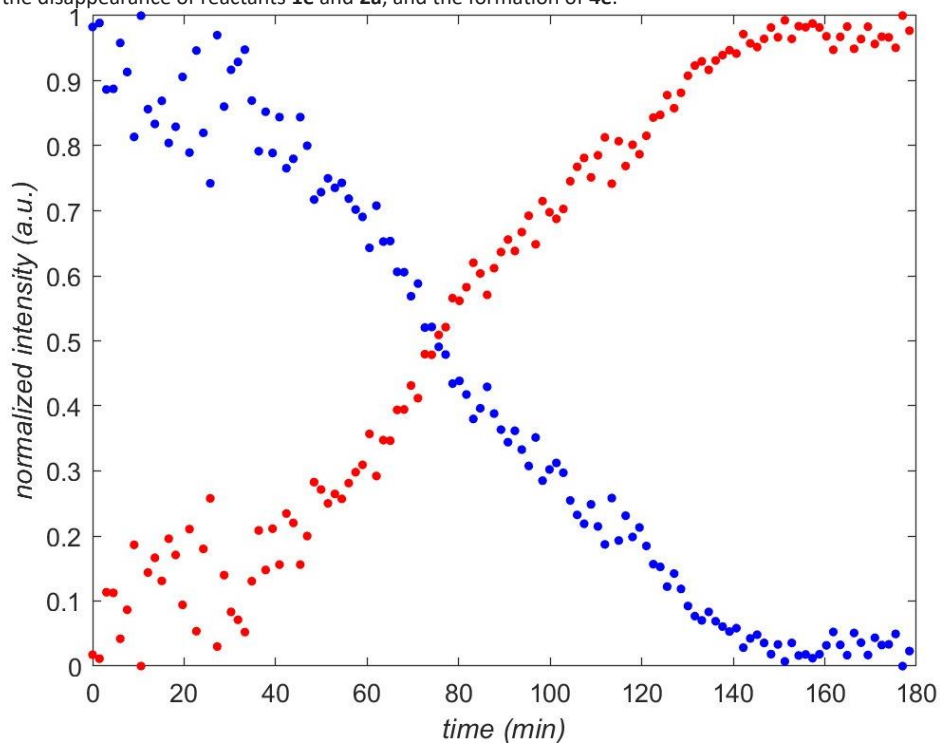


Figure S12.2 Time-resolved changes in intensity of Raman absorbance bands corresponding to **2a** (blue) and the formation of **4e** (red).

S13. Single crystal x-ray diffraction data

Table S16.1 Crystallographic data for compound **4e**.

CCDC deposition No. : 2223762	
Molecular formula	C ₁₇ H ₁₇ N ₃ O ₂
<i>M_r</i> (g/mol)	295.33
Crystal system	triclinic
Crystal colour	colorless
Space group	<i>P</i> -1
<i>T</i> (K/°)	298
Unit cell dimensions (Å, °)	
<i>a</i>	5.6650(1)
<i>b</i>	11.8408(2)
<i>c</i>	12.1314(2)
α	107.953(1)
β	101.480(1)
γ	92.508(1)
<i>V</i> (Å ³)	753.806
<i>Z</i>	2
ρ_{calc} (g/cm ³)	1.301
μ (mm ⁻¹)	0.707
<i>F</i> (000)	312.0
Independent reflections	2937 [<i>R</i> _{int} = 0.1194, <i>R</i> _{sigma} = 0.0591]
Data/restraints/parameters	2937/0/202
Goodness-of-fit on <i>F</i> ²	0.963
Final <i>R</i> indices [<i>I</i> >= 2σ (<i>I</i>)]	<i>R</i> ₁ = 0.0504, <i>wR</i> ₂ = 0.1332
Final <i>R</i> indices [all data]	<i>R</i> ₁ = 0.0675, <i>wR</i> ₂ = 0.1604
Largest diff. peak/hole / e Å ⁻³	0.15/-0.15

S14. References

[1] NIST XPS Database (2012). NIST X-ray photoelectron spectroscopy database. <http://srdata.nist.gov/xps> (accessed November 2022).